
**Role of the *Nodule Inception* promoter in
the evolutionary gain of the nitrogen-
fixing root nodule symbiosis**

Dissertation
zur Erlangung des
Doktorgrades der Naturwissenschaften
an der
Fakultät für Biologie
der
Ludwig-Maximilians-Universität München

vorgelegt von

Chloé Cathebras

München, August 2022

Erstgutachter:	Prof. Dr. Martin Parniske
Zweitgutachter:	Prof. Dr. Claude Becker
Dissertation eingereicht am:	2. August 2022
Tag der mündlichen Prüfung:	4. Oktober 2022

Eidesstattliche Erklärung

Ich versichere hiermit an Eides statt, dass die vorgelegte Dissertation von mir selbständig und ohne unerlaubte Hilfe angefertigt ist.

München, den 02. August 2022

Chloé Cathebras

Erklärung

Hiermit erkläre ich, dass die Dissertation nicht ganz oder in wesentlichen Teilen einer anderen Prüfungskommission vorgelegt worden ist. Ich habe mich nicht anderweitig einer Doktorprüfung ohne Erfolg unterzogen.

München, den 02. August 2022

Chloé Cathebras

Table of Contents

1.	Abbreviation index	1
2.	List of manuscripts in preparation and declaration of contributions of other researchers.....	5
3.	Summary.....	7
4.	Introduction	9
4.1.	Plant root endosymbioses.....	9
4.2.	The arbuscular mycorrhiza symbiosis	10
4.3.	The nitrogen-fixing root nodule symbiosis.....	11
4.3.1.	Evolution of the nitrogen-fixing root nodule symbiosis.....	11
4.3.2.	Establishment of the nitrogen-fixing root nodule symbiosis in legumes	13
4.4.	Recruitment of gene regulatory networks during the evolution of the nitrogen-fixing root nodule symbiosis	21
4.4.1.	Recruitment of AM genes for intracellular uptake of bacteria.....	22
4.4.2.	Recruitment of the lateral root developmental program for nodule organogenesis	23
4.4.3.	The role of <i>NIN</i> in the evolution of nodulation.....	24
5.	Aim of the thesis	25
6.	Results	27
6.1.	Acquisition of a <i>cis</i> -regulatory element in the <i>NIN</i> promoter enabled bacterial uptake by plant cells.....	27
6.1.1.	Discovery of <i>PACE</i>	27
6.1.2.	<i>PACE</i> drives the expression of <i>NIN</i> during infection thread development in the cortex....	29
6.1.3.	Mutational dissection of <i>PACE</i> reveals a quantitative impact of regions flanking the <i>CYC</i> - <i>box</i> on infection thread development.....	33
6.1.4.	<i>PACE</i> s from different nodulating FaFaCuRo species are functionally equivalent.....	41
6.1.5.	Loss of <i>PACE</i> is associated with a loss of nodulation	43
6.1.6.	<i>PACE</i> is sufficient to restore cortical infection thread formation in <i>nin-15</i>	45
6.1.7.	<i>PACE</i> insertion into the tomato <i>NIN</i> promoter confers RNS capability	46
6.2.	Lateral root formation is stimulated by deregulated versions of common symbiosis genes in <i>Lotus japonicus</i> and <i>Dryas drummondii</i> via the activation of <i>NIN</i>	51
6.2.1.	Arbuscular mycorrhiza and rhizobia impact root system architecture in <i>Lotus japonicus</i> .	51
6.2.2.	<i>NIN</i> is required for both AM fungi and rhizobia-mediated increase in lateral root density .	51
6.2.3.	Activation of arbuscular mycorrhiza and nodulation signalling stimulates lateral root formation in root organ liquid cultures.....	52
6.2.4.	Auto-active CCaMK stimulates lateral root formation in the absence of <i>Cyclops</i>	56
6.2.5.	Ectopic expression of <i>NIN</i> stimulates lateral root formation.....	57
6.2.6.	<i>NIN</i> is required for lateral root formation stimulated by auto-active CCaMK	59
6.2.7.	Lateral root induction mediated by auto-active CCaMK is conserved in <i>Dryas drummondii</i> but not in <i>Fragaria vesca</i>	60
7.	Discussion	63
7.1.	Acquisition of <i>PACE</i> in the last common ancestor of the FaFaCuRo clade enabled the formation of infection threads in the root cortex.....	63

7.2. Activation of <i>NIN</i> induces the formation of lateral roots.....	66
7.2.1. Components of the common symbiosis pathway trigger lateral root development via the activation of <i>NIN</i>	66
7.2.2. Genetic redundancy in the lateral root signalling pathway mediated by auto-active CCaMK	67
7.2.3. <i>NIN</i> orchestrates nodule organogenesis and lateral root formation	68
7.2.4. The evolution of the <i>NIN</i> regulon	68
8. Materials and Methods	71
8.1. Plant material, bacterial and fungal strains	71
8.2. Cultivation of chive and inoculation with AM spores.....	71
8.3. Cultivation of bacterial strains	71
8.4. <i>Lotus japonicus</i> growth conditions, symbiotic inoculations and root organ liquid cultures	72
8.5. Phenotypic analysis and quantification of infection events	73
8.6. Phenotypic analysis and quantification of primary root length and lateral root numbers under sterile conditions and symbiotic treatments	74
8.7. Promoter activity analysis	74
8.8. <i>Dryas drummondii</i> and <i>Fragaria vesca</i> growth conditions and root transformation	75
8.9. Cloning and DNA constructs	76
8.10. Imaging	76
8.11. Data visualization and statistical analysis	76
9. References	79
10. List of Figures and Table.....	95
11. Supplementary Figures and Tables	97
11.1. List of Supplementary Figures and Supplementary Tables.....	97
11.2. Supplementary Figures.....	98
11.3. Supplementary Tables.....	109
12. Acknowledgements	119
13. Curriculum Vitae	121

1. Abbreviation index

AM	Arbuscular mycorrhiza
ANOVA	Analysis of variance
AON	Autoregulation of nodulation
<i>A. rhizogenes</i>	<i>Agrobacterium rhizogenes</i>
ASL18a/LBD16	Asymmetric leaves 2-like 18a/Lob-domain protein 16
<i>A. thaliana</i>	<i>Arabidopsis thaliana</i>
bp	Base pair
BF	Brightfield
CaM	Calmodulin
CEP	C-terminally encoded peptide
ChIP-seq	Chromatin immunoprecipitation followed by sequencing
<i>C. glauca</i> & <i>Cg</i>	<i>Casuarina glauca</i>
CaM	Calmodulin
CCaMK	Calcium and Calmodulin-dependent kinase
CE	Cytokinin element
ChIP	Chromatin immunoprecipitation sequencing
CLSM	Confocal laser scanning microscopy
CYC-RE	Cyclops response element
CFP	Cyan fluorescent protein
CIP73	CCaMK interacting protein 73
CLE	Clavata3/embryo surrounding region-related
CLSM	Confocal laser scanning microscopy
CNGC15	Cyclic nucleotide-gated channel 15
CO	Chitin oligomer
CRE1	Cytokinin response 1
<i>D. drummondii</i> & <i>Dd</i>	<i>Dryas drummondii</i>
<i>D. glomerata</i> & <i>Dg</i>	<i>Datisca glomerata</i>
DNA	Deoxyribonucleic acid
dpg	Days post germination
dpi	Days post inoculation
dpt	Days post transfer
<i>DsRed</i>	<i>Discosoma sp.</i> red fluorescent protein
ENOD11	Early nodulin 11
EPR3	Exopolysaccharide receptor 3
EPS	Exopolysaccharide
ERF	Ethylene responsive factor
ERN1	ERF required for nodulation 1
EV	Empty vector

FaFaCuRo	Fagales, Fabales, Cucurbitales and Rosales
GARP	Glycoprotein A repetitions predominant
GFP	Green fluorescent protein
<i>G. max</i>	Glycine max
GUS	β -glucuronidase
HAR1	Hypernodulation aberrant root formation 1
HMGR1	3-hydroxy-3-methylglutaryl CoA reductase 1
IPN2	Interacting protein of NSP2
IT	Infection thread
<i>J. regia & Jr</i>	<i>Juglans regia</i>
kb	Kilo base
LCO	Lipo-chito-oligosaccharide
LHK1	Lotus histidine kinase 1
<i>L. japonicus & Lj</i>	<i>Lotus japonicus</i>
LB	Luria-Bertani broth
LORE1	<i>Lotus Retrotransposon 1</i>
LR	Lateral root
LysM	Lysin motif
Mb	Mega base
MF	Myc factor
<i>M. loti</i>	<i>Mesorhizobium loti</i>
<i>M. truncatula & Mt</i>	<i>Medicago truncatula</i>
Mya	Million years ago
<i>N. benthamiana</i>	<i>Nicotiana benthamiana</i>
NF	Nodulation factor
NFR1	Nod factor receptor 1
NFR5	Nod factor receptor 5
NF-Y	Nuclear Factor Y
NIN	Nodule inception
NLP	NIN-like protein
NOOT1	Nodule root 1
NPL	Nodulation pectate lyase
NRD	Nitrate responsive domain
NRE	Nitrate-responsive <i>cis</i> -regulatory element
NSP1	Nodulation signalling pathway 1
NSP2	Nodulation signalling pathway 2
NUP	Nucleoporin
PACE	Predisposition associated <i>cis</i> -regulatory element
<i>P. andersonii</i>	<i>Parasponia andersonii</i>
PB1	Phox and Bem1
PCR	Polymerase chain reaction

PIT	Pre-infection thread
PM	Plasma membrane
PPA	Pre-penetration apparatus
<i>P. persica & Pp</i>	<i>Prunus persica</i>
RAM1	Reduced arbuscular mycorrhization 1
RINRK1	Rhizobial infection receptor-like kinase 1
<i>R. irregularis</i>	<i>Rhizophagus irregularis</i>
RNA	Ribonucleic acid
RNS	Nitrogen-fixing root nodule symbiosis
RPG	Rhizobia-directed polar growth
Rpm	Revolutions per minute
SCAR	Suppressor of cyclic adenosine monophosphate receptor
SCARN	SCAR-nodulation
SCR	SCARECROW
SHR	SHORTROOT
<i>S. lycopersicum & Sl</i>	<i>Solanum lycopersicum</i>
<i>snf1</i>	<i>spontaneous nodule formation 1</i>
<i>snf2</i>	<i>spontaneous nodule formation 2</i>
<i>spp.</i>	Species
SymRK	Symbiosis receptor-like kinase
SYP132	Syntaxin of plant protein 132
TY	Tryptone yeast extract
Ubq	Ubiquitin
UTR	Untranslated region
VAMP	Vesicle associated membrane protein
YFP	Yellow fluorescent protein
WLI	White light illumination
WT	Wild-type
<i>Z. jujuba & Zj</i>	<i>Ziziphus jujuba</i>

2. List of manuscripts in preparation and declaration of contributions of other researchers

(1) The following manuscript presented in this work has been submitted to *eLife* and is currently under review:

Cathebras C*, Gong X*, Andrade RE, Vondenhoff K, Keller J, Delaux P-M, Hayashi M, Griesmann M & Parniske M. A novel *cis*-element enabled bacterial uptake by plant cells. Manuscript under review.

* these authors contributed equally to this work

The relevant data is found in section 7.1. The data presented in Figures 2 - 11 and Supplementary Figures 1 - 6 was a result of collaborative efforts between Chloé Cathebras (CC), Rosa Elena Andrade (RA), Xiaoyun Gong (XG), Ksenia Vondenhoff (KV) and Max Griesmann (MG). CC generated the data presented in Figure 3 and 8 and Supplementary Figure 5 and prepared all confocal and light microscopy images of root hairs and nodule sections (Figure 4, 5, 8, 10 and 11). CC, RA and XG collected the data displayed in Figure 5, 9, and 10. CC and RA collected the data displayed in Figure 4. CC and XG collected the data displayed in Figures 6, 7 and 11 and Supplementary Figure 4. MG generated the data presented in Figure 2. KV generated the data presented in Supplementary Figure 1. XG generated the data presented in Supplementary Figure 2, 3 and 6. CC, RA and XG all participated in the formulation of the research hypothesis, design of the experiments and analysis and interpretation of the data. Contributors are listed in each figure legend.

(2) The following manuscript presented in this work is in preparation:

Cathebras C, Sandré A, Ried MK & Parniske M. Lateral root formation is stimulated by deregulated versions of common symbiosis genes in *Lotus japonicus* and *Dryas drummondii*.

The relevant data is found in section 7.2. The data presented in Figures 12 - 22 and Supplementary Figures 7 - 10 was a result of collaborative efforts between Chloé Cathebras (CC), Aline Sandré (AS) and Martina Katharina Ried (MR). CC generated the data presented in Figures 12 - 21 and Supplementary Figures 7 - 10. CC and AS collected the data displayed in Figure 22. MR generated the data presented in Figure 19B. Contributors are listed in each figure legend.

Figure 1 in section 4.3.2.2 was designed by Xiaoyun Gong and modified by Chloé Cathebras.

Figures 23 and 24 in sections 7.1 and 7.2 were designed by Chloé Cathebras.

3. Summary

To overcome nutrient limitations, plants engage in two main types of root endosymbioses with beneficial microbes. Arbuscular mycorrhiza (AM) is an ancient symbiosis formed by about 70-90 % of land plants and phosphate-acquiring fungi of the phylum Glomeromycota. By contrast, root nodule symbiosis (RNS) with nitrogen-fixing bacteria is evolutionary much younger and is phylogenetically restricted to a single clade of flowering plants comprising only four orders, the Fabales, Fagales, Cucurbitales and Rosales (FaFaCuRo). AM and RNS require a common set of plant genes – the common symbiosis genes – and it is believed that genes that evolved for AM development have been recruited during the evolution of RNS to enable intracellular uptake and accommodation of bacteria. Moreover, RNS is characterised by the formation of a novel organ, the root nodule, and it was hypothesised that part of the lateral root (LR) developmental program was co-opted for nodule formation.

The restricted occurrence of RNS calls for yet unidentified trait acquisitions and genetic changes in the last common ancestor of the FaFaCuRo clade. Using a phylogenomic approach, a *cis*-regulatory element (*PACE*) was discovered to be exclusively present in the promoter of the transcription factor gene *Nodule Inception* (*NIN*) of FaFaCuRo member species. *NIN* is positioned at the top of a RNS-specific transcriptional regulatory cascade and is indispensable for RNS. We found that *PACE* is essential for restoring infection threads (ITs) in *Lotus japonicus nin* mutants. *PACE* sequence variants from RNS-competent species appear functionally equivalent. Evolutionary loss or mutation of *PACE* is associated with loss of this symbiosis. *PACE* dictates gene expression in cortical cells forming IT and *PACE*-driven *NIN* expression restores the formation of cortical ITs, also when engineered into the *NIN* promoter of tomato. Our data pinpoint *PACE* as a key evolutionary invention that connected *NIN* to a pre-existing signal transduction cascade that governs the intracellular accommodation of AM fungi. This connection enabled bacterial uptake into plant cells via ITs, a unique and unifying feature of this symbiosis.

Symbiosis signalling and LR development are tightly interconnected and treatment with lipochito-oligosaccharide molecules produced by AM fungi and rhizobia induce LR formation. To gain insight into the molecular players that connect these two distinct signalling programs, we studied the role of three common symbiosis genes *Symbiosis Receptor Kinase* (*SymRK*), *Calcium Calmodulin-dependent kinase* (*CCaMK*) and *Cyclops*, and of *NIN* in the formation of LRs. We reported that deregulated versions of *SymRK*, *CCaMK*, and *Cyclops* significantly increase the number of LRs in *L. japonicus* in a *NIN*-dependent manner and that ectopic expression of *NIN* likewise results in a significant increase in LR numbers. Additionally, *NIN* is necessary for LR induction mediated by both AM fungi and rhizobia bacteria. Our data reveal *NIN* as a key transcriptional regulator that does not only employ parts of the LR developmental program for nodule organogenesis but also directly activates the development of LRs in a symbiotic context.

Taken together, our data underpin the essential role of *NIN* in the evolutionary gain of RNS.

4. Introduction

4.1. Plant root endosymbioses

Plant growth and development relies on the availability of water and nutrients in the soil in which they root. In terrestrial ecosystems, phosphorus (P) and nitrogen (N) constitute the two main limiting macronutrients. P is mainly present in organic form such as minerals which are inaccessible for the plants. Instead, plants rely on soluble inorganic P form such as H_2PO_4^- or HPO_4^{2-} (Chen et al., 2008b; Shen et al., 2011) that can be directly taken up by the roots, but represents only a small fraction of the total soil's P pool (Schachtman et al., 1998). N makes up 78% of the earth's atmosphere in the form of di-nitrogen gas (N_2), however, it is inaccessible in that form for most organisms. Plants take up N predominantly as ammonium (NH_4^+) or nitrate (NO_3^-), that are produced through the fixation and nitrification processes, respectively, in the N cycle (Thamdrup, 2012), and are often deficient in soils. To increase crop yield, both macronutrients are supplied in the form of chemical fertilizers produced from non-renewable resources: N-based fertilizers are almost exclusively generated by the Haber-Bosch process that currently requires extensive use of fossil fuels (Erisman et al., 2008); and P-based fertilizers are produced from mining of rock phosphate reserves (Walan et al., 2014). The current over-use of these fertilizers in agricultural settings result in a run-off into ground water and oceans leading to water pollution, eutrophication, altered biodiversity and greenhouse effect (Erisman et al., 2013; Diaz and Rosenberg, 2008).

During the course of evolution, plants have developed multiple strategies to overcome nutrient limitation such as the ability to engage in symbiosis with nutrient-delivering microorganisms. Approximately 70-90 % of land plants engage in symbiosis with fungi of the monophyletic phylum Glomeromycota to form the arbuscular mycorrhiza symbiosis (AM). Fossil records of AM structures were dated to approximately 450 million years ago (Mya), raising the hypothesis that AM could have play a crucial role for the colonization of land by plants (Remy et al., 1994). AM is an endomycorrhiza that connects plants to an extensive hyphal network that unlocks P from inorganic complexes of low solubility in the soil (Javot et al., 2007). Fungal hyphae penetrate the plant roots intracellularly and form tree-shaped subcellular structures called arbuscules within cortical cells, which are thought to be the main site for nutrients exchange between the two partners (Gutjahr and Parniske, 2013). AM fungi mainly deliver P and water to the host plants (Joner et al., 2000; Javot et al., 2007; Kakouridis et al., 2022). In return, plants deliver up to 20% of its photosynthetically fixed carbon to the fungi in the form of hexoses and fatty acids (Bago et al., 2000; Keymer et al., 2017; Bravo et al., 2017; Jiang et al., 2017; Helber et al., 2011; Pfeffer et al., 1999; Shachar-Hill et al., 1995; Luginbuehl et al., 2017). AM fungi play a significant role in global P cycle as well as carbon cycle as approximately 5 billion tons of carbon per year are estimated to be consumed by AM fungi (Parniske, 2008; Bago et al., 2000). In addition to the nutrient supply, AM-forming plants benefit from an enhanced biotic and abiotic stress resistance and improved soil stability (reviewed in (Gianinazzi et al., 2010)).

To overcome N limitation, certain plants evolved the capacity to engage in symbiosis with N-fixing bacteria to form the N-fixing root nodule symbiosis (RNS). RNS is exclusively formed by species that belong to a single clade comprising four orders: the Fabales, Fagales, Cucurbitales and Rosales (thereafter termed “the FaFaCuRo clade”) (Soltis et al., 1995). Members of the Fabales engage in symbiosis with Gram-negative α - and β - protobacteria collectively referred to as rhizobia, whereas species belonging to the Fagales, Cucurbitales and Rosales (called actinorhiza plants) engage in symbiosis with Gram-positive actinobacteria of the genus *Frankia* (Sprent, 2007; Svistoonoff et al., 2014), with the only exception of *Parasponia* species (Rosales) that interact with rhizobia bacteria (van Velzen et al., 2019). RNS is characterised by the formation of a new organ – the root nodule – in which N-fixing bacteria are hosted intracellularly. The root nodule provides a low oxygen environment, enabling the conversion of atmospheric dinitrogen into ammonia by the bacterial nitrogenase enzyme complex (Hoffman et al., 2014). In return, plants deliver reduced carbon and various nutrients to the bacteria such as malate and amino acids (Colebatch et al., 2004; White et al., 2007; Roy et al., 2020).

Due to their ecological and economical importance, researches on the molecular mechanisms governing AM and RNS development have been conducted extensively. Since RNS is restricted to a single clade of flowering plants, it has long been a goal for scientists to transfer this ability to engage in symbiosis with N-fixing bacteria to important non-host crop plants (Charpentier and Oldroyd, 2010). To this end, understanding the evolutionary origin of the RNS and uncovering its genetic requirements is fundamental. Over the last decades, scientists have characterized almost 200 genes that play a role in the establishment of RNS, principally using the legumes (Fabales) *Medicago truncatula* and *Lotus japonicus* as model plants (Roy et al., 2020). In addition, the availability of numerous genomes has enabled genome-wide comparative phylogenomic analyses that provided insights on the evolutionary origins of RNS (Griesmann et al., 2018; van Velzen et al., 2018). Despite a lot of progress, it is still a long walk toward the identification of all the evolutionary inventions necessary to engineer RNS on roots of non-host plants (Pankievicz et al., 2019).

4.2. The arbuscular mycorrhiza symbiosis

Plants control AM development depending on their nutritional, in particular P, status (Carbonnel and Gutjahr, 2014). AM is inhibited under high P supply, but promoted under P deficiency in the soil. The molecular mechanisms underlying this regulation have been recently identified (Das et al., 2022). The establishment of AM starts with a reciprocal exchange of diffusible signal molecules between the two partners. Plant roots secrete in particular strigolactones which are carotenoid-derived phytohormones that are released in the soil. The perception of these compounds by AM fungi induces hyphal growth and branching as well as cell proliferation and spore germination (reviewed in (Gutjahr and Parniske, 2013)). In return, AM fungi secrete signal molecules called Myc factors that were identified to be a mixture of sulphated and non-sulphated lipochitoooligosaccharides

(LCOs) and short-chain chitin oligomers (COs) (Maillet et al., 2011; Genre et al., 2013). LCOs perception by the host plant induces multiple responses such as the transcriptional activation of symbiosis-related genes (Kosuta et al., 2003; Ortu et al., 2012; Navazio et al., 2007; Kuhn et al., 2010; Mukherjee and Ané, 2011), induction of rhythmic calcium oscillations in and around the nucleus (referred to as calcium spiking; (Kosuta et al., 2008; Chabaud et al., 2011; Sun et al., 2015; Sieberer et al., 2009)), starch accumulation (Gutjahr et al., 2009b) and lateral root (LR) formation and elongation (Oláh et al., 2005; Sun et al., 2015; Tanaka et al., 2015). Additionally, LCOs were recently found to have regulatory functions in fungal development (Rush et al., 2020).

Upon physical contact with the plant root, the fungal hyphae differentiate to form an attachment structure called hyphopodium which penetrate the rhizodermal cells (Gutjahr and Parniske, 2013). Concomitantly, the nucleus in the rhizodermal cells migrate below the hyphopodium site and then move through the vacuole toward the opposite side of the cell to initiate an accommodation structure called pre-penetration apparatus (PPA) (Genre et al., 2005). The PPA constitutes a cytoplasmic bridge across the vacuole that guides the fungus inside the rhizodermal and outer cortical cells (Parniske, 2008; Genre et al., 2008, 2005). Once the fungal hyphae reach the inner cortex, they grow longitudinally in the apoplastic space and enter the cells by invagination of the plant plasma membrane (PM) where they differentiate into arbuscules. This *de novo* plant synthesised membrane, termed as peri-arbuscular membrane, separates the fungi from the host cytoplasm and constitutes, together with the fungal PM and the peri-arbuscular space in between, the symbiotic interface for nutrient exchanges between the symbionts (Gutjahr and Parniske, 2013).

Beside the formation of accommodation structures for AM fungi, the intra-radical AM colonization process induces changes in the root system architecture of the host plant, predominantly resulting in an increase in root volume and LR proliferation (reviewed in (Gutjahr and Paszkowski, 2013)).

4.3. The nitrogen-fixing root nodule symbiosis

4.3.1. Evolution of the nitrogen-fixing root nodule symbiosis

While fossils of AM structures were detected in early land plants, RNS evolved later. The oldest fossil records of putative nodules were dated back to 84 Mya (Herendeen et al., 1999), whereas the last putative RNS-forming common ancestor was dated back to 92-110 Mya (Wang et al., 2009; Bell et al., 2010). Phylogenetic analyses revealed that the occurrence of the RNS is restricted to a single clade of flowering plants, the FaFaCuRo clade, within which the distribution of RNS is scattered: only 10 out of 28 families contain RNS-forming species and in 9 out of these 10 families, RNS-forming genera represent the minority (Soltis et al., 1995; Doyle, 2011). This restricted and scattered distribution has led to two hypotheses underlying the evolutionary origin and dynamic of the RNS.

The first one is the **multiple origin hypothesis**, also called the “predisposition hypothesis”. This hypothesis predicts a genetic change, a “predisposition event”, in the common ancestor of the FaFaCuRo clade leading to a precursor state that enabled the subsequent independent evolution of the RNS in some descendants, followed by parallel losses of this trait in few species (Soltis et al., 1995; Doyle, 2011; Werner et al., 2014). Hence, this model predicts nodulation as a non-homologous trait and implies that the yet unidentified propensity for nodulation has been maintained for approximately 30 million years before the emergence of RNS in the earliest nodulating lineage, therefore bridging the conceptual gap between the date of the oldest nodule fossils and the common ancestor that acquired the nodulation predisposition. The **multiple origin hypothesis** is the most commonly accepted evolutionary scenario and is supported by recent quantitative phylogenetic modelling studies (Li et al., 2015; Werner et al., 2014) as well as by the diversity observed in the nodule ontogeny, type of microsymbionts and infection modes among nodulating plants (Doyle, 2011; van Velzen et al., 2019).

First, two groups of bacteria engage in RNS: the Gram-negative proteobacteria referred to as rhizobia and the Gram-positive actinobacteria of the genus *Frankia*. The infection mechanisms through which these bacteria are accommodated within the nodule cells greatly differ between plant species. In most of the leguminous plants (Fabales), rhizobia enter the root via the formation of host-constructed tubular structures called infection threads (ITs) within root hairs (Oldroyd et al., 2011). This infection mode has also been described in plants belonging to the Fagales order such as *Casuarina glauca* (Svistoonoff et al., 2003). In other species such as *Discaria trinervis* (Rosales), *Frankia* bacteria enter the root through intercellular spaces between epidermal and cortical cells (Fournier et al., 2018). In a different manner, *Bradyrhizobium* strains penetrate the root of *Aeschynomene* (Fabales) species intercellularly through epidermal fissures generated by the emergence of LR_s (Bonaldi et al., 2011).

Additionally, nodule morphologies greatly vary between plant species. Two major types of root nodules are found in legume species, namely indeterminate and determinate nodules. Indeterminate nodules such as the ones formed on *M. truncatula* and *Pisum sativum* have a persistent apical meristem and are continuously infected. By contrast, determinate nodules such as the ones formed on *L. japonicus* and *Glycine max* lose their meristem upon maturation and have a defined lifespan. These two nodule types are characterised by peripheral vasculatures. Conversely, nodules formed on *Parasponia* species (infected by rhizobia) and actinorhizal plants (infected by *Frankia*) are characterised by a central vasculature and the presence of a persistent apical meristem (Popp and Ott, 2011; Xiao et al., 2014; Soyano et al., 2021). Furthermore, nodulating species employ different strategies to accommodate the symbiont intracellularly as well as to provide a low oxygen environment which is necessary for bacterial nitrogenase activity. Altogether, these phenotypic variations have fuelled the hypothesis that nodulation is a non-homologous trait that evolved multiple times independently in different lineages (Doyle, 2011; van Velzen et al., 2019).

The second model is the *single origin hypothesis*. This hypothesis predicts a single gain of RNS in the last common ancestor of the FaFaCuRo clade followed by multiple parallel loss of this trait in most descendants (Soltis et al., 1995; Doyle, 2011). This model predicts nodulation as a homologous trait in all lineages and is supported by multiple lines of evidences (van Velzen et al., 2019). The first one came from the observation that several genes essential for RNS development have a similar function within distantly related nodulating plants and are therefore considered as orthologous (Gherbi et al., 2008; Markmann et al., 2008; Svistoonoff et al., 2014; Clavijo et al., 2015; Granqvist et al., 2015; Fabre et al., 2015; Das et al., 2019). The second one came from the similarities in nodule ontology from leguminous and actinorhizal plants. Although the anatomy and developmental features of both nodule types differ, a recent study constructed detailed fate maps of nodules formed on *Alnus glutinosa* (Fagales), *Medicago truncatula* (Fabales) and *Parasponia andersonii* (Rosales) roots and revealed that the ontogeny of the legume-type nodules and actinorhizal-type nodules is much more similar than previously thought (Xiao et al., 2014; Shen et al., 2020). In addition, the authors reported that a homeotic mutation in *NODULE ROOT1* (*MtNOOT1*) in *M. truncatula* partially converts the ontology of legume-type nodules into actinorhizal-type nodules, therefore suggesting that both nodule types share an evolutionary origin (Shen et al., 2020). Moreover, two recent phylogenomic studies revealed that the scattered distribution of nodulating species among the FaFaCuRo clade is a consequence of massive independent losses of RNS caused by the loss or mutation of genes essential for RNS establishment (Griesmann et al., 2018; van Velzen et al., 2018). Altogether, these findings are consistent with a *single gain* of this symbiosis in the most recent common ancestor of the FaFaCuRo clade.

Currently, both hypotheses lack direct evidences and despite decades of research, the genetic causes associated with the emergence of the RNS remain a mystery (Doyle, 2016; Griesmann et al., 2018). In a recent opinion article, Martin Parniske (Parniske, 2018) proposed that the ability to uptake bacteria into living plant cells with intracellular physical support structures might be tightly linked to the predisposition event acquired in the last common ancestor of the FaFaCuRo clade.

4.3.2. Establishment of the nitrogen-fixing root nodule symbiosis in legumes

Over the last decades, the molecular and cellular processes underpinning the establishment of RNS have been extensively studied through forward and reverse genetics in the two model legumes *L. japonicus* (*Lj*) and *M. truncatula* (*Mt*). Up to date, nearly 200 genes required for RNS in legumes have been identified (Roy et al., 2020).

4.3.2.1. Cellular processes during rhizobial infection and nodule development

The establishment of RNS is a process strictly controlled by the host plant. Under N limiting conditions, legume plants increase their secretion of flavonoids in the rhizosphere (Coronado et al., 1995) which are perceived by rhizobia via their bacterial transcriptional activator *nodD* proteins (Peck et al., 2006). Subsequently, *nodD* proteins activate the expression of the bacterial *nod* genes, leading to the synthesis of strain-specific nodulation factors (Nod factors, NFs) (Liu and Murray, 2016). NFs are highly similar to AM fungal LCOs and consist of a chitin backbone, generally made up of five to six β -(1-4)-linked *N*-acetylglucosamine residues, which is acylated at the non-reducing terminal glucosamine (Oldroyd, 2013; Fliegmann and Bono, 2015). NFs produced by different rhizobia differ in the length and degree of saturation of the *N*-acyl group and can be decorated by various substituents (e.g. methyl, fucosyl, acetyl or sulphate groups) on the *N*-acetylglucosamine subunits (Oldroyd, 2013). These strain-specific modifications are essential for stringent host-rhizobium compatibility (Poole et al., 2018; Radutoiu et al., 2007). Apart from NFs, bacteria synthesise exopolysaccharides (EPSs) which were reported to also contribute to host-symbiont compatibility (Kawaharada et al., 2015).

The perception of the NFs in the plant root hairs induces multiple cellular responses such as the induction of calcium spiking (Ehrhardt et al., 1996), membrane potential depolarisation (Ehrhardt et al., 1992), modifications of the root hair cytoskeleton and root hair deformation (Heidstra et al., 1994; Sieberer et al., 2005; Esseling et al., 2003). NFs recognition additionally induces cellular responses in deeper cell layers such as the formation of tube-shape like-structure called pre-infection threads (PITs) (Van Brussel et al., 1992) and the induction of cell divisions leading to the formation of a nodule primordium (Truchet et al., 1991; Van Spronsen et al., 2001). These cellular responses are accompanied by the induction of symbiosis-related genes (Breakspear et al., 2014). Furthermore, the perception of NFs was found to stimulate the formation of LRs (Oláh et al., 2005; Herrbach et al., 2017).

Rhizobia infect legumes using intercellular and/or intracellular entry modes (Deakin and Broughton, 2009; Madsen et al., 2010). The best studied infection mode takes place through the root hair cells and is initiated by a physical attachment of rhizobia to the root hair tip which curls and entraps the bacteria within a so-called infection pocket. Entrapped bacteria continue to divide and form a so-called infection foci (Oldroyd et al., 2011). Subsequently, the cell wall of the root hair is locally hydrolysed and a tubular invagination of the PM initiates the development of an infection thread (IT), in which rhizobia are guided towards the cortex (Oldroyd et al., 2011). In analogy to the PPA formed during AM, IT progression is preceded by the formation of a PIT, which consists of ER-rich cytoplasmic bridges aligned with the cytoskeleton traversing the central vacuole of the cells (Van Brussel et al., 1992; Yokota et al., 2009). Concomitantly to IT development, cell divisions in the pericycle and cortical cells are initiated to form nodule primordium (Popp and Ott, 2011; Xiao et al., 2014). Although they are happening in a precisely coordinated way, the rhizobia infection and

nodule organogenesis processes are at least partially independent and can be uncoupled from each other (Tirichine et al., 2006, 2007; Murray et al., 2007). Once ITs have reached the cortical cells in the nodule primordium, they ramify and subsequently release bacteria into plant membrane-enclosed compartments called symbiosomes where they differentiate into a N-fixing state (Popp and Ott, 2011). Because RNS is an energetically costly process, plants control the number of nodules formed on their roots via a systemic pathway called autoregulation of nodulation (AON) (Magori and Kawaguchi, 2009).

4.3.2.2. Signalling during the nitrogen-fixing root nodule symbiosis

The establishment of the RNS requires a network of genetic regulators that activate a specific symbiotic signalling pathway which triggers extensive transcriptional responses in the host cells (Chakraborty et al., 2022). This transcriptional reprogramming starts with the recognition of the bacteria NFs. In the legume *L. japonicus*, NFs are perceived by lysin motif (LysM) domain-containing receptors Nod Factor Receptor (NFR) 1 and NFR5 which form heterodimers at the PM ((Broghammer et al., 2012; Madsen et al., 2003; Radutoiu et al., 2003); in this thesis the name of the *L. japonicus* genes will be used). Besides NFs, bacterial EPSs are recognized by the LysM receptor kinase Exopolysaccharide Receptor 3 (EPR3; (Kawaharada et al., 2015, 2017)). The NF-induced signalling involves the activation of the receptor-like kinase SymRK (Stracke et al., 2002; Ried et al., 2014) which interacts with NFR1 and NFR5 as well as several other cytosolic proteins and is believed to start the transmission of secondary signal from the PM to the nucleus (Figure 1). Two possible signalling pathways have been proposed to link microbial perception at the PM to the generation of calcium spiking in the nucleus (Charpentier, 2018). The first one may involve heterotrimeric G-protein complexes and regulator of G-protein signalling (RGS), a GTPase that interacts and is phosphorylated by NFR1 and plays a role in the regulation of nodulation in *G. max* (Choudhury and Pandey, 2015). The second one requires the SymRK-interacting protein 3-hydroxy-3-methylglutaryl CoA reductase 1 (HMGR1) which catalyses the conversion of HMG-CoA to mevalonate (MVA) (Kevei et al., 2007) and was reported to be involved in the generation of nuclear calcium oscillations (Venkateshwaran et al., 2015). Interestingly, Ried et al. (Ried et al., 2014) observed that strong expression of NFR1, NFR5 and SymRK results in the activation of symbiosis-related genes and is sufficient to activate a signalling cascade leading to the formation of spontaneous nodules in the absence of a symbiont. Nonetheless, whether the over-abundance of these proteins also induces calcium spiking remains to be determined.

The induction of rhythmic calcium oscillations in and around the nucleus is a hallmark of symbiotic signal transduction (Ehrhardt et al., 1996; Oldroyd, 2013). Calcium spiking requires multiple components that localise to the nuclear envelope, including the nuclear core complex components nucleoporine 85 (NUP85), NUP133 and Nena (Kanamori et al., 2006; Saito et al., 2007; Groth et al., 2010), the ions channels Castor, Pollux, and CNGC15 proteins (Ané et al., 2004; Imaizumi-Anraku et al., 2005; Charpentier et al., 2008; Kim et al.,

2019; Charpentier et al., 2016), and the calcium-dependent adenosine triphosphatase MCA8 (Capoen et al., 2011) (Figure 1).

Within the nucleus, the calcium and calmodulin-dependant protein kinase CCaMK is believed to decode and transduce the calcium signal into downstream symbiotic gene activation (Singh and Parniske, 2012). CCaMK contains an N-terminal serine/threonine kinase domain, followed by a calmodulin (CaM) binding domain overlapping with an autoinhibitory region, and a C-terminal visinin-like domain which contains three EF hands (Sathyanarayanan et al., 2000; Takeda et al., 2012; Ramachandiran et al., 1997; Poovaiah et al., 2013). Biochemical studies and structural analyses established a model for CCaMK activation and revealed that CCaMK's kinase activity is regulated by calcium concentrations (Sathyanarayanan et al., 2000; Miller et al., 2013). At basal calcium concentration, T265 in the kinase domain is phosphorylated, which stabilizes an autoinhibitory conformation rendering CCaMK inactive for target phosphorylation. Upon calcium spiking, CaM binds to CCaMK inducing conformational changes that overrides the impact of T265 phosphorylation thus leading to CCaMK activation (Miller et al., 2013). CCaMK is essential for the establishment of both AM and RNS. *ccamk* mutants are completely impaired in rhizobial and fungal infections as well as nodule organogenesis, but retain the capacity to elicit root hair deformation and calcium spiking upon NF or AM fungal exudate treatment (Lévy et al., 2004; Mitra et al., 2004; Chabaud et al., 2011).

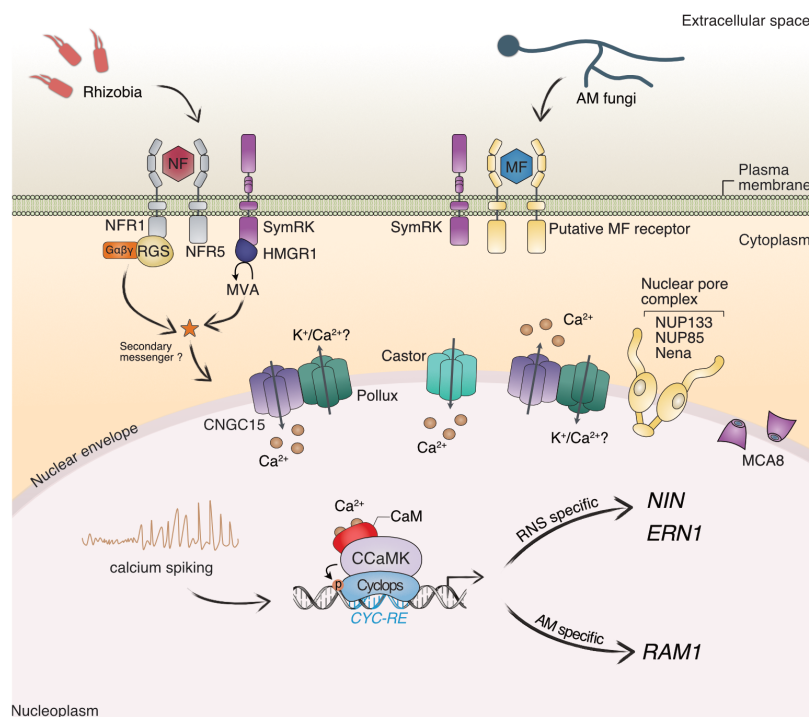


Figure 1: Overview of the symbiotic signal transduction in plant root cells. Signalling molecules produced by rhizobia or AM fungi are recognised by plant receptors at the plasma membrane. Rhizobia secrete in particular Nod factors (NFs) which are perceived by the LysM domain-containing receptors NFR1 and NFR5 (Broghammer et al., 2012; Madsen et al., 2003; Radutoiu et al., 2003). (continuation of figure legend on the next page)

Legend Figure 1: continued

AM fungi secrete Myc factors (MF) which are perceived by a hypothetical yet to be identified LysM-receptor-like kinase. NFR1 and NFR5 associate with the receptor-like kinase SymRK, which is required for both AM and RNS development (Stracke et al., 2002; Ried et al., 2014). HMGR1 interacts with SymRK and produces MVA, an activator of nuclear calcium oscillations (Kevei et al., 2007; Venkateshwaran et al., 2015). NFR1 interacts with and phosphorylates RGS proteins, which play a role in the regulation of nodulation (Choudhury and Pandey, 2015). MVA and the G-protein signalling pathway might be necessary to induce the production of a so far unidentified secondary messenger, leading to calcium release in the nucleus (Charpentier, 2018). The nuclear pore complex components NUP85, NUP133 and Nena (Kanamori et al., 2006; Saito et al., 2007; Groth et al., 2010), the ion channels Castor, Pollux (Ané et al., 2004; Imaizumi-Anraku et al., 2005; Charpentier et al., 2008; Kim et al., 2019) and CNGC15a,b,c (Charpentier et al., 2016), as well as the calcium pump MCA8 (Capoen et al., 2011) are required to generate rhythmic calcium oscillations (calcium spiking) in and around the nucleus (Ehrhardt et al., 1996; Sieberer et al., 2009; Kosuta et al., 2008). Calcium spiking is believed to be decoded by CCaMK which interacts with and phosphorylates the transcription factor Cyclops (Lévy et al., 2004; Tirichine et al., 2006; Yano et al., 2008; Singh et al., 2014). Cyclops recognises and binds to palindrome-containing *cis*-regulatory elements (CYC-REs) in the promoters of its target genes that are specifically required for AM (*Reduced Arbuscular Mycorrhization 1*, *RAM1*) or RNS (*NIN* and *ERN1*) (Pimprikar et al., 2016; Singh et al., 2014; Cerri et al., 2017). p, phosphate group; CaM, calmodulin; MVA, mevalonate. Figure was initially created by Xiaoyun Gong and modified based on Charpentier (2018).

The identification of CCaMK auto-active versions enabled to position this kinase in the genetic pathway required for root endosymbiosis. Mutation of the autophosphorylation residue T265, CCaMK^{T265D} or CCaMK^{T265I} in the *snf1-1* mutant, leads to the formation of spontaneous nodules as well as the induction of RNS-specific genes in the absence of rhizobia (Tirichine et al., 2006; Takeda et al., 2012). In addition, CCaMK^{T265D} and CCaMK^{T265I} are both able to restore nodule organogenesis and rhizobia infection in calcium-spiking deficient mutants, with the exception of *nfr* mutants (Hayashi et al., 2010; Madsen et al., 2010; Singh and Parniske, 2012), and strong ectopic expression of CCaMK^{T265D} induces the formation of LRs (Martina Katharina Ried, unpublished data). Moreover, strong expression of the kinase domain alone of CCaMK (CCaMK^{1-314 T265D}) is sufficient to spontaneously induce both AM and RNS-specific genes as well as to trigger the development of spontaneous nodules and the formation of structures that resemble PPA in the absence of a symbiont (Takeda et al., 2012). Importantly, CCaMK^{1-314 T265D} is also able to restore fungal but not rhizobial infection in the *ccamk-3* mutant (Takeda et al., 2012), thus highlighting the importance of the autoregulatory domain for maintaining downstream signalling specificity (Singh and Parniske, 2012).

CCaMK interacts with and phosphorylates the DNA-binding transcriptional activator factor Cyclops (Yano et al., 2008; Singh et al., 2014). *cyclops* mutants are impaired in both bacterial and fungal infection but retain the capacity to develop empty nodule primordia upon rhizobia inoculation (Yano et al., 2008). Interestingly, strong expression of *SymRK* or CCaMK^{T265D} in *cyclops* mutants induces the formation of spontaneous nodules, revealing genetic redundancy in the nodule organogenesis pathway at the hierarchical level of *Cyclops* (Yano et al., 2008; Ried et al., 2014). Using mass spectrometry, Singh et al. (Singh et al., 2014) identified five phosphorylated serines of which two (Cyclops S50 and S154) appeared to be essential for fungal and rhizobial infection. Additionally, phosphomimetic replacement of S50 and S154 by aspartic acid (Cyclops^{DD}) triggers spontaneous nodules

formation in *ccamk* mutants and wild-type roots (Singh et al., 2014) and stimulates the formation of LRs in wild-type roots (Martina Katharina Ried, unpublished data).

Cyclops binds and transactivates the promoters of *Nodule Inception (NIN)* and an APETALA2/Ethylene Responsive Factor (AP2/ERF) *ERF Required for Nodulation 1 (ERN1)* in a phosphorylation dependent manner (Singh et al., 2014; Cerri et al., 2017). Both genes encode transcription factors that are essential for rhizobia infection, and *NIN* also controls nodule organogenesis (Cerri et al., 2017; Schauser et al., 1999).

4.3.2.3. Nodule inception, a central regulatory hub

Nodule inception (NIN) was the first gene identified for its role in nodulation (Schauser et al., 1999). *NIN* encodes an RWP-RK domain containing transcription factor and is the founding member of NIN-like proteins (NLPs), a protein family present in all land plants (Chardin et al., 2014). Phylogenetic analyses identified *NLP1* as the closest relative of *NIN* and it was hypothesised that these two subgroups result from a duplication event that occurred at the base of the eudicots (Clavijo et al., 2015; Liu and Bisseling, 2020; Soyano and Hayashi, 2014). *NIN* is structurally similar to NLP proteins that were described to contain three major domains, the nitrate responsive domain (NRD), RWP-RK domain and Phox and Bem1 (PB1) domain (Schauser et al., 2005). The C-terminal region of *NIN* and NLPs is highly conserved and contains the RWP-RK domain which mediates DNA-binding and the PB1 domain which mediates protein-protein interactions (Korasick et al., 2015). The main difference between these two classes of proteins resides in their N-terminal region that contain the NRD. *NIN* carries deletions in its NRD and this was attributed to its lack of nitrate responsiveness. In the presence of nitrate, NLPs move from the cytosol to the nucleus and bind conserved nitrate-responsive *cis*-regulatory elements (*NREs*) to activate the transcription of nitrate-induced genes (Konishi and Yanagisawa, 2013; Marchive et al., 2013; Nishida et al., 2018). By contrast, *NIN* localises to the nucleus and activates transcription of its target genes regardless of the concentration of nitrate (Suzuki et al., 2013). It has been hypothesised that the loss of nitrate responsiveness of *NIN* is one of the key steps that enabled the emergence of the RNS (Suzuki et al., 2013; Soyano and Hayashi, 2014).

NIN is positioned downstream of NF-signalling and plays an essential role in bacterial infection and nodule organogenesis (Schauser et al., 1999). *nin* loss-of-function mutants are characterised by extensive root hair curling and swelling upon NF perception, but infection chamber inside curled root hairs and IT development as well as nodule organogenesis are completely blocked (Fournier et al., 2015; Schauser et al., 1999). Although *NIN* is only known to have RNS-specific functions, many non-nodulating species outside of the FaFaCuRo clade have maintained a *NIN* orthologue in their genome, therefore suggesting that *NIN* has a yet unidentified non-symbiotic function in these species (Griesmann et al., 2018; Clavijo et al., 2015; Liu and Bisseling, 2020).

An increase in the abundance of *NIN* transcripts can be detected as early as 2 hours following NF application which makes *NIN* one of the earliest induced gene during RNS (Schauser et al., 1999). *NIN* regulates the expression of several infection-related genes by direct binding to their promoter: *Nodulation Pectate Lyase (NPL)* encoding a pectate lyase (Xie et al., 2012); *EPR3* encoding a LysM type exopolysaccharide receptor (Kawaharada et al., 2015, 2017); *Rhizobial Infection Receptor-like Kinase 1 (RINRK1)* encoding an atypical leucine-rich repeat receptor-like kinase (Li et al., 2019); *SCAR-Nodulation (SCARN)* encoding a Suppressor of cAMP Receptor defect (SCAR) protein (Qiu et al., 2015); *Early Nodulin 11 (ENOD11)* encoding a putative repetitive proline-rich cell wall protein (Journet et al., 2001; Vernié et al., 2015), *Cytokinin Response 1 (CRE1)* encoding a cytokinin receptor (Vernié et al., 2015) as well as *Rhizobia-directed Polar Growth (RPG)* encoding a coil-coiled protein (Liu et al., 2019b; Soyano et al., 2014; Arrighi et al., 2008). All these genes were found to be either essential or at least involved in the development of ITs, with the exception of *ENOD11* for which its symbiotic function has not been characterized yet. A recent study transcriptionally profiled the *M. truncatula nin-1* mutant in root hairs during the early stages of rhizobia infection and revealed *NIN* as a central hub in gene regulatory networks directing rhizobial infection (Liu et al., 2019b). Gene network analysis and a comparison to Chromatin Immunoprecipitation Sequencing (ChIP-seq) data from an earlier study (Soyano et al., 2014) suggested that at least 100 genes might be directly regulated by *NIN* (Liu et al., 2019b).

NIN plays an essential role in nodule organogenesis and strong ectopic expression of *NIN* induces the formation of enlarged bumps in the absence of a symbiont (Soyano et al., 2013; Dong et al., 2021). *NIN* binds and transactivates the promoters of two genes that encode subunits of the heteromeric CCAAT-box-binding Nuclear Factor Y (NF-Y) protein complex, *NF-YA1* and *NF-YB1*, which are believed to regulate the expression of cell cycle genes in plants (Caretta et al., 2003; Soyano et al., 2013). In *L. japonicus*, *M. truncatula* and *Parasponia andersonii*, *nf-ya1* mutants are characterised by the formation of small nodules and/or reduced nodule number (Comber et al., 2008; Bu et al., 2020; Soyano et al., 2019). Moreover, *NF-Y* genes were reported to be involved in the bacterial infection process in *M. truncatula* and *P. andersonii* (Laporte et al., 2014; Bu et al., 2020), which is consistent with the entry of root hair cells into the cell cycle upon NF application and rhizobial inoculation (Breakspear et al., 2014). *NIN* directly regulates the expression of *Asymmetric Leaves 2-like 18a/Lateral organ Boundaries Domain 16a (ASL18a/LBD16)* (Soyano et al., 2019), a gene required for LR development in non-legumes plants (Goh et al., 2012, 2019). *asl18a/lbd16* mutants are characterized by a low LR density and a reduction of nodule number and size under high nitrate concentrations suggesting that this gene is involved in nodule growth (Soyano et al., 2019; Schiessl et al., 2019). Interestingly, *ASL18a/LBD16* directly interacts with both *NF-YA1* and *NF-YB1* and the ectopic expression of *NF-YA1/NF-YB1* together with *ASL18a* increases by six-fold LR densities and induced bump formation in *L. japonicus* wild-type and in the *Ljnin-9* mutant (Soyano et al., 2019). Additionally, Dong et al. (Dong et al., 2021) reported that the SHORTROOT-SCARECROW (SHR-SCR) module regulates cortical cell

division during nodule organogenesis and *NIN*, *LBD16* and *SHR-SCR* appear to regulate each other in a positive feedback loop. Cytokinin plays an essential role in nodule organogenesis and this can be exemplified with the *L. japonicus snf2* mutant which carries a gain-of-function mutation in the cytokinin receptor *Lotus Histidine Kinase 1 (LHK1)* and develops spontaneous nodules (Tirichine et al., 2007). Application of cytokinin on roots is sufficient to induce *NIN* expression and leads to the formation structure resembling nodules (Heckmann et al., 2011). Moreover, Vernié et al. (Vernié et al., 2015) reported that *NIN* binds to the promoter of the *M. truncatula LHK1* orthologue *Cytokinin Response 1 (MtCRE1)* and activates *CRE1* expression in the cortex.

The role of *NIN* extends beyond the two aforementioned processes. *NIN* plays dual roles in the regulation of nodule numbers. On one hand, *NIN* directly binds to the promoters of the genes encoding peptides *Clavata3/embryo surrounding region-related (CLE) CLE-RS1* and *CLE-RS2* and activates their transcription, leading to the activation of the AON pathway that restricts the number of nodules (Soyano et al., 2014; Chaulagain and Frugoli, 2021). On the other hand, *NIN* directly regulates the expression of C-terminally encoded peptides (CEPs) that function antagonistically to CLE peptides in the root and promote nodulation (Laffont et al., 2020). Furthermore, *NIN* was reported to be involved in symbiosome formation (Liu et al., 2021; Feng et al., 2021), maturation of nodules to a nitrogen-fixing state (Feng et al., 2021), nutrient uptake (Liu et al., 2019b) and defence responses (Liu et al., 2019b).

The fine-tuned spatiotemporal regulation of *NIN* expression is crucial for RNS development and was found to be highly complex. Several transcription factors that have been reported to bind to the *NIN* promoter to direct *NIN* expression (Hirsch et al., 2009; Xiao et al., 2020; Singh et al., 2014; Zhu et al., 2008). The GRAS-type transcription regulator Nodulation Signalling Pathway 1 (*NSP1*) forms a complex with *NSP2* and was the first protein to be reported to bind to the *NIN* promoter through a AATTT *cis*-element and potentially modulate its expression (Hirsch et al., 2009). *nsp1* and *nsp2* mutants are impaired in rhizobial infection and nodule formation but retain the ability to initiate calcium spiking. Both *NSPs* are genetically positioned downstream of *CCaMK* and *LHK1* and are required for *NIN* induction upon rhizobia inoculation (Wais et al., 2000; Catoira et al., 2000; Oldroyd and Long, 2003; Kaló et al., 2005; Gleason et al., 2006; Hayashi et al., 2010; Madsen et al., 2010; Mitra et al., 2004; Smit et al., 2005; Hirsch et al., 2009; Heckmann et al., 2006; Limpens and Bisseling, 2014). *IPN2* (Interacting Protein of *NSP2*), a MYB coiled-coil type transcription factor belonging to the GARP protein family, was also reported to bind and transactivate the *NIN* promoter through a 31 bp *cis*-element called *IPN2-RE* (Kang et al., 2013; Xiao et al., 2020). *IPN2* is required for *NIN* induction upon rhizobial inoculation and the *L. japonicus ipn2-1* mutant is severely impaired in rhizobia infection and nodule formation and displays defective phloem cells in the vascular tissue (Xiao et al., 2020). Interestingly, co-transformation of *Nicotiana benthamiana* leaves with constructs expressing *NSP1* and *NSP2* together with *IPN2* enhances the transactivation of the *NIN* promoter mediated by *IPN2*. Xiao et al. proposed a model where *IPN2*, *NSP1*, and *NSP2* form a

trimeric complex involved in the transcriptional regulation of *NIN*. Cyclops directly regulates the expression of the *NIN* promoter through binding to a *cis*-regulatory element called *CYC-RE* (Singh et al., 2014). *CYC-RE* encompasses a palindromic sequence, referred to as *CYC-box*, and was reported to be essential for *NIN* expression in the epidermis (Liu et al., 2019c). Furthermore, Cyclops and NSP2 interact with the GRAS domain protein DELLA and it was recently hypothesised that DELLA might bridge the NSP1/NPS2 and CCaMK/Cyclops complexes which may act in concert to regulate the expression of the *NIN* promoter (Jin et al., 2016; Pimprikar et al., 2016). In *M. truncatula*, a remote upstream *cis*-regulatory region encompassing several putative cytokinin response elements (called *CE*) was recently reported to be essential for *NIN* expression in pericycle cells to initiate nodule organogenesis (Liu et al., 2019c). *CE* is necessary for cytokinin-induced *NIN* expression and both *CE* and the 5 kb proximal promoter of the *NIN* gene are necessary to rescue bacterial infection and nodule development in the *Mtnin-1* mutant (Liu et al., 2019c).

NIN is also regulated at the protein level. A recent study revealed that proteolytic processing of *NIN* controls the transition of nodules to a nitrogen-fixing state (Feng et al., 2021). *NIN* processing is mediated by a signal peptidase complex and results in a carboxyl-terminal *NIN* fragment containing the RWP-RK domain, which activates a suite of genes associated with symbiosome development and nitrogen fixation (Feng et al., 2021).

4.4. Recruitment of gene regulatory networks during the evolution of the nitrogen-fixing root nodule symbiosis

RNS is a complex trait that requires a large network of genetic regulators. Understanding how this trait evolved might provide keys to engineer it in crops and has been subject to extensive research over the last decades. Complex traits can arise by altering existing mechanisms via gains or losses of *cis*- and *trans*-regulatory elements leading to the co-option of ancestral genes or from evolution of completely new genes. To explore the evolutionary origin of RNS, a genome-wide comparative phylogenomic analysis has recently been performed (Griesmann et al., 2018). Using a total of 37 plant species, this analysis did not detect gene gains specific to the FaFaCuRo clade and the authors suggested that the putative predisposition event postulated by Soltis et al. (Soltis et al., 1995) did not involve the acquisition of novel genes but rather the co-option of pre-existing genes and their corresponding pathways. This hypothesis was previously put forward by Soyano and Hayashi (Soyano and Hayashi, 2014) and is further supported by the common requirement of genes for RNS and more ancient developmental programs, such as AM or LR development (Kistner and Parniske, 2002; Kistner et al., 2005; Soyano et al., 2019; Schiessl et al., 2019).

4.4.1. Recruitment of AM genes for intracellular uptake of bacteria

The hypothesis that pre-existing AM genes were recruited during the evolution of nodulation was inspired by the discovery of a set of genes required for the establishment of both AM and RNS (Kistner and Parniske, 2002). These genes are referred to as “common symbiosis genes” and their products are involved in symbiont signal perception (SymRK, HMGR1), generation of calcium spiking within the nucleus (Castor, Pollux, NUP85, NUP133, Nena, CNGC15a,b,c and MCA8), symbiotic signal transduction (CCaMK and Cyclops) (Figure 1) and cellular processes such as vesicle transport (VAMP72s, Vapyrin and SYP132) (Kistner and Parniske, 2002; Kistner et al., 2005; Venkateshwaran et al., 2015; Capoen et al., 2011; Charpentier et al., 2016; Ivanov et al., 2012; Murray et al., 2011; Pumplin et al., 2010; Catalano et al., 2007; Huisman et al., 2016; Pan et al., 2016).

With the exception of SymRK, common symbiosis genes are structurally conserved between dicot and monocot angiosperms, such as *L. japonicus* and rice (*Oryza sativa*) (reviewed in (Markmann and Parniske, 2009)). *Castor*, *Cyclops* and *CCaMK* are indispensable for AM development in rice and can fully restore both AM and RNS in respective mutants of legume plants (Banba et al., 2008; Yano et al., 2008; Chen et al., 2007, 2008a; Godfroy et al., 2006). Moreover, it was recently reported that *CCaMK* and *Cyclops* from the phylogenetically distant AM-forming liverwort *Marchantia paleacea* can rescue RNS in the respective *M. truncatula* mutants (Radhakrishnan et al., 2020). These common symbiosis proteins from non-nodulating and distant lineages can thus support RNS without sequence adaptation. Conversely, SymRK might constitute the entry point to the common program between AM and RNS and displays variations in gene structure and domain composition across angiosperm lineages (Markmann et al., 2008). *SymRK* genes from rice or different dicots can restore AM but not RNS in the *L. japonicus symrk-10* mutant (Markmann et al., 2008). Only the longest and rosid-specific version of SymRK can fully support both AM and RNS and it was hypothesised that this sequence adaptation was a crucial step in mediating the recruitment of the AM program for intracellular uptake of bacteria (Gherbi et al., 2008; Markmann et al., 2008; Markmann and Parniske, 2009).

The recruitment of the AM program for bacterial uptake is further underpinned by similarities in intracellular accommodation structures for AM fungi and N-fixing bacteria (Parniske, 2000). AM fungal and bacterial infections are preceded by the formation of PPA and PIT, respectively, that dictate the path of symbiont progression (Van Brussel et al., 1992; Genre et al., 2005). These cytological structures are both associated with transcellular nuclear migration as well as rearrangements of the cytoskeleton and organelles (Timmers et al., 1999; Genre et al., 2005; Fournier et al., 2008; Yokota et al., 2009). Common symbiosis gene mutants are impaired in intracellular fungal and bacterial infections thus strengthening the hypothesis that the ability to host bacteria inside living plant cells evolved by AM gene recruitment (Markmann and Parniske, 2009). At later stages, several proteins of the exocytotic pathway were reported to be necessary for the formation of the symbiotic membrane interface that surrounds the symbiont in both interactions, suggesting that this ancient exocytotic pathway forming the peri-arbuscular membrane compartment

was also co-opted during the evolution of RNS (Liu et al., 2019a; Harrison and Ivanov, 2017). Nonetheless, the mechanisms by which the AM program was co-opted remain so far elusive.

4.4.2. Recruitment of the lateral root developmental program for nodule organogenesis

The recruitment of the LR developmental program for nodule organogenesis during the evolution of RNS is a long-standing hypothesis that builds on the similarities in anatomy between actinorhiza nodules and LRs, both characterised by a pericycle-derived central vasculature and the presence of an apical meristematic region (Hirsch and Larue, 1997; Pawlowski and Demchenko, 2012). Recently, detailed fate maps of LRs and indeterminate nodules formed on *M. truncatula* roots have revealed that both organs originate from the same root cell layers (Herrbach et al., 2014; Xiao et al., 2014; Shen et al., 2020; Xiao et al., 2019). Furthermore, it was observed that early abortion of rhizobial infection in the root hair leads to the development of abnormal nodules featuring a central vasculature in *M. truncatula* and *Phaseolus vulgaris* (Ferraioli et al., 2004; Guan et al., 2013) and mutation of *MtNOOT1* results in abnormal root development that emerge from the meristematic region of the nodules (Couzigou et al., 2012; Magne et al., 2018).

Beside these anatomical similarities, the co-option of the LR developmental program is further supported by the discovery of genetic components functioning in both LR and nodule development such as *Hypernodulation Aberrant Root Formation 1 (HAR1)* that encodes a leucine-rich repeat containing receptor kinase involved in the AON pathway (Wopereis et al., 2000) and *LATD* (Bright et al., 2005). Moreover, downregulation of *MtCRE1* significantly increases LR density and negatively impacts nodule formation (Gonzalez-Rizzo et al., 2006).

Very recently, Soyano et al. reported the first molecular genetic evidence linking nodule development with LR development (Soyano et al., 2019). The authors identified a NIN binding site in the intron of *ASL18a/LBD16*, a gene that encodes a key transcription factor involved in LR initiation in *Arabidopsis thaliana* (Goh et al., 2012, 2019). Similar to *A. thaliana* loss of function mutants, leguminous *asl18a/lbd16* mutants exhibit fewer LRs and are additionally impaired in nodule growth under high nitrate concentrations. NIN positively regulates the expression of *ASL18a/LBD16* (Soyano et al., 2019) and RNA sequencing in *M. truncatula* roots revealed that 95% of the genes whose expression is influenced by NIN during nodule initiation overlap with the differentially expressed genes in the *lbd16* mutant, thereby indicating that LRs and nodules share overlapping developmental programs (Schiessl et al., 2019). Further supporting this notion, strong ectopic expression of *ASL18a* together with its interacting partners *NF-YA1* and *NF-YB1* lead to the formation of infected nodules in the *L. japonicus daphne* mutant, which has lost the CE region within the NIN promoter due to chromosome translocation and is completely impaired in nodule organogenesis but retains the capacity to form ITs (Soyano et al., 2019; Yoro et al., 2014).

Importantly, the intronic *NIN*-targeting *cis*-element is highly conserved in legumes (Fabales) but is absent from other lineages (Soyano et al., 2019). Together with the fact that the *CE* region is restricted to legume species (Liu and Bisseling, 2020) and the observation that legumes and actinorhizal plants differ in their responses to cytokinin treatment (Gauthier-Coles et al., 2019), these findings indicate that legumes and actinorhizal plants have developed distinct mechanisms to regulate nodule organogenesis.

4.4.3. The role of *NIN* in the evolution of nodulation

The co-option of several pre-existing AM genes - the common symbiosis genes - is thought to have been a crucial step during the evolution of RNS and it was hypothesised that the genetic basis for this recruitment might be identical to the enigmatic predisposition event at the base of the FaFaCuRo clade (Kistner and Parniske, 2002; Markmann and Parniske, 2009; Soyano and Hayashi, 2014). Up to date, the mechanism that enabled the co-option of this set of genes for RNS remains elusive. Common symbiosis genes are structurally conserved between species from the FaFaCuRo clade and other angiosperm lineages suggesting that their protein products did not undergo changes that enabled their role in RNS, they are therefore not candidate genes associated with the predisposition (reviewed in (Markmann and Parniske, 2009)). The sequence divergence observed in *SymRK* was postulated to be a critical step in mediating the recruitment of the AM genetic program, however, this sequence adaptation extends beyond the FaFaCuRo clade and it was reported that *SymRK* from the Brassicales *Tropaeolum majus* can restore RNS in the *L. japonicus symrk-10* mutant, indicating that this evolutionary step precedes the origin of nodulation (Markmann et al., 2008).

In an inspiring opinion article, Soyano and Hayashi (Soyano and Hayashi, 2014) hypothesised that the co-option of the common symbiosis genes was achieved through the recruitment of *NIN* in the common ancestor of the FaFaCuRo clade. The authors proposed that gain of *cis*-regulatory elements in the *NIN* promoter enabled its regulation by the common symbiosis genes, a model supported by the finding that the transcription factor Cyclops binds to and transcriptionally activates the *L. japonicus NIN* promoter (Singh et al., 2014) and by the hierarchical position of *NIN* within the RNS-specific transcriptional network (Soyano and Hayashi, 2014; Liu et al., 2019b). The regulation of *NIN* by the common symbiosis genes, in combination with the loss of the nitrate responsive domain (NRD) in *NIN* (Suzuki et al., 2013), and the subsequent gain of *cis*-regulatory elements bound by *NIN* in the promoters of downstream genes such as *ASL18a/LBD16*, *NF-Y* and *NPL* (Soyano et al., 2013, 2019; Xie et al., 2012) was highlighted by the authors as key steps that enabled the evolution of RNS (Soyano and Hayashi, 2014).

5. Aim of the thesis

RNS is a complex trait which is believed to have evolved by co-opting genes from the ancient AM and LR developmental programs. *Nodule Inception (NIN)* encodes a transcription factor that plays an essential role in two processes during the establishment of RNS, namely bacterial infection and nodule organogenesis. The fine-tuned spatiotemporal regulation of *NIN* expression is crucial for RNS development and it is controlled, at least partially, by a cohort of transcription factors that have been reported to bind to its promoter, including the CCaMK/Cyclops complex (Singh et al., 2014). *NIN* and *ERN1* have been positioned at the top hierarchical level of the RNS-specific transcriptional network (Liu et al., 2019b), and it was previously hypothesised that gain of a *cis*-regulatory element within the *NIN* promoter enabled the recruitment of genes that evolved in the context of AM – the common symbiosis genes – for RNS development (Soyano and Hayashi, 2014). However, genetic evidences for this hypothesis were still missing. Using a phylogenomic approach, a *cis*-regulatory element (*PACE*) was discovered to be conserved and exclusively present in the *NIN* promoter of FaFaCuRo member species, thus carrying the hallmarks of a possible critical genetic acquisition by the last common ancestor of the FaFaCuRo clade (analysis performed by Maximilian Griesmann, Figure 2).

One goal of this thesis was to access the **role of *PACE* in the establishment of RNS**. Using the model legume *L. japonicus* in combination with its compatible nitrogen-fixing bacterium *Mesorhizobium loti* as experimental system, we I) studied the impact of *PACE* on the expression of *NIN* utilising promoter:reporter fusion constructs; II) tested the relevance and specific role of *PACE* in nodule and IT development by transgenic complementation using *nin* mutant alleles; and III) examined the functional conservation of *PACE* sequences from different FaFaCuRo species.

Symbiosis signalling and LR development were previously found to be tightly interconnected (Martina Katharina Ried, unpublished data; see section 4.3.2.2) and AM colonization as well as treatment with symbiotic LCO molecules were reported to induce LR formation in several species belonging to phylogenetically distant lineages (Maillet et al., 2011; Oláh et al., 2005; Mukherjee and Ané, 2011; Gutjahr et al., 2009a; Sun et al., 2015). The second goal of this thesis was **to gain insight into the molecular players that connect these two distinct signalling programs**. To address this issue, we I) took advantage of deregulated versions of common symbiosis genes that spontaneously activate symbiosis signalling to dissect their roles in the formation of LRs in *L. japonicus* and the two Rosaceae *Dryas drummondii* and *Fragaria vesca* (experimental setup established by Martina Katharina Ried; see Figure 14); II) access the role of these genes and of *NIN* in the induction of LRs mediated by bacterial or fungal microsymbiont.

Aim of the thesis

6. Results

6.1. Acquisition of a *cis*-regulatory element in the *NIN* promoter enabled bacterial uptake by plant cells

6.1.1. Discovery of *PACE*

We asked which evolutionary acquisitions by the last common ancestor, in the form of novel traits and the underlying genetic causes, enabled the evolution of the RNS. From a phylogenetic perspective, such acquisitions should be: 1) exclusively present in the FaFaCuRo clade and absent outside of this clade and 2) conserved throughout the FaFaCuRo clade or at least maintained in RNS-competent (hereafter called “nodulating”) species. A systematic comparison of features associated with the RNS across the entire FaFaCuRo clade pinpoints a single unique and shared trait – the uptake of bacteria into living plant cells with intracellular physical support structures – that fulfils both abovementioned criteria to be acquired by the common ancestor (Parniske, 2018). These structures come in a diversity of shapes (infection threads (ITs) and infection pegs) and in at least two different cell types (epidermal and cortical), but are all characterised by the apposition of matrix material which is thought to maintain cell integrity during the localised lysis of the plant cell wall, necessary for bacterial uptake. While this matrix material is a common feature of all analysed successful bacteria uptake events in FaFaCuRo species, only one type, cortical ITs, can be found in almost all nodulating species (Parniske, 2018). Cortical IT formation is an evolutionary breakthrough because it allowed clonal selection of bacteria (Gage, 2002), specific control of nutrient exchange and increased nitrogen fixation efficiency (Carvalho et al., 2014). To search for gene gains specific for the FaFaCuRo clade, a genome-wide comparative phylogenomic analysis was performed, however, not a single gene following the aforementioned evolutionary pattern was identified (Griesmann et al., 2018).

We tested the hypothesis that the “predisposition” event postulated by Soltis et al. (Soltis et al., 1995), involved gain of novel *cis*-regulatory elements. It has been shown that changes in gene regulation are important drivers of functional and morphological evolution. Emergence or loss of even a single *cis*-regulatory element can lead to dramatic phenotypic consequences, e.g. novel organ formation (Wittkopp and Kalay, 2011; Kvon et al., 2016). Phylogeny has dated the common ancestor of the FaFaCuRo clade to approximately 90 Mya (Wang et al., 2009; Bell et al., 2010; Li et al., 2015). A long standing hypothesis states that the evolution of RNS involved co-opting genes from the AM symbiosis (Parniske, 2000; Kistner and Parniske, 2002), which can be traced back to the earliest land plant fossils 450 Mya (Remy et al., 1994; Redecker et al., 2000). This hypothesis is underpinned by similarities in intracellular accommodation structures (Parniske, 2018) and the common requirement of both symbioses for a set of so-called “common symbiosis genes” (Kistner and Parniske, 2002) that are conserved across land plant species able to form AM, and encode symbiotic

signal transduction and intracellular restructuring machineries (Yano et al., 2008; Gutjahr et al., 2008; Markmann et al., 2008; Banba et al., 2008; Chen et al., 2007).

The transcription factor-encoding *Nodule Inception (NIN)* gene (Schauser et al., 1999; Soyano et al., 2013) is positioned at the top of a RNS-specific transcriptional regulatory cascade and is indispensable for RNS (Schauser et al., 1999; Singh et al., 2014; Soyano and Hayashi, 2014). The promoter of *NIN* is a potential physical target for such a co-option event, because it defines the molecular interface between common symbiotic signal transduction and the specific transcriptional networks underlying RNS development (Soyano and Hayashi, 2014). We therefore compared the *NIN* promoter sequences of 37 angiosperm species including 27 FaFaCuRo members and identified only one motif fulfilling the aforementioned criteria, which we called *Predisposition-Associated Cis-regulatory Element (PACE)* (Figure 2). The phylogenetic distribution of *PACE* was further investigated in an expanded search comprising 163 plant species in the promoter of *NIN* and the entire *NIN-like protein (NLP)* gene family, including *NLP1* from which *NIN* diverged at the base of the eudicots (Soyano and Hayashi, 2014). *PACE* was found in all nodulating FaFaCuRo members and four non-nodulating species that have lost RNS but maintained *NIN* (Jean Keller, unpublished data). Importantly, *PACE* was absent from all the *NLP* promoters analysed (Jean Keller, unpublished data). Thus, the phylogenetic distribution pattern of *PACE* is FaFaCuRo-clade specific and is consistent with a model in which *PACE* was acquired by the *NIN* promoter of the last common FaFaCuRo ancestor. Intriguingly, the 29 nucleotides-long *PACE* encompassed and extended beyond the previously identified binding site of the transcription factor Cyclops, encoded by a common symbiosis gene required for the development of both AM and RNS (Yano et al., 2008; Singh et al., 2014). Given this clade-specific distribution of *PACE*, we searched for conserved motifs in the promoter sequences of two genes encoding transcriptional regulators, *ERF Required for Nodulation 1 (ERN1)* (Cerri et al., 2017) and *Reduced Arbuscular Mycorrhiza 1 (RAM1)* (Pimprikar et al., 2016) that are also known Cyclops targets. We identified motifs within the promoters of both, *ERN1* and *RAM1*, encompassing the previously identified Cyclops binding sites (Cerri et al., 2017; Pimprikar et al., 2016). In sharp contrast to *PACE*, their presence extended beyond the FaFaCuRo clade (Jean Keller, unpublished data).

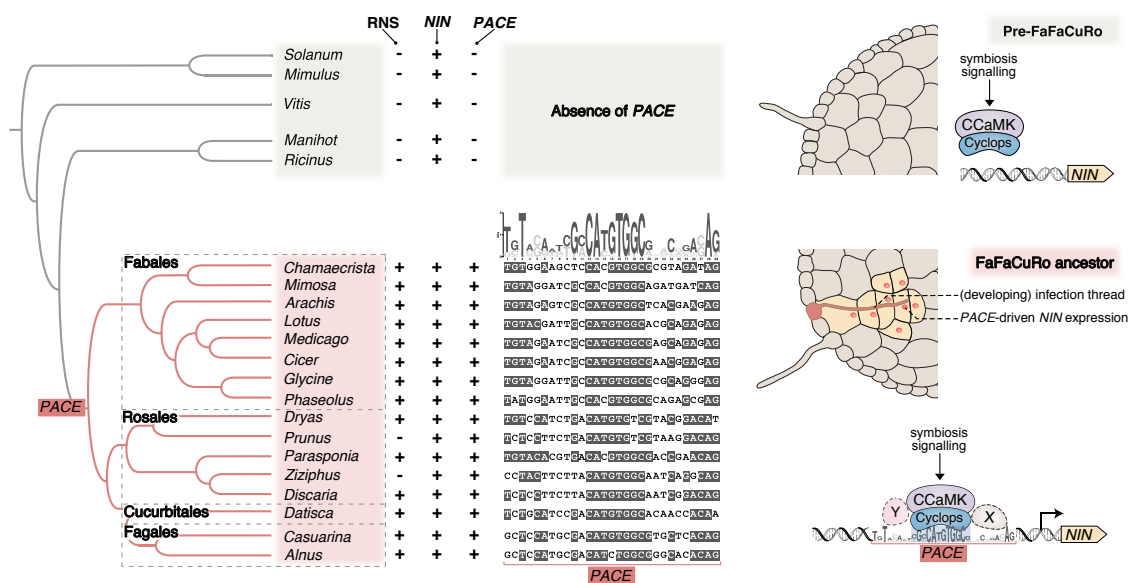


Figure 2: Acquisition of *PACE* was a key step in the evolution of RNS. **Left:** Schematic illustration of phylogenetic relationships between species inside (light red shade) and outside (light grey shade) the FaFaCuRo clade and presence (+) and absence (-) pattern of RNS, *NIN* and *PACE*. **Middle:** *PACE* sequence alignment of the displayed species in which grey shadings indicate more than 50% sequence identity. On top of the alignment the *PACE* consensus sequence depicted as Position Weight Matrix calculated from the displayed RNS-competent species. **Right:** Graphical illustration of how *PACE* connected *NIN* to symbiotic transcriptional regulation by CCaMK/Cyclops, enabling IT development in the root cortex. This acquisition coincided with the predisposition event. X and Y: hypothetical proteins binding to *PACE* outside of the Cyclops binding site. The discovery of *PACE* by MEME analyses was performed by Maximilian Griesmann. The phylogenetic tree and graphical illustration were created by Ksenia Vondenhoff and Xiaoyun Gong.

We tested the functional relevance of these distinct phylogenetic distribution patterns in transcriptional activation assays in *Nicotiana benthamiana* leaf cells. Transactivation by Cyclops was restricted to *NIN* promoters from FaFaCuRo species, but extended to non-FaFaCuRo species for *RAM1* promoters (Supplementary Figure 1). Importantly, *PACE* was necessary and sufficient for the activation of the *NIN* promoter by Cyclops (Supplementary Figure 2). Together with the exclusive occurrence of *PACE* in the *NIN* promoter of the FaFaCuRo clade, these results are in line with the hypothesis that the mechanistic link between Cyclops and the *NIN* promoter was established in the last common ancestor of this clade (Figure 2).

6.1.2. *PACE* drives the expression of *NIN* during infection thread development in the cortex

NIN is indispensable for IT development (Schauser et al., 1999; Soyano et al., 2013) and its precise spatiotemporal expression is essential for this process (Soyano et al., 2013; Vernié et al., 2015; Yoro et al., 2014; Liu et al., 2019c). Because *cis*-regulatory elements are master determinants of gene expression patterns (Buecker and Wysocka, 2012), we investigated the impact of *PACE* on the expression of *NIN* in physical relation to the bacterial uptake and accommodation stages during nodule development. We used the model legume *Lotus*

japonicus in combination with its compatible nitrogen-fixing bacterium *Mesorhizobium loti* as experimental system. The process by which *M. loti* is taken up by *L. japonicus* can be subdivided into successive stages: (1) entrapment of bacteria in a pocket formed by a curled root hair (Perrine-Walker et al., 2014), (2) development of an IT within that root hair (Perrine-Walker et al., 2014), (3) IT progression into and through the outer cortical cell layers (Van Spronsen et al., 2001), (4) IT branching and extension within the nodule primordium (Yoon et al., 2014) (5) release of bacteria from ITs into plant membrane-enclosed organelle-like structures called symbiosomes (Yoon et al., 2014) leading to (6) mature nodules characterised by infected cells densely packed with symbiosomes and the pink colour of leghemoglobin (Ott et al., 2005).

To determine the *PACE*-mediated spatiotemporal expression domain, we introduced a *GUS* reporter gene driven by *PACE* fused to a region comprising the *NIN* minimal promoter and the 5'UTR (Singh et al., 2014) (*PACE:NIN_{min}_{pro}:GUS*) into *L. japonicus* wild-type roots. Roots were subsequently inoculated with *M. loti* MAFF 303099 expressing *DsRed* (*M. loti DsRed*) facilitating detection of the bacteria through their fluorescence signal in root hairs and nodules. The *NIN* minimal promoter did not mediate reporter gene expression at any stage of bacterial infection (Supplementary Figure 3E). Intriguingly, the earliest detectable *GUS* activity mediated by *PACE:NIN_{min}_{pro}:GUS* was clearly restricted to a zone in the nodule primordia (panel I - II in Supplementary Figure 3D) that roughly correlated with the site of bacterial infection (indicated by a local accumulation of *DsRed* signal) and later expanded to the entire central tissue of the nodule (panel III in Supplementary Figure 3D). *PACE*-driven reporter expression was neither detected in root hairs harbouring ITs (Supplementary Figure 3G) nor in nodules in which cortical cells were filled with symbiosomes (panel IV in Supplementary Figure 3D). Importantly, *PACE*-mediated expression was distinct from that mediated by the *LjNIN* 3 kb promoter (*NIN_{pro}*) or the *NIN_{pro}* with *PACE* mutated or deleted (*NIN_{pro}::mPACE* and *NIN_{pro}::ΔPACE*, respectively) that conferred reporter expression across the central tissue of the nodule (panels II - IV in Supplementary Figure 3A - C). We concluded based on these observations that the *PACE*-mediated expression domain is temporally and spatially restricted and possibly accompanies the development of bacterial accommodation structures in the nodule.

To further resolve this relationship between *PACE* driven gene expression and bacterial accommodation at the cellular level, we compared – simultaneously in the same tissue – the progression of bacterial infection with the expression pattern mediated by *PACE* fused to the *NIN* minimal promoter (*PACE:NIN_{min}*) and by a *NIN* promoter with mutated *PACE* (*NIN_{pro}::mPACE*). A red and a yellow fluorescent protein (mCherry and YFP, respectively) targeted to the nucleus by fusion to a nuclear localization signal (NLS) were used as reporters. The resulting promoter:reporter fusions (*PACE:NIN_{min}_{pro}:NLS-mCherry* and *NIN_{pro}::mPACE:NLS-YFP*) were placed in tandem on the same T-DNA allowing a nucleus-by-nucleus comparison of their relative expression. This T-DNA construct was introduced into *L. japonicus* wild-type roots that were subsequently inoculated with *M. loti* R7A expressing the cyan fluorescent protein (CFP) to facilitate detection (Figure 3). In sections

of developing nodules, in which infection had progressed to stage 3 or 4, *PACE*-mediated *mCherry* was expressed specifically in a – hereafter called “infection zone” – comprising cortical cells that carried ITs and in some, but not all, directly adjacent cells (25 out of 29 nodules inspected; Figure 3A). Intriguingly, the expression domains marked by *mCherry* and YFP fluorescence were distinct from each other: while the *PACE*-driven *mCherry* signal was consistently marking the infection zone, the *NIN_{pro}::mPACE*-driven YFP signal was observed in cortical cells surrounding this zone (16 out of 18 nodules inspected; Figure 3A, 3C). The thin (approx. 1-2 cells thick) border between the two domains was characterised by nuclei emitting both YFP and *mCherry* signals (Figure 3A). In so-marked cells, ITs were typically not detected. The expression pattern mediated by the *NIN* promoter (containing *PACE*) was congruent with the sum of both promoter fragments (8 out of 8 nodules inspected; Figure 3B, 3C).

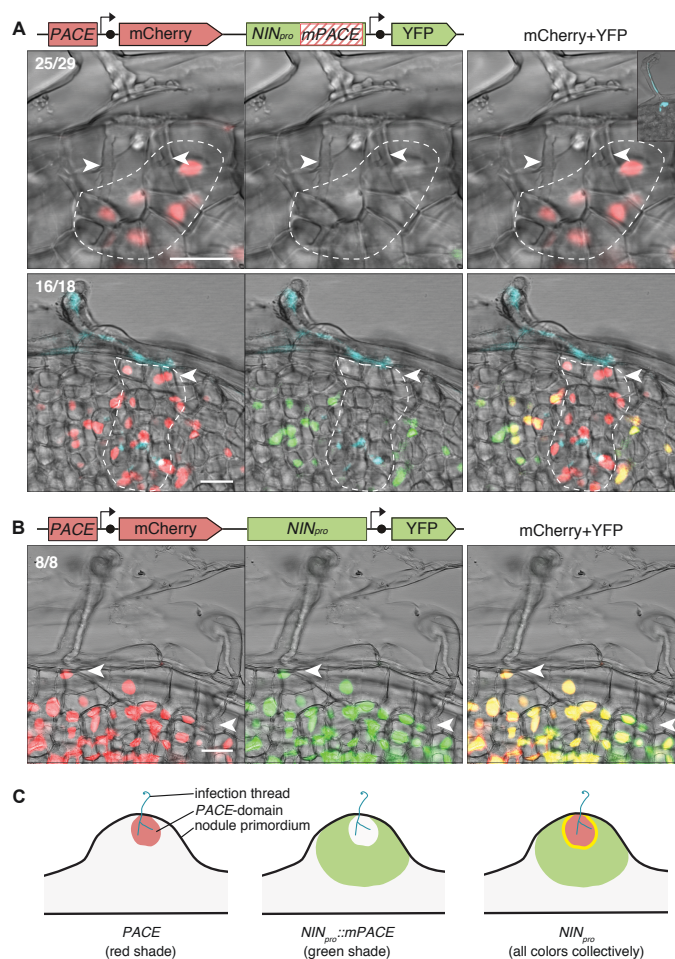


Figure 3: *PACE* drives the expression of *NIN* during IT development in the cortex. Sections of representative *L. japonicus* nodule primordia formed upon inoculation with *M. loti* R7A expressing CFP (blue) imaged by confocal laser-scanning microscopy. Comparison of the expression domains determined by (A) *PACE* (*PACE:NIN_{min}_{pro}:NLS-mCherry*; red) and a *NIN* promoter carrying a mutated *PACE* (*NIN_{pro}::mPACE:NLS-YFP*; green); or (B) *PACE* (red) and the intact *NIN* promoter (*NIN_{pro}:NLS-YFP*; green). Dashed lines demarcate a group of cortical cells in the *PACE* core territory. Arrowheads indicate ITs. Numbers: nodule primordia showing the presented expression pattern / total number of nodule primordia sectioned and inspected. Bars, 20 μ m. (C) graphical interpretation of expression patterns presented in (A and B). Yellow: overlapping region. The graphical illustration (C) was created by Xiaoyun Gong.

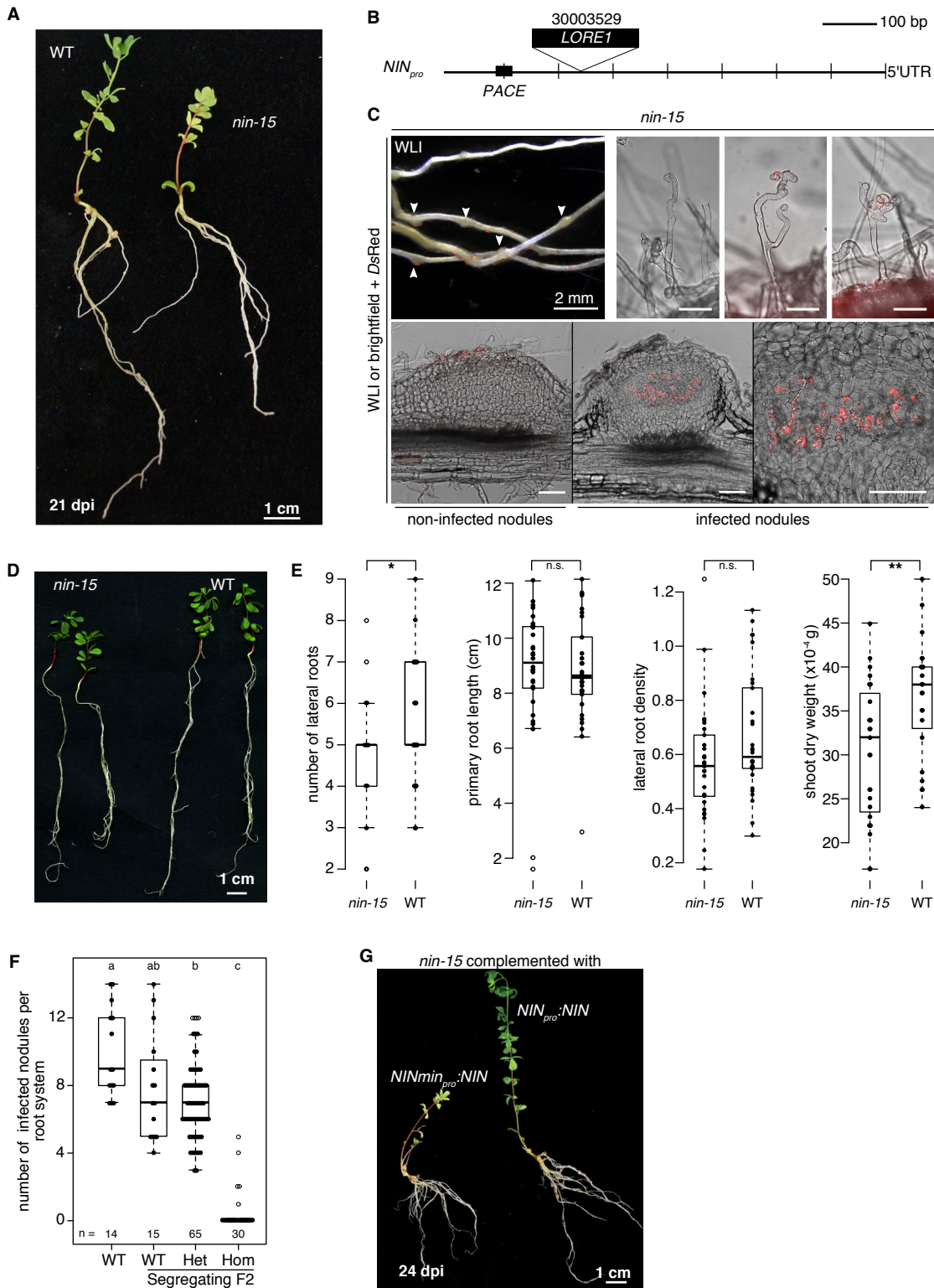


Figure 4: *L. japonicus nin-15* mutant phenotype. (A) A representative picture of *L. japonicus* wild-type (WT, left) and *nin-15* (right) plants 21 dpi with *M. loti* DsRed. (B) Position of the *Lotus Retrotransposon 1* (LORE1) insertion within the *NIN* promoter in the *nin-15* mutant. (C) Representative pictures of *nin-15* root hairs and nodule sections 21 dpi with *M. loti* DsRed. Forty-nine plants with a total number of 436 nodules were analysed: only four plants bore one or two IT(s) within root hairs and seven plants bore one or two infected nodule(s). Deformed or curled root hairs in the presence of *M. loti* DsRed were abundant but infection threads were rarely found. Arrowheads: uninfected nodules. Unlabelled bars, 100 μ m. (continuation of figure legend on the next page)

Legend Figure 4: continued

(D - E) Phenotype of *nin-15* in the presence of a symbiosis-independent nitrogen source (15 mM KNO₃) for 28 days. (D) Pictures documenting the healthy status of *L. japonicus* WT and *nin-15* plants (compare (D) and (A)) and (E) quantitative assessment of parameters displayed in boxplots. Thirty plants per genotype were analysed. Each dot represents one plant. Lateral root density: number of lateral roots/primary root length (cm). The applied statistical method was pairwise *t*-test: **p* < 0.05; ***p* < 0.01; n.s.: not significant. (F) Segregation analysis of *nin-15*. The applied statistical method was ANOVA with *post hoc* Tukey: $F_{3,120} = 84.1$, $p = 2 \times 10^{-16}$. Different small letters indicate significant difference. (G) Representative pictures of *nin-15* plants with hairy roots transformed with the *NIN* gene driven by the *L. japonicus* *NIN* minimal promoter (*NIN_{min_{pro}}*) or the 3 kb *NIN* promoter (*NIN_{pro}*) 24 dpi with *M. loti* DsRed. WLI: white light illumination. The data presented in this figure were generated by Chloé Cathebras (C, E), Rosa Elena Andrade (A, B, F, G) and Xiaoyun Gong (D, E).

Based on these clearly distinct and complementary reporter expression domains governed by *PACE* versus the remaining promoter, we concluded that 1) *PACE* directs *NIN* expression to a specific infection zone and that 2) the *NIN* promoter comprises *cis*-regulatory elements that drive expression outside the *PACE* territory i.e. in root hairs (together with *PACE*), non-infected cortical cells and cells filled with symbiosomes. These additional *cis*-regulatory elements might be addressed by other transcription factors that have been reported to bind to this promoter (Hirsch et al., 2009; Xiao et al., 2020; Singh et al., 2014; Zhu et al., 2008).

6.1.3. Mutational dissection of *PACE* reveals a quantitative impact of regions flanking the *CYC*-box on infection thread development

To test the relevance and specific role of *PACE* in nodule and IT development, we performed complementation experiments using plants homozygous for the *nin-2* or *nin-15* mutant alleles (Schauser et al., 1999). The *nin-2* mutant allele harbours a frameshift mutation of the *NIN* gene, leading to a *NIN* loss-of-function phenotype, i.e. absence of both IT formation and nodule organogenesis (Schauser et al., 1999) while the *nin-15* mutant allele carries a *Lotus Retrotransposon 1* insertion within the *NIN* promoter 143 bp 3' of *PACE* (Figure 4). We examined the restoration of bacterial infection 21 days after inoculation with *M. loti* DsRed by quantifying the number of root hairs harbouring ITs and the number of infected nodules (Figure 5).

Nodule development in the legume *Medicago truncatula* is dependent on *NIN* expression mediated by a regulatory region containing several putative cytokinin responsive elements (*CE*) (Liu et al., 2019c). In *L. japonicus*, a similar *CE* region is positioned 45 kb upstream of the *NIN* transcriptional start site (Liu et al., 2019c). To enable transgenic complementation experiments, we synthetically fused a 1 kb or 5 kb region encompassing this distant *CE* to the 5' end of a 3 kb *NIN* promoter. The *NIN* gene driven by these promoters (*CE_{1kb}:NIN_{pro}:NIN* and *CE_{5kb}:NIN_{pro}:NIN*) restored the formation of root hair ITs on 78% and 95% and infected nodules on 40% and 88% of *nin-2* transgenic root systems, respectively (Figure 5A, 6, 7 and 8; Supplementary Figure 4 and 5). Importantly, this complementation

success relied on the presence of *PACE*; *nin-2* roots transformed with the same fusion design but carrying a mutation of *PACE* ($CE_{1kb}:NIN_{pro}::mPACE:NIN$ and $CE_{5kb}:NIN_{pro}::mPACE:NIN$) did not restore root hair ITs but nodule formation was not impaired when using the cytokinin element-containing region of 5 kb ($CE_{5kb}:NIN_{pro}::mPACE:NIN$). We concluded that *PACE* is indispensable for bacterial infection but not for nodule development.

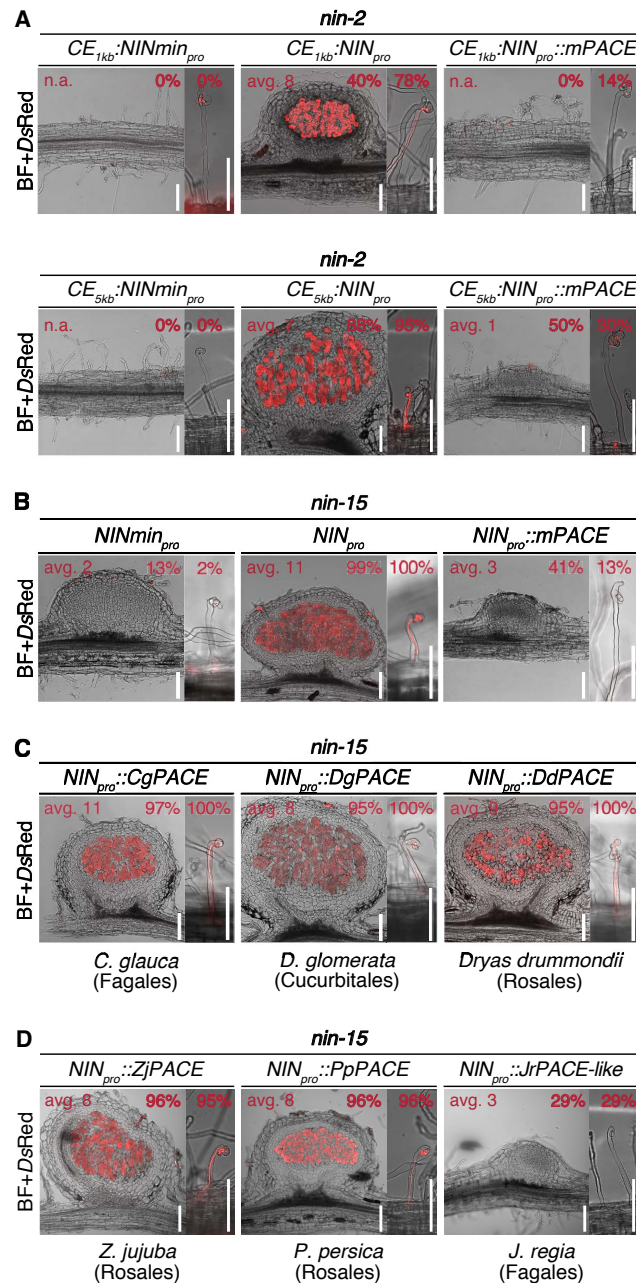


Figure 5: *PACE* is necessary for bacterial infection and functionally conserved across the FaFaCuRo clade. Microscopy images of representative nodule sections or root hairs harbouring an IT or an infection pocket from (A) *nin-2* or (B - D) *nin-15* roots transformed with the *LjNIN* gene driven by: (A - B) indicated promoters, and in (C - D) the *L. japonicus* *NIN* promoter in which *LjPACE* was replaced by *PACE* from (C) nodulating and (D) non-nodulating FaFaCuRo species or with a *PACE*-like sequence identified in the *JrNLP1b* promoter. %: percentage of transgenic root systems carrying infected nodules or root hair ITs. Avg.: average number of infected nodules on plants carrying infected nodules. n.a.: not applicable. Bars, 100 μ m. The quantification of the infection events presented in this figure were generated by Chloé Cathebras (A - D), Rosa Elena Andrade (B - D) and Xiaoyun Gong (A - D).

The 29 bp long *PACE* sequence encompasses and extends beyond the previously identified Cyclops binding site (Figure 2). To dissect the specific contributions of the Cyclops binding site (*CYC-box* (Singh et al., 2014), “box”) and *PACE* sequences flanking the *CYC-box* (“flanking”) to *PACE* function, we mutated the box and the flanking region independently (*CE:NIN_{pro}::mbox:NIN* and *CE:NIN_{pro}::mflanking:NIN*, respectively). Mutation of the *CYC-box* abolished root hair ITs. Interestingly, mutation of the flanking sequences led to a 50% reduction of the number of transgenic root systems carrying infected nodules, while the formation of root hair ITs was not impaired (Figure 6, 7 and 8; Supplementary Figure 4 and 5). This mutational dissection revealed two separable functions of *PACE*: while the *PACE*-Cyclops connection is essential for IT development, the flanking sequences are positively regulating the infection of newly developed nodules and possibly act as binding sites for additional, yet undefined, transcription factors (Figure 2). The existence of transcription factors that act synergistically with Cyclops is in line with the original *cyclops* mutant phenotype description which called for the existence of CCaMK phosphorylation targets that can partially compensate for the loss of Cyclops in nodule development but not in infection (Yano et al., 2008). Our data suggest that *PACE* comprises synergistic binding sites for both Cyclops and cooperating transcription factors.

PACE-mediated *NIN* expression defined an infection zone in the nodule cortex (Figure 3). To genetically separate the initiation of nodule development from IT formation and thereby enable a focussed analysis of the role of *PACE* in cortical IT formation, we utilised the *nin-15* mutant, which is impaired in IT formation but retains the capacity to form nodules. Most of these nodules were uninfected (92% and 86% plants carrying no root hair ITs and no infected nodules, respectively) and cortical cells filled with symbiosomes were never observed (Figure 4). This mutant therefore provided an ideal background to study the role of *PACE* in cortical IT formation, circumventing the negative epistatic effect of the inability of *nin* loss-of-function mutants to initiate cell divisions (Schauser et al., 1999; Yoro et al., 2014; Clavijo et al., 2015; Vernié et al., 2015; Liu et al., 2019c) (Figure 5B – D, 9, 10 and 11). Transformation with the *L. japonicus* *NIN* gene driven by the *NIN* minimal promoter (*NIN_{minpro}:NIN*) did not alter the symbiotic phenotype of *nin-15* roots (Figure 5B). In contrast, the *NIN* gene driven by the *NIN* promoter (*NIN_{pro}:NIN*) led to restoration of the complete infection process in *nin-15* roots from root hair ITs to symbiosome formation (100% and 92% of transgenic root systems carried root hairs ITs and infected nodules, respectively; Figure 5B). Similar to observations in complementation experiments of *nin-2*, mutation or deletion of *PACE* (*NIN_{pro}::mPACE:NIN* and *NIN_{pro}::ΔPACE:NIN*, respectively) drastically reduced the restoration of bacterial infection in root hairs and nodules in *nin-15* (Figure 3B; Figure 3 – figure supplement 2, 3, 4, 5, 6 and 7).

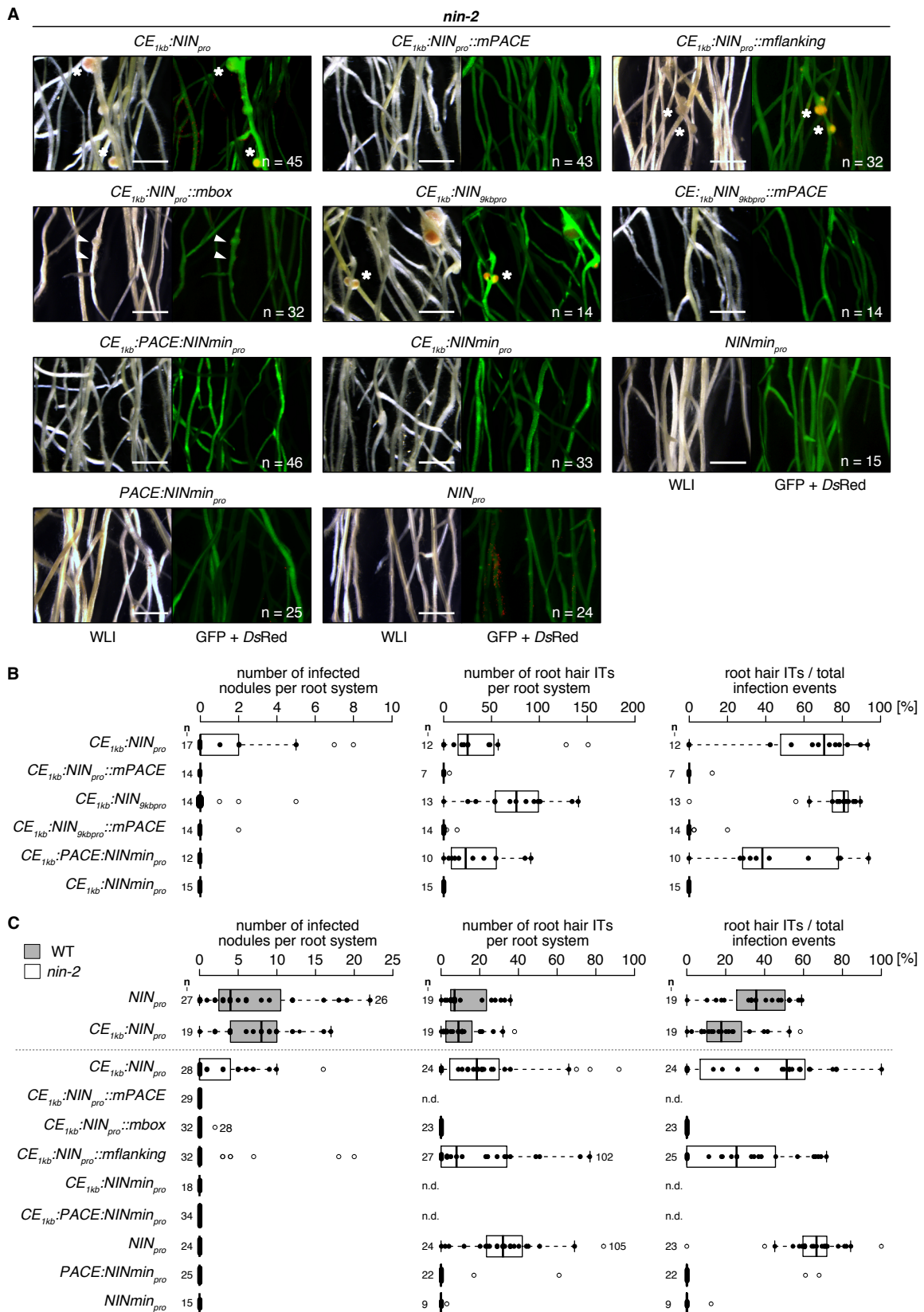


Figure 6: The *CYC*-box and flanking sequences of *PACE* are required for the full restoration of the bacterial infection process in the *L. japonicus nin-2* mutant. (continuation of figure legend on the next page)

Legend Figure 6: continued

nin-2 roots were transformed with T-DNAs carrying a *Ubq10_{pro}:NLS-GFP* transformation marker in tandem with the *LjNIN* gene driven by either of the following promoter versions: the cytokinin element-containing region of 1 kb (*CE_{1kb}*) fused to the 3 kb or 9 kb *LjNIN* promoter (*CE_{1kb}:NIN_{pro}* or *CE_{1kb}:NIN_{9kbpro}*, respectively); *CE_{1kb}:NIN_{pro}* or *CE_{1kb}:NIN_{9kbpro}* with *PACE* mutated (*CE_{1kb}:NIN_{pro}::mPACE* or *CE_{1kb}:NIN_{9kbpro}::mPACE*, respectively); *CE_{1kb}:NIN_{pro}* carrying a mutated Cyclops binding site (*CYC-box*) (*CE_{1kb}:NIN_{pro}::mbox*); *CE_{1kb}:NIN_{pro}* carrying mutated sequences flanking the *CYC-box* in *PACE* (*CE_{1kb}:NIN_{pro}::mflanking*); *CE_{1kb}* fused to the *LjNIN* minimal promoter (*CE_{1kb}:NIN_{minpro}*); *CE_{1kb}* fused to *PACE* and to *NIN_{minpro}* (*CE_{1kb}:PACE:NIN_{minpro}*); *NIN_{pro}*, *PACE:NIN_{minpro}* or *NIN_{minpro}*. (A) Representative overview pictures of transgenic root systems. Roots were analysed 21 dpi with *M. loti* DsRed. White asterisks and arrowheads: infected and non-infected nodules, respectively. Bars, 2 mm. (B - C) Boxplots displaying the number of root hair ITs or infected nodules and the percentage of root hair ITs among total infection events (sum of bacterial entrapments and ITs). Each dot represents one transgenic *nin-2* root system or root piece. *L. japonicus* WT roots transformed with *NIN_{pro}:NIN* or *CE_{1kb}:NIN_{pro}:NIN* were included as controls. Note the loss of restoration of nodules and IT formation associated with the mutation of *PACE* or only the *CYC-box* in *PACE*; and the reduction of same when sequences flanking the *CYC-box* in *PACE* were mutated. n: number of transgenic root systems or root pieces analysed. Numbers above the boxplots: the value of individual data points outside of the plotting area. n.d.: not determined. WLI: white light illumination. The data presented in this figure were generated by Chloé Cathebras and Xiaoyun Gong.

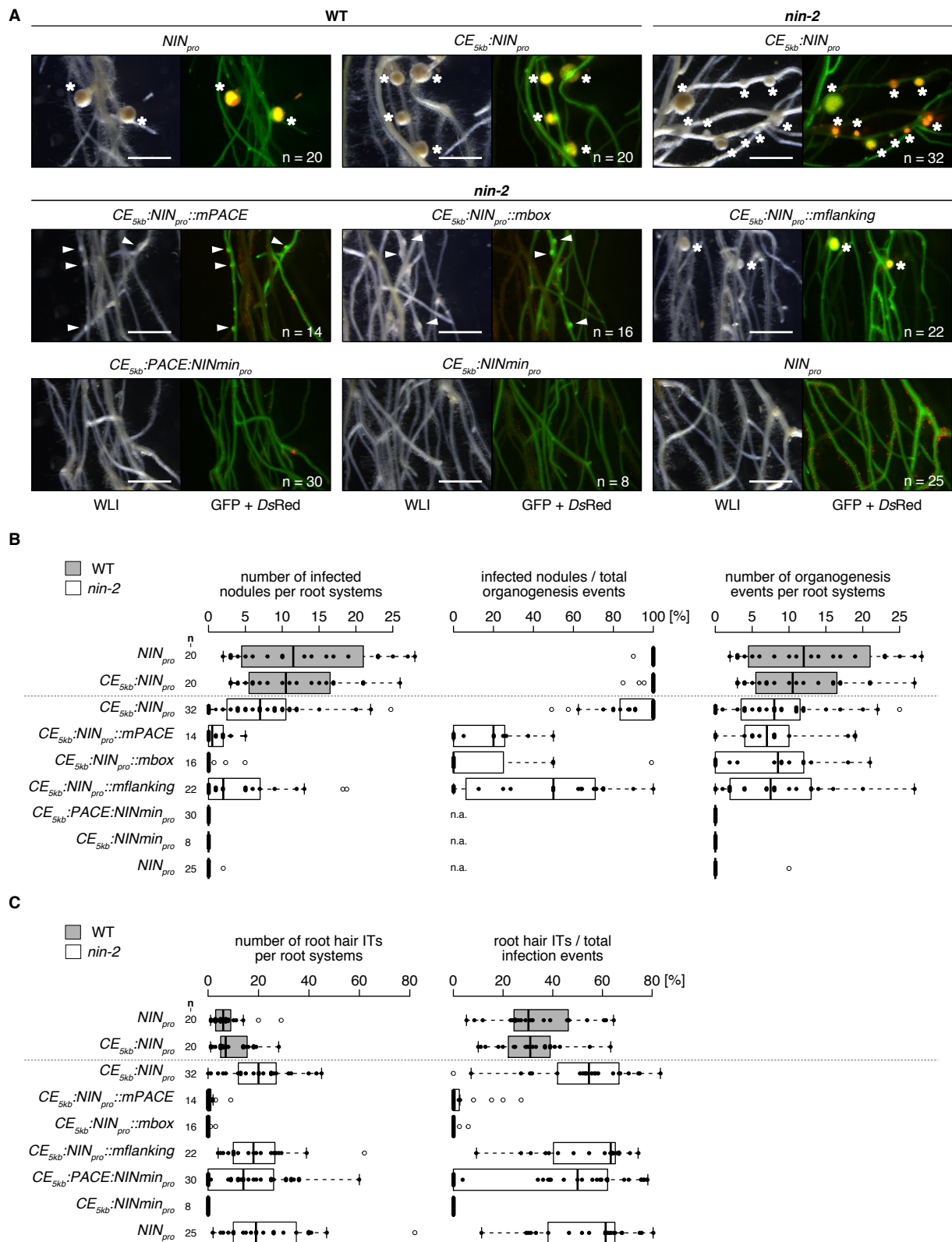


Figure 7: The *CYC*-box and flanking sequences of *PACE* are required for the full restoration of the bacterial infection process but are dispensable for the nodule organogenesis process in the *L. japonicus nin-2* mutant. (continuation of figure legend on the next page)

Legend Figure 7: continued

nin-2 roots were transformed with T-DNAs carrying a *Ubq10_{pro}:NLS-GFP* transformation marker in tandem with the *LjNIN* gene driven by either of the following promoter versions: the cytokinin element-containing region of 5 kb (*CE_{5kb}*) fused to the 3 kb *LjNIN* promoter (*CE_{5kb}:NIN_{pro}*); *CE_{5kb}:NIN_{pro}* with *PACE* mutated (*CE_{5kb}:NIN_{pro}:mPACE*); *CE_{5kb}:NIN_{pro}* carrying a mutated Cyclops binding site (*CYC-box*) (*CE_{5kb}:NIN_{pro}:mbox*); *CE_{5kb}:NIN_{pro}* carrying mutated sequences flanking the *CYC-box* in *PACE* (*CE_{5kb}:NIN_{pro}:mflanking*); *CE_{5kb}* fused to the *LjNIN* minimal promoter (*CE_{5kb}:NIN_{min_{pro}}*); *CE_{5kb}* fused to *PACE* and to *NIN_{min_{pro}}* (*CE_{5kb}:PACE:NIN_{min_{pro}}*) or *NIN_{pro}*. **(A)** Representative overview pictures of transgenic root systems. Roots were analysed 21 dpi with *M. loti* DsRed. White asterisks and arrowheads: infected and non-infected nodules, respectively. Bars, 2 mm. **(B)** Boxplots displaying the number of infected nodules, the percentage of infected nodules among total organogenesis events (sum of infected and non-infected nodules) and the number of organogenesis events. **(C)** Boxplots displaying the number of root hair ITs and the percentage of root hair ITs among total infection events (sum of bacterial entrapments and ITs). Each dot represents one transgenic *nin-2* root system or root piece. *L. japonicus* WT roots transformed with *NIN_{pro}:NIN* or *CE_{5kb}:NIN_{pro}:NIN* were included as controls. Note that the mutation of *PACE* or only the *CYC-box* in *PACE* led to an almost complete loss of IT formation and infected nodules per root system while nodule organogenesis was not significantly reduced; and that mutation of sequences flanking the *CYC-box* in *PACE* led to a reduction of the number of infected nodules per root systems. n: number of transgenic root systems or root pieces analysed. Numbers above the boxplots: the value of individual data points outside of the plotting area. n.a.: not applicable. WLI: white light illumination. The data presented in this figure were generated by Chloé Cathebras and Xiaoyun Gong.

Results

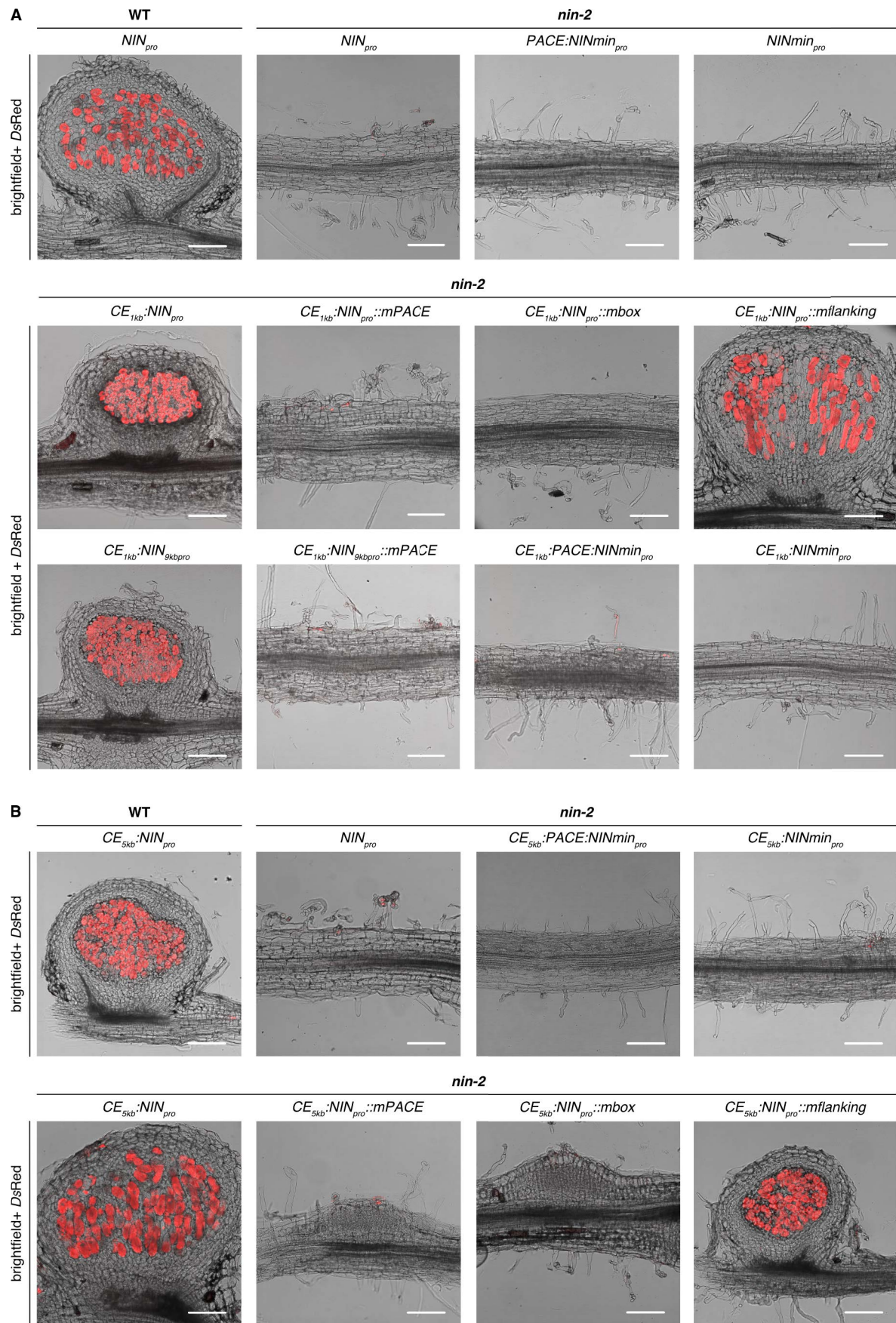


Figure 8: The *CYC-box* and flanking sequences of *PACE* are required for the full restoration of the bacterial infection process but are dispensable for the nodule organogenesis process in the *L. japonicus nin-2* mutant. (continuation of figure legend on the next page)

Legend Figure 8: continued

Pictures of nodule sections or roots from *L. japonicus nin-2* roots 21 dpi with *M. loti* DsRed from the same experiments depicted in **Figure 6 (A)** and **Figure 7 (B)**. Nodule sections from *L. japonicus* WT roots transformed with $NIN_{pro}:NIN$ and $CE_{5kb}NIN_{pro}:NIN$ were included for comparison. Note that when the cytokinin element-containing region of 1 kb was fused to NIN_{pro} nodule organogenesis was abolished by mutation of *PACE* or only the *CYC-box* in *PACE* and that these mutations did not abolish organogenesis when the cytokinin element-containing region of 5 kb was fused to NIN_{pro} . Bars, 100 μ m.

6.1.4. *PACEs* from different nodulating FaFaCuRo species are functionally equivalent

PACE was detected by MEME searches as a conserved motif within *NIN* promoters of the FaFaCuRo clade. However, the individual *PACE* sequences from different species differed from each other (Figure 2). We therefore tested whether and to what extent this sequence variation of *PACE* would affect its function. Replacement of *PACE* within the *L. japonicus* (Fabales) 3 kb *NIN* promoter with *PACE* sequence variants ($NIN_{pro}::\textit{Species abbreviation PACE:NIN}$) originating from *Casuarina glauca* (Cg, Fagales), *Datisca glomerata* (Dg, Cucurbitales) or *Dryas drummondii* (Dd, Rosales) restored the complete infection process in *nin-15* to similar level as $NIN_{pro}:NIN$, demonstrating the functional conservation of *PACE* from nodulating species across the entire FaFaCuRo clade (Figure 5C and 9). Similarly, the *PACE* versions from two non-nodulating Rosales that maintained the *NIN* gene, *Ziziphus jujuba* and *Prunus persica*, restored the complete infection process in *nin-15* (Figure 5D and 9). The results of these complementation experiments were consistent with the conserved expression pattern mediated by *PACEs* in *L. japonicus* (Supplementary Figure 6) and the CCaMK/Cyclops-mediated transactivation via these *PACE* variants (Supplementary Figure 2A) or chimeric promoter:reporter fusions (Supplementary Figure 2B) tested in *N. benthamiana* leaves.

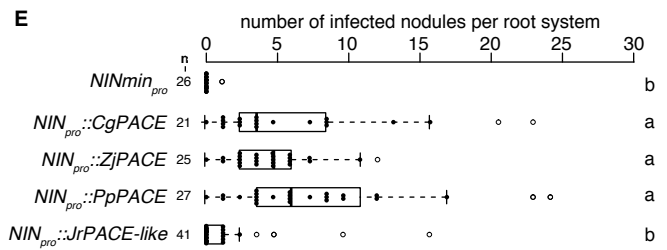
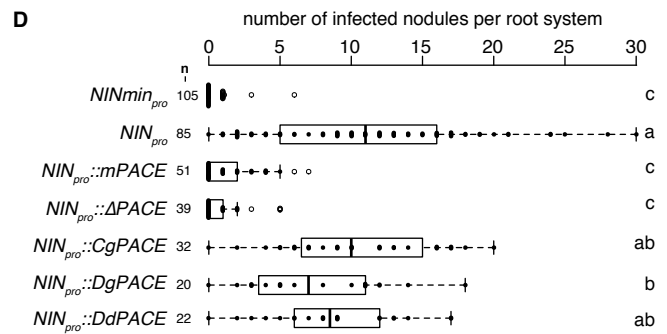
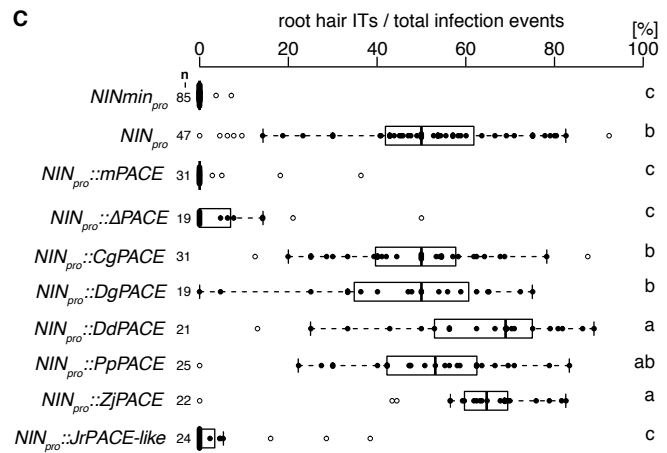
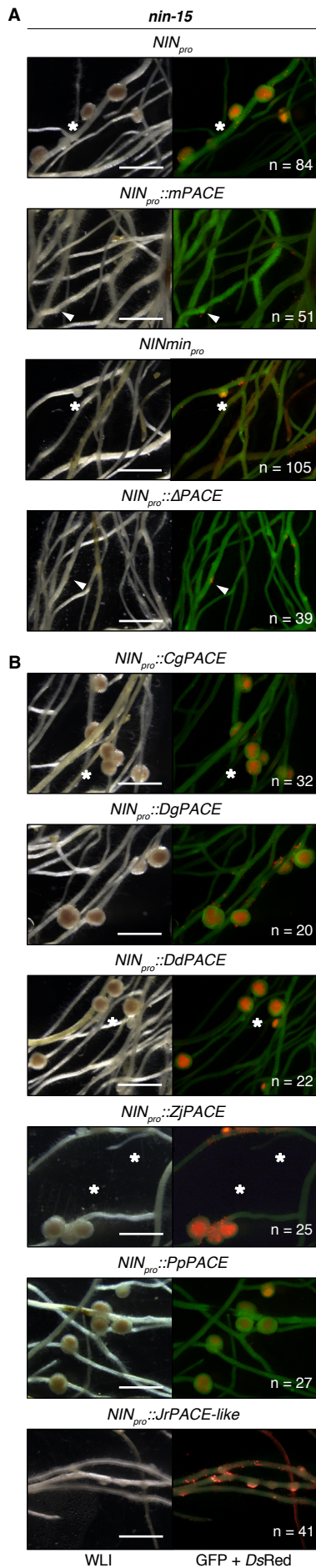


Figure 9: PACEs from FaFaCuRo species are functionally equivalent in restoring bacterial infection in the *L. japonicus nin-15* mutant. *L. japonicus nin-15* roots were transformed with T-DNAs carrying a *Ubg10_{pro}:NLS-GFP* transformation marker in tandem with the *LjNIN* gene driven by either of the following promoters: (A) the 3 kb *LjNIN* promoter (*NIN_{pro}*), the *LjNIN* minimal promoter (*NIN_{min_{pro}}*), the 3 kb *LjNIN* promoter with *PACE* deleted (*NIN_{pro}::ΔPACE*) or mutated (*NIN_{pro}::mPACE*); (B) the 3 kb *LjNIN* promoter with *LjPACE* replaced with either of the *PACE* sequence variants from nodulating or non-nodulating FaFaCuRo species and analysed 21 dpi with *M. loti* DsRed. (A - B) Representative overview pictures of *nin-15* transgenic roots systems. Sections of representative nodules are displayed in Figure 4. Note the drastic reduction of restoration of infection in nodules and root hairs associated with the mutation or deletion of *PACE* as well as the replacement of *PACE* with *JrPACE-like* in the context of the *LjNIN* promoter. White asterisks and arrowheads: infected and non-infected nodules, respectively. (C - E) Boxplots displaying *c*, the percentage of root hair ITs among total infection events (sum of bacterial entrapments and ITs) and (D - E) the number of infected nodules from two independent experiments. Each dot in (D - E) represents one *nin-15* transgenic root system. (C) displays merged data from all experiments as the percentage represents a normalised value calculated for each root piece. *n*: number of transgenic root systems or root pieces analysed. For species abbreviations see Supplementary Figure 1. The applied statistical method was ANOVA with *post hoc* Tukey: (C) $F_{9,313} = 106.7$, $p < 2 \times 10^{-16}$; (D) $F_{6,346} = 82.89$, $p < 2 \times 10^{-16}$; (E) $F_{4,135} = 20.18$, $p = 4.76 \times 10^{-13}$. Different small letters indicate significant differences. Bars, 2 mm. WLI: white light illumination. The data presented in this figure were generated by Chloé Cathebras, Rosa Elena Andrade and Xiaoyun Gong.

6.1.5. Loss of *PACE* is associated with a loss of nodulation

Griesmann et al. (Griesmann et al., 2018) and van Velzen et al. (van Velzen et al., 2018) discovered that RNS was lost multiple times independently during evolution, via independent truncations or losses of the *NIN* gene. However, at least 10 out of 28 FaFaCuRo species that lost RNS have maintained a full-length *NIN* open reading frame (Table 1). Based on our complementation data, *PACE* is indispensable for the *NIN* promoter function in symbiosis (Figure 5, 6, 7, 8, and 9; Supplementary Figure 4 and 5). Therefore, the absence of *PACE* from 5 out of these 10 species (Table 1), is potentially sufficient to explain these losses of RNS. Consequently, at least 82% of all losses can now be attributed to either the *NIN* ORF (18/28, 64%) or loss of *PACE* (5/28, 18%) (Table 1). The presence of *PACE* in all nodulating species together with a correlation between the absence of *PACE* with the absence of RNS adds strong support for the evolutionary relevance of *PACE* both in the gain and potential loss of RNS.

PACE was not detected in the promoters of *NIN-like protein* (*NLP*) genes (Jean Keller and Maximilian Griesmann, unpublished data) with the possible exception of the curious case of *Juglans regia* (Fagales). While it was also absent from the promoter of the so-annotated *NIN* gene, a *PACE*-like motif was identified in the promoter of the closest gene family member, *NIN-like protein 1 JrNLP1b* (*JrPACE-like*; Maximilian Griesmann, unpublished data). This *PACE*-like element was not able to restore IT formation in *nin-15* (Figure 5D and 9). Regardless of whether this exceptional presence/absence pattern of *PACE* may be caused by a miss-annotation of *NIN* and *NLP1* in *J. regia*, either a loss-of-function mutation within *PACE* or a loss of the entire *PACE* element in the *JrNIN* promoter could explain the absence of the RNS observed in this species.

Table 1: Status of PACE and NIN in non-nodulating FaFaCuRo species. Species highlighted in grey: non-nodulating FaFaCuRo species that possess a full length NIN open reading frame.

Species_Abbreviation	Species	Genus	Order	Family	RNS (+/-)	NIN presence	PACE presence (+/-)
Begfuc	<i>Begonia fuchsoides</i>	<i>Begonia</i>	Cucurbitales	Begoniaceae	-	Lost*	n. d.
Betpen	<i>Betula pendula</i>	<i>Betula</i>	Fagales	Fagaceae	-	+	-
Cansat	<i>Cannabis sativa</i>	<i>Cannabis</i>	Rosales	Cannabaceae	-	+	-
Carfan	<i>Carpinus fangiana</i>	<i>Carpinus</i>	Fagales	Betulaceae	-	+	-
Casaus	<i>Castanospermum australe</i>	<i>Castanospermum</i>	Fabales	Fabaceae	-	Lost*	n. d.
Casmol	<i>Castanea mollissima</i>	<i>Castanea</i>	Fabales	Fagaceae	-	+	+
Cercan	<i>Cercis canadensis</i>	<i>Cercis</i>	Fabales	Caesalpiaceae	-	Fragmented*	n. d.
Citian	<i>Citrus latifolius ssp vulgaris 97103</i>	<i>Citrus</i>	Cucurbitales	Cucurbitaceae	-	Fragmented*	n. d.
Cucsat	<i>Cucumis sativus P183967</i>	<i>Cucumis</i>	Cucurbitales	Cucurbitaceae	-	Fragmented*	n. d.
Ficere	<i>Ficus erecta</i>	<i>Ficus</i>	Rosales	Moraceae	-	+	+
Fraves	<i>Fragaria vesca</i>	<i>Fragaria</i>	Rosales	Rosaceae	-	Lost*	n. d.
Humlup	<i>Humulus lupulus</i>	<i>Humulus</i>	Rosales	Cannabaceae	-	Fragmented*	-
Jugreg	<i>Juglans regia</i>	<i>Juglans</i>	Fagales	Juglandaceae	-	+	-
Miomot	<i>Morus notabilis</i>	<i>Morus</i>	Rosales	Moraceae	-	Fragmented	-
Nissch	<i>Nissolia schottii</i>	<i>Nissolia</i>	Fabales	Fabaceae	-	Lost*	n. d.
Pruavi	<i>Prunus avium</i>	<i>Prunus</i>	Rosales	Rosaceae	-	Fragmented	+
Prudul	<i>Prunus dulcis</i>	<i>Prunus</i>	Rosales	Rosaceae	-	Fragmented	+
Prumum	<i>Prunus mume</i>	<i>Prunus</i>	Rosales	Rosaceae	-	+	+
Pruper	<i>Prunus persica</i>	<i>Prunus</i>	Rosales	Rosaceae	-	Fragmented	+
Pruyed	<i>Prunus yedoensis</i>	<i>Prunus</i>	Rosales	Rosaceae	-	Fragmented	-
Pyrcom	<i>Pyrus communis</i>	<i>Pyrus</i>	Rosales	Rosaceae	-	Lost*	n. d.
Quelob	<i>Quercus lobata</i>	<i>Quercus</i>	Fagales	Fagaceae	-	+	+
Querob	<i>Quercus robur</i>	<i>Quercus</i>	Fagales	Fagaceae	-	+	-
Rharub	<i>Rhamnella rubrinervis</i>	<i>Rhamnella</i>	Rosales	Rhamnaceae	-	Fragmented	-
Roschi	<i>Rosa chinensis</i>	<i>Rosa</i>	Rosales	Rosaceae	-	Fragmented	+
Rubocc	<i>Rubus occidentalis</i>	<i>Rubus</i>	Rosales	Rosaceae	-	Lost*	n. d.
Treori	<i>Trema orientalis</i>	<i>Trema</i>	Rosales	Cannabaceae	-	Fragmented	-
Zizluj	<i>Ziziphus jujuba cv. Dongzao</i>	<i>Ziziphus</i>	Rosales	Rhamnaceae	-	+	+

Lost* : species that lost NIN according to Griesmann et al. (2018)

Fragmented* : species that have a fragmented NIN according to Griesmann et al. (2018)

Fragmented : species that have a fragmented NIN (less than 85% identity - including absence - of the RWP domain; less than 65% identity - including absence - of the PBI domain or containing premature stop codon(s))

"+" : species that have an intact NIN open reading frame

n. d. : not determined

The data presented in this figure were generated by Maximilian Griesmann and Jean Keller.

6.1.6. *PACE* is sufficient to restore cortical infection thread formation in *nin-15*

We tested whether *PACE* on its own, only supported by the minimal *NIN* promoter (*PACE:NIN_{min_{pro}}*) is sufficient to restore IT development in cortical cells. For this purpose, we transformed *nin-15* roots with *PACE:NIN_{min_{pro}}* fused to the transcribed region of the *NIN* gene. *PACE*-mediated *NIN* expression led to an increased success in restoration of infection (49% of transgenic root systems carried infected nodules) compared to *NIN_{min_{pro}}:NIN*-transformed roots (17%; Figure 10A and 11). Root hair ITs were rarely observed on *PACE:NIN_{min_{pro}}:NIN*-transformed *nin-15* roots (Figure 10A) and infected nodules harbouring cortical cells filled with symbiosomes were never observed (Figure 11A - B), consistent with the restricted expression domain defined by *PACE* (Supplementary Figure 3).

Strikingly, the vast majority of infected nodules transformed with *PACE:NIN_{min_{pro}}:NIN* (25 out of 28 nodules inspected) carried ITs in the outer cortex, originating from a focused hyperaccumulation of bacteria, locally constricted by root cell wall boundaries (Figure 10A). This phenomenon was not observed in most of the rarely occurring infected nodules formed on *NIN_{min_{pro}}:NIN*-transformed *nin-15* roots (11 out of the 16 nodules inspected did not carry ITs in the outer cortex). Bacterial colonies within cell wall boundaries resembling this phenomenon have been described in a variety of legumes including *Sesbania* and *Mimosa* (D'Haese et al., 1998; De Faria et al., 1988). Our data imply that *PACE* promotes this type of cortical IT initiation. Altogether, these findings revealed that *PACE* promotes IT development in cortex cells but not within root hairs.

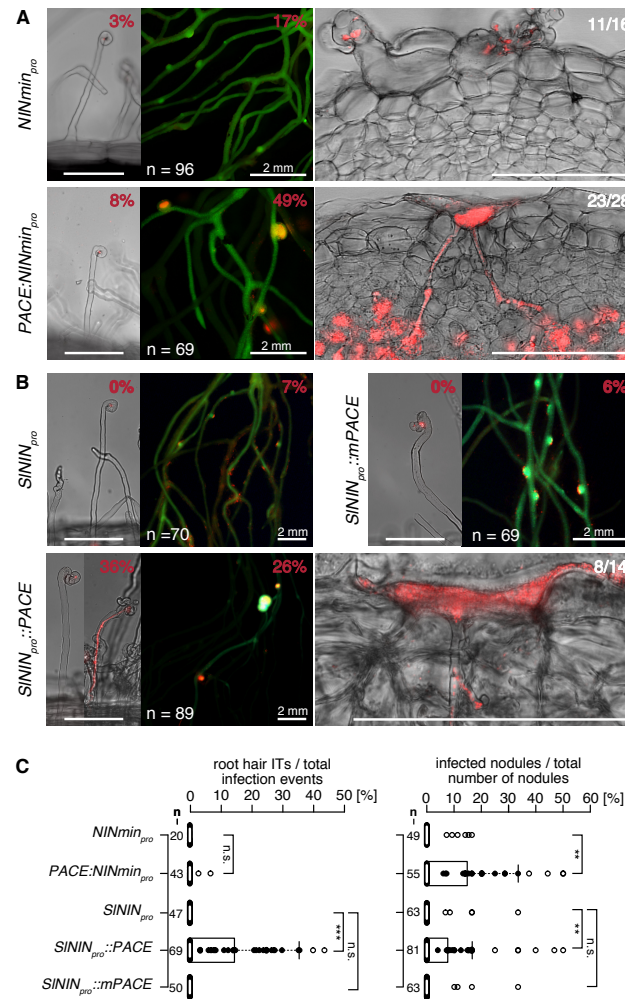


Figure 10: PACE enables IT formation in the cortex. Representative pictures of *nin-15* root hairs, root and nodule sections (see **Figure 11** for overview pictures), transformed with the *L. japonicus* *NIN* gene driven by (A) *NINmin_{pro}* or *PACE:NINmin_{pro}*; (B) *S. lycopersicum* *NIN* promoter (*SININ_{pro}*) and *SININ_{pro}* with *LjPACE* or *mPACE* inserted. %: percentage of transgenic root systems carrying root hair ITs or infected nodules; Ratios: number of nodules showing the presented pattern / total number of nodules sectioned and inspected. (C) Boxplots displaying the percentage of root hair ITs and infected nodules per transgenic root system. n, number of transgenic root systems or root pieces analysed. The applied statistical method was Fisher's exact test: ** $p < 0.01$; *** $p < 0.001$; n.s., not significant. Unlabelled scale bars, 100 μ m. The quantification of the infection events presented in this figure were generated by Chloé Cathebras, Rosa Elena Andrade and Xiaoyun Gong.

6.1.7. PACE insertion into the tomato *NIN* promoter confers RNS capability

To artificially recapitulate the functional consequence of *PACE* acquisition into a non-FaFaCuRo *NIN* promoter, we chose tomato (*Solanum lycopersicum*) which belongs to the Solanaceae, a family phylogenetically distant from the FaFaCuRo clade. Consistent with the absence of *PACE*, a *GUS* reporter gene driven by the tomato *NIN* promoter (*SININ_{pro}*) was not transactivated by Cyclops in *N. benthamiana* leaf cells (Figure 1 and Supplementary Figure 1B and 2C), while the insertion of the *L. japonicus* *PACE* (*SININ_{pro}::PACE*), but not of a mutated *PACE* (*SININ_{pro}::mPACE*) conferred transactivation by Cyclops (Supplementary Figure 2C). We tested the ability of the *LjNIN* expressed under the control of these synthetic

promoters to restore the bacterial infection process in *nin-15*. Similar to *NIN_{min_{pro}}:NIN*-transformed *nin-15* roots, *SININ_{pro}:NIN* did not restore bacterial infection (0% and 7% of transgenic root systems carried root hair ITs and infected nodules, respectively; Figure 10A - C). In contrast, *nin-15* roots transformed with *SININ_{pro}::PACE:NIN* restored the formation of root hair ITs and infected nodules on 36% and 26% of transgenic root systems, respectively (Figure 10B and 11). This increase in infection success was not observed on *SININ_{pro}::mPACE:NIN*-transformed roots. ITs in the outer cortex that originated from a focal accumulation of bacteria were also observed in the *SININ_{pro}::PACE:NIN*-transformed *nin-15* nodules (8 out of 14 nodules inspected; Figure 10B) resembling those in the *PACE:NIN_{min_{pro}}:NIN*-transformed *nin-15* nodules (Figure 10A). The gained ability of the *SININ::PACE* promoter to restore root hair ITs suggested that additional *cis*-regulatory elements within the *SININ* promoter function together with *PACE* for root hair IT formation. All together, these findings obtained with the tomato *NIN* promoter carrying an artificially inserted *PACE* agree with the hypothesis that the acquisition of *PACE* by a non-FaFaCuRo *NIN* promoter enabled its regulation via Cyclops and laid the foundation for IT formation in cortical cells.

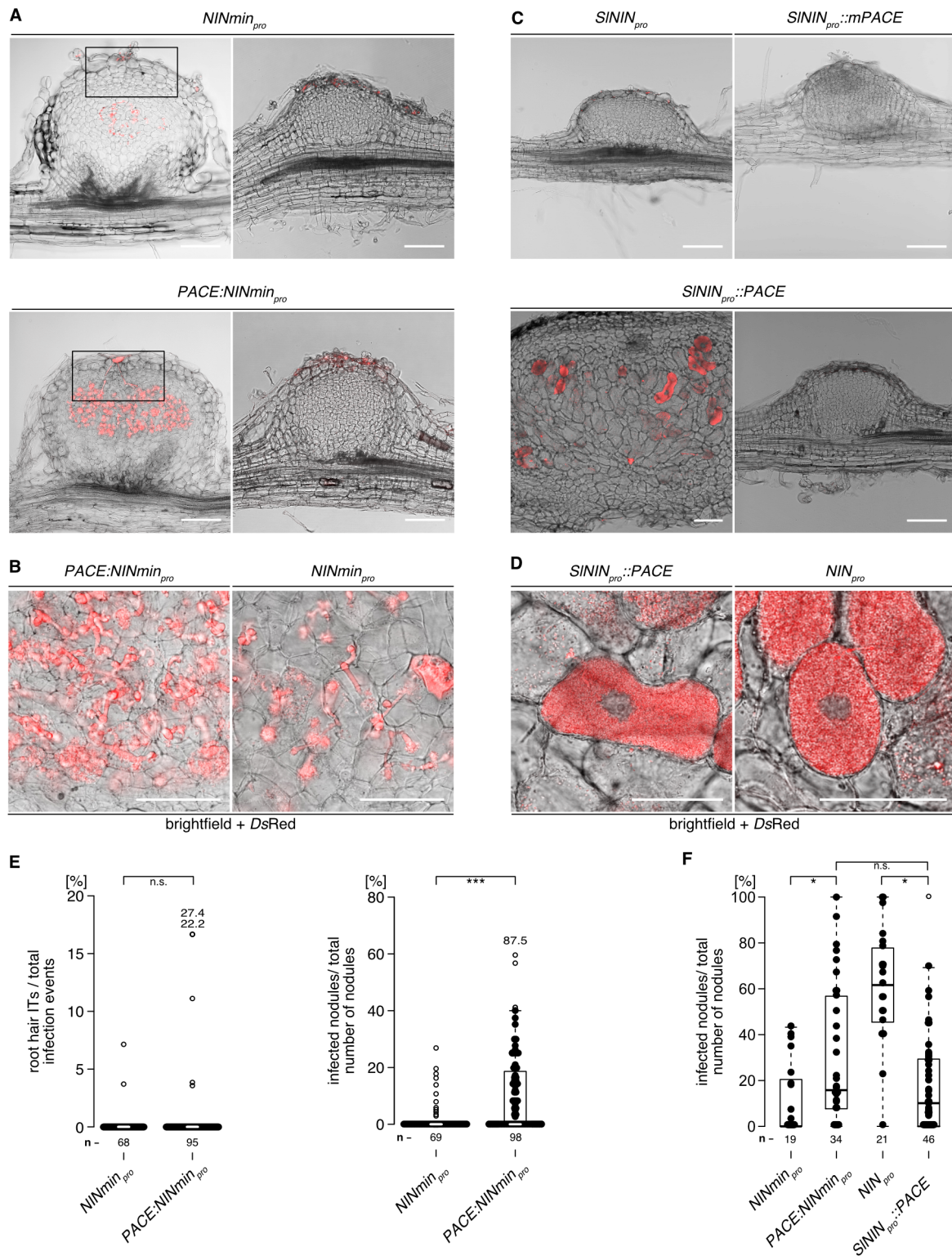


Figure 11: PACE alone or in the context of the *S. lycopersicum* NIN promoter (a species outside of the FaFaCuRo clade) enables IT formation in the cortex. (A - D) Representative pictures of sections of nodules formed on *L. japonicus nin-15* roots transformed with T-DNAs carrying a *Ubq10_{pro}:NLS-GFP* transformation marker together with the *LjNIN* gene driven by either of the following promoters: (A - B) the *L. japonicus* NIN minimal promoter (*NINmin_{pro}*) or *PACE* fused to *NINmin_{pro}* (*PACE:NINmin_{pro}*); (C - D) the 3 kb *S. lycopersicum* NIN promoter (*SININ_{pro}*), the 3 kb *SININ* promoter with mutated *PACE* (*SININ_{pro}::mPACE*) or with *L. japonicus* *PACE* inserted (*SININ_{pro}::PACE*), 21 dpi with *M. loti* *DsRed* (from the same experiments depicted in Figure 10). Black rectangles in (A) demarcate the enlarged area displayed in Figure 10A to focus on the initial infection structures. Note the absence of cells filled with symbiosomes in nodules transformed with the *LjNIN* gene driven by *PACE:NINmin_{pro}* or *NINmin_{pro}*. (continuation of figure legend on the next page)

Legend figure 11: continued

By contrast, infected cells were often filled with symbiosomes in the *SININ_{pro}::PACE:NIN*-transformed nodules, like those resulted by *NIN_{pro}::NIN* (see **(C)** and compare the two sections in **(D)**). **(E - F)** Boxplots displaying the percentage of root hair ITs among total infection events (sum of bacterial entrapments and ITs) or the percentage of infected nodules among total number of nodules **(E)** 21 dpi and **(F)** 35 dpi with *M. loti* DsRed, respectively. Each dot represents one *nin-15* transgenic root system or root piece. **(E)** displays results from an independent repetition from the experiment depicted in **Figure 10**. n: number of transgenic root systems or root pieces analysed. Numbers above the boxplots: the value of individual data points outside of the plotting area. The applied statistical method was Fisher's exact test: * $p < 0.05$; *** $p < 0.001$; n.s.: not significant. Bars, **(A and C)** 100 μm ; **(B and D)** 50 μm . The data presented in this figure were generated by Chloé Cathebras **(A - F)**, Rosa Elena Andrade **(E - F)** and Xiaoyun Gong **(E - F)**.

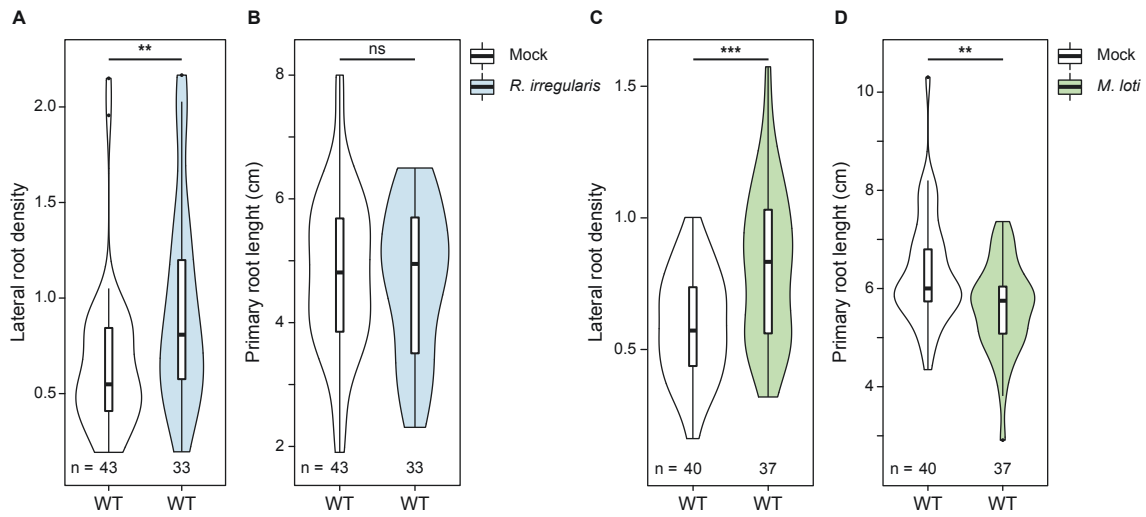


Figure 12: *Rhizopagus irregularis* and *Mesorhizobium loti* impact root system architecture in *L. japonicus*. Violin plots represent the lateral root density and primary root length of *L. japonicus* WT plants inoculated for 10 days with *R. irregularis* (A and B) or *M. loti* (C and D). Data were subjected to pairwise *t*-test: * $p < 0.05$; ** $p < 0.01$; *** $p < 0.001$. ns: not significant. n: number of plants analysed. Lateral root density: number of lateral roots/cm of primary root.

6.2. Lateral root formation is stimulated by deregulated versions of common symbiosis genes in *Lotus japonicus* and *Dryas drummondii* via the activation of *NIN*

6.2.1. Arbuscular mycorrhiza and rhizobia impact root system architecture in *Lotus japonicus*

The AM colonization process as well as treatment with LCO molecules produced by AM fungi and rhizobia were previously reported to induce changes in the root system architecture of the host plant (Oláh et al., 2005; Gutjahr et al., 2009a; Maillet et al., 2011; Gutjahr and Paszkowski, 2013). To confirm the effects of colonization by these symbionts on root architecture and examine the potential connections between symbioses signalling and the formation of LRs, we inoculated *L. japonicus* Gifu wild-type (WT) seedlings with the AM fungus *Rhizophagus irregularis* or the rhizobium *Mesorhizobium loti* MAFF 303099 7 days after imbibition and counted the number of LRs 10 days post inoculation (dpi). We observed that the LR density (number of LRs per primary root length) was increased by approximately 145 % upon inoculation with AM (Figure 12A) and by 155 % upon inoculation with rhizobia (Figure 12B) in comparison to the mock treated roots (100 %). Moreover, primary root length was significantly reduced upon inoculation with *M. loti* while no significant changes were observed upon inoculation with *R. irregularis* (Figure 12B and D). Based on these results, we conclude that compatible AM fungi as well as rhizobia impact root system architecture in *L. japonicus*; while inoculation with AM fungi results in a significant increase in LR numbers, inoculation with rhizobia does not change the overall number of LRs significantly, but inhibits primary root growth likewise resulting in higher LR density.

6.2.2. *NIN* is required for both AM fungi and rhizobia-mediated increase in lateral root density

Roots of *L. japonicus* mutants affected in common symbiosis genes block rhizobia and AM colonization. We investigated whether the common symbiosis genes *CCaMK* and *Cyclops*, and their downstream target gene *NIN* are required for AM and rhizobia-mediated LR induction. To that end, we inoculated the *ccamk-3*, *cyclops-3* and *nin-2* mutants with *R. irregularis* or *M. loti* and analysed their root phenotype 10 dpi. Surprisingly, we observed that *CCaMK*, *Cyclops* and *NIN* were all required for the increase in LR density mediated by *R. irregularis* (Figure 13A). Similar to WT seedlings, no significant changes in the primary root length were observed in any of these mutants (Figure 12A and Supplemental Figure 7A). We found that *CCaMK*, *Cyclops* and *NIN* were also required for the significant increase in LR density mediated by *M. loti* (Figure 13B). Interestingly, a significant reduction in the primary root length was still observed in all these mutants indicating that this root response is independent of the tested common symbiosis genes and *NIN* (Supplemental Figure 7B).

Taken together, these data indicate that *CCaMK*, *Cyclops* and *NIN* are required for both AM fungi- and rhizobia-mediated increase in LR density and reveal a function of *NIN* not specific to RNS.

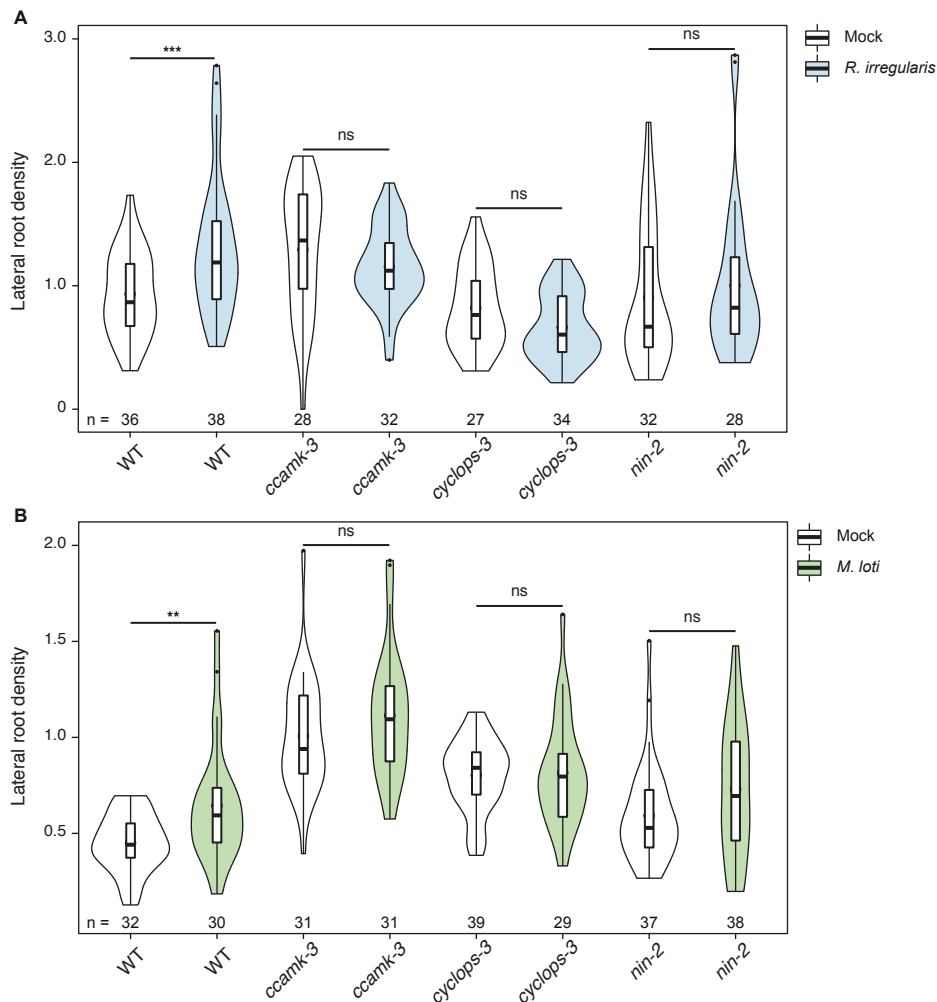


Figure 13: *Rhizophagus irregularis* and *Mesorhizobium loti*-mediated increase in lateral root density requires *NIN*. Violin plots represent the lateral root density of *L. japonicus* WT, *ccamk-3*, *cyclops-3* and *nin-2* plants inoculated for 10 days with *R. irregularis* (A) or *M. loti* (B). Data were subjected to pairwise *t*-test: * $p < 0.05$; ** $p < 0.01$; *** $p < 0.001$. ns: not significant. n: number of plants analysed. Lateral root density: number of lateral roots/cm of primary root.

6.2.3. Activation of arbuscular mycorrhiza and nodulation signalling stimulates lateral root formation in root organ liquid cultures

To further investigate potential connections between symbioses signalling and LR formation, we developed a quantitative LR induction assay and studied the effect of spontaneous activation of the symbiotic program mediated by deregulated versions of symbiosis genes on the formation of LRs. We generated transgenic *L. japonicus* root systems transformed with an empty vector control (EV) or ectopically expressing *SymRK*, *CCaMK*¹⁻

³¹⁴, *CCaMK*^{T265D} or *Cyclops*^{DD} under the control of the *L. japonicus* Ubiquitin promoter (*Ubq*_{pro}, (Maekawa et al., 2008)). All transgenic root systems expressed free GFP as a visual transformation marker. In order to standardize the assay, root tips of equal length were cut off and grown individually in liquid medium (Figure 14). Intriguingly, ectopic expression of *SymRK* or of deregulated versions of *CCaMK* or *Cyclops* significantly stimulated LR formation (Figure 15A). The overall increase of LR number was in the range of 175 % with *Ubq*_{pro}:*SymRK*-*mOrange* and 210 % with *Ubq*_{pro}:*CCaMK*¹⁻³¹⁴, *Ubq*_{pro}:*CCaMK*^{T265D} and *Ubq*_{pro}:*3xHA-Cyclops*^{DD} 10 days post transfer (dpt) to the liquid medium, in comparison to roots transformed with the EV (100 %). Additionally, the significantly higher numbers of LRs were maintained over a time course of 30 days and no significant changes in the percentage of LR induction were observed (Supplemental Figure 8). Likewise, roots ectopically expressing a phosphoablative *Cyclops* mutant version in which S50 and S154 were mutated to alanine (A) (*Ubq*_{pro}:*3xHA-Cyclops*^{AA}) displayed a similar number of LRs as roots transformed with the EV (Figure 16). Although root organ cultures retain the capacity to establish AM (Fortin et al., 2002; Keymer et al., 2017), none of the tested deregulated versions of symbiosis genes, which spontaneously activate root nodule organogenesis when expressed in roots of intact *L. japonicus* plants, were able to induce spontaneous nodules on any of the 2063 roots generated throughout the course of this study. This suggests that shoot-derived signals are required to permit spontaneous nodule development in *L. japonicus* (Raggio et al., 1957; Tsikou et al., 2018).

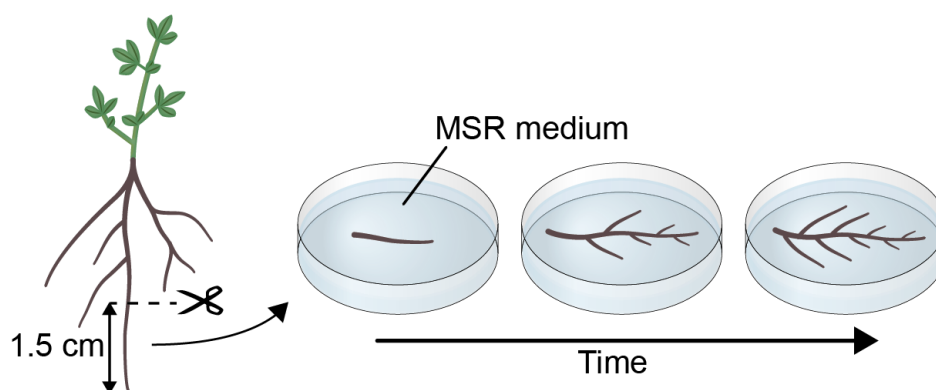


Figure 14: Schematic illustration of the experimental setup for the cultivation of root organ liquid cultures. Primary root tips (1.5 cm) of 4 weeks old transformed *L. japonicus* roots were cut off and transferred to Petri dishes containing 18 ml of liquid modified Strullu-Romand (MSR) medium. Plates were sealed with micropore tape and placed at 22 °C in the dark. Emerged lateral roots were counted 10, 20 or 30 days post incubation.

While over-abundance or ectopic expression of *SymRK* is responsible for spontaneous activation of symbiosis signalling (Ried et al., 2014), deregulated *CCaMK*^{T265D} and *Cyclops*^{DD} are both able to spontaneously trigger nodule organogenesis when expressed from their native promoters (Tirichine et al., 2006; Singh et al., 2014). To examine whether stimulation of LR formation mediated by *CCaMK*^{T265D} or *Cyclops*^{DD} requires expression from the *L.*

japonicus Ubiquitin promoter, we transformed *L. japonicus* WT roots with *Cyclops_{pro}:HA-Cyclops^{DD}* or *CCaMK_{pro}:Myc-CCaMK^{T265D}*, and compared the effects on LR induction to those obtained with the *Ubiquitin* promoter-driven constructs. We observed that deregulated versions of CCaMK or Cyclops either controlled by their native promoters or the *L. japonicus Ubiquitin* promoter stimulate LR formation to the same extent (Figure 15B). Consistent with this result, the *snf1-1* mutant that carries another deregulated version of CCaMK (CCaMK^{T265I}; (Tirichine et al., 2006)) displayed a higher LR density and number of LRs than WT plants (Figure 17). Taken together, these results indicate that spontaneous activation of a symbiosis signalling pathway mediated by gain-of-function versions of *SymRK*, *CCaMK* or *Cyclops* results in the stimulation of the LR developmental program.

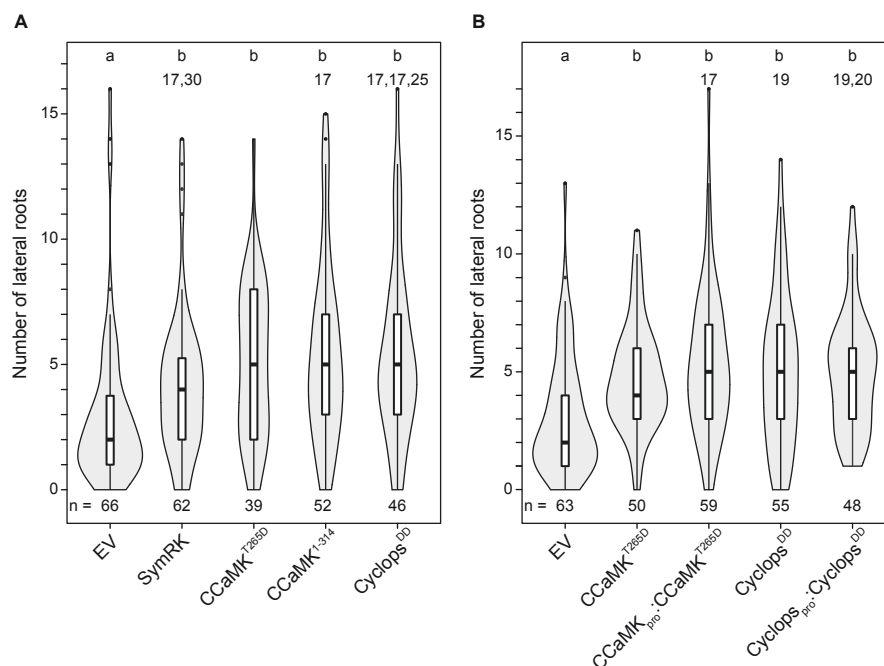


Figure 15: Expression of deregulated versions of *SymRK*, *CCaMK* or *Cyclops* stimulates lateral root formation. Liquid cultures of *L. japonicus* WT roots transformed with the empty vector (EV), *Ubq_{pro}:SymRK-mOrange* (SymRK), *Ubq_{pro}:CCaMK^{T265D}* (CCaMK^{T265D}), *Ubq_{pro}:CCaMK¹⁻³¹⁴* (CCaMK¹⁻³¹⁴), and *Ubq_{pro}:3xHA-Cyclops^{DD}* (Cyclops^{DD}) (A), or with the empty vector (EV), *Ubq_{pro}:CCaMK^{T265D}* (CCaMK^{T265D}), *CCaMK_{pro}:Myc-CCaMK^{T265D}* (CCaMK_{pro}:CCaMK^{T265D}), *Ubq_{pro}:3xHA-Cyclops^{DD}* (Cyclops^{DD}) and *Cyclops_{pro}:HA-Cyclops^{DD}* (Cyclops_{pro}:Cyclops^{DD}) (B) were generated. Violin plots represent the number of lateral roots per root system 10 dpt. Data were subjected to Kruskal-Wallis test followed by Dunn's *post-hoc* analysis; $p < 0.05$. n: number of roots analysed. Numbers above Violin plots: the value of individual data points outside of the plotting area.

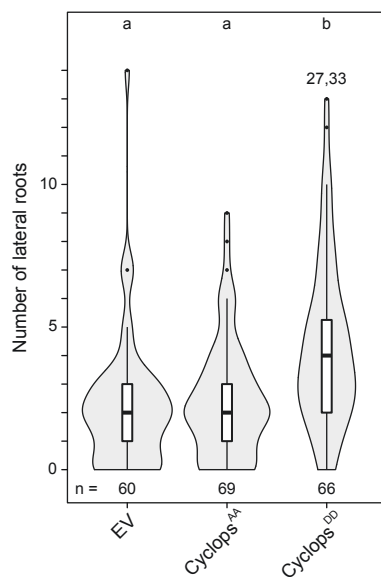


Figure 16: Expression of a phosphomimetic version of Cyclops but not its phosphoablative version stimulates lateral root formation. Liquid cultures of *L. japonicus* WT roots transformed with the empty vector (EV), *Ubq_{pro}:3xHA-Cyclops^{AA}* (Cyclops^{AA}) or *Ubq_{pro}:3xHA-Cyclops^{DD}* (Cyclops^{DD}) were generated. Violin plots represent the number of lateral roots per root system 10 dpt. Data were subjected to Kruskal-Wallis test followed by Dunn's post-hoc analysis; $p < 0.05$. n: number of roots analysed. Numbers above Violin plots: the value of individual data points outside of the plotting area.

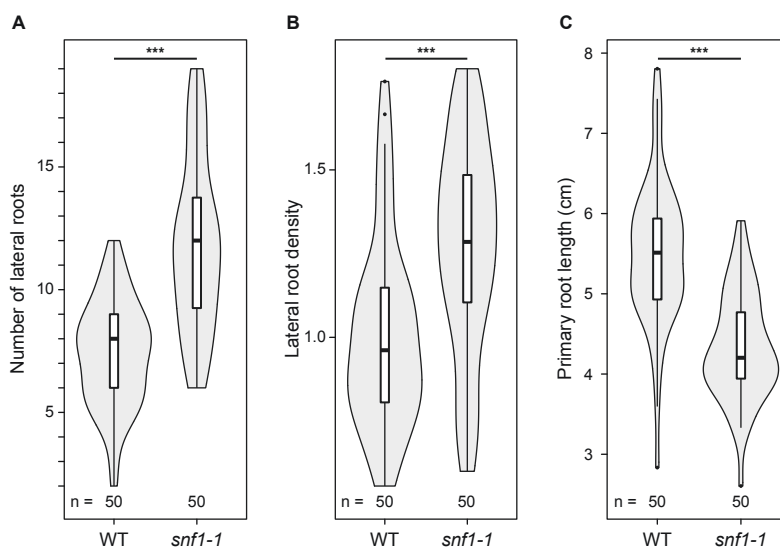


Figure 17: Deregulation of CCaMK in the *snf1-1* mutant stimulates lateral root formation. Violin plots represent the number of lateral roots (A), lateral root density (B) and primary root length (C) of 30 days old *L. japonicus* WT and *snf1-1* plants. Data were subjected to pairwise t-test: * $p < 0.05$; ** $p < 0.01$; *** $p < 0.001$. ns: not significant. n: number of plants analysed. Lateral root density: number of lateral roots/cm of primary root.

6.2.4. Auto-active CCaMK stimulates lateral root formation in the absence of *Cyclops*

While *Cyclops* is indispensable for bacterial penetration, *L. japonicus* and *M. truncatula cyclops* mutants retain the ability to initiate cortical cell divisions leading to the formation of nodule primordia and fully developed nodules, respectively, upon rhizobial inoculation (Yano et al., 2008; Horváth et al., 2011; Ovchinnikova et al., 2011). Moreover, ectopic expression of SymRK or CCaMK^{T265D} results in the development of full-sized spontaneous nodules in a *cyclops* mutant background, revealing genetic redundancy in the organogenesis pathway at the hierarchical level of *Cyclops* (Ried et al., 2014; Yano et al., 2008). To elucidate whether *Cyclops* is also dispensable for the stimulation of LR formation mediated by auto-active CCaMK, we transformed roots of the *cyclops-3* mutant with *Ubq_{pro}:CCaMK^{T265D}* and generated root organ cultures. Similar to WT roots expressing CCaMK^{T265D}, we observed a significant increase in the number of LRs in *cyclops-3* roots transformed with *Ubq_{pro}:CCaMK^{T265D}* in comparison to the EV-transformed roots (Figure 18). This indicates that CCaMK^{T265D}-mediated activation of LR induction can be uncoupled from *Cyclops*. This finding, together with the observation that Cyclops^{DD} alone is able to increase LR formation, highlights the relevance of redundant signalling components downstream of CCaMK at the hierarchical level of *Cyclops*.

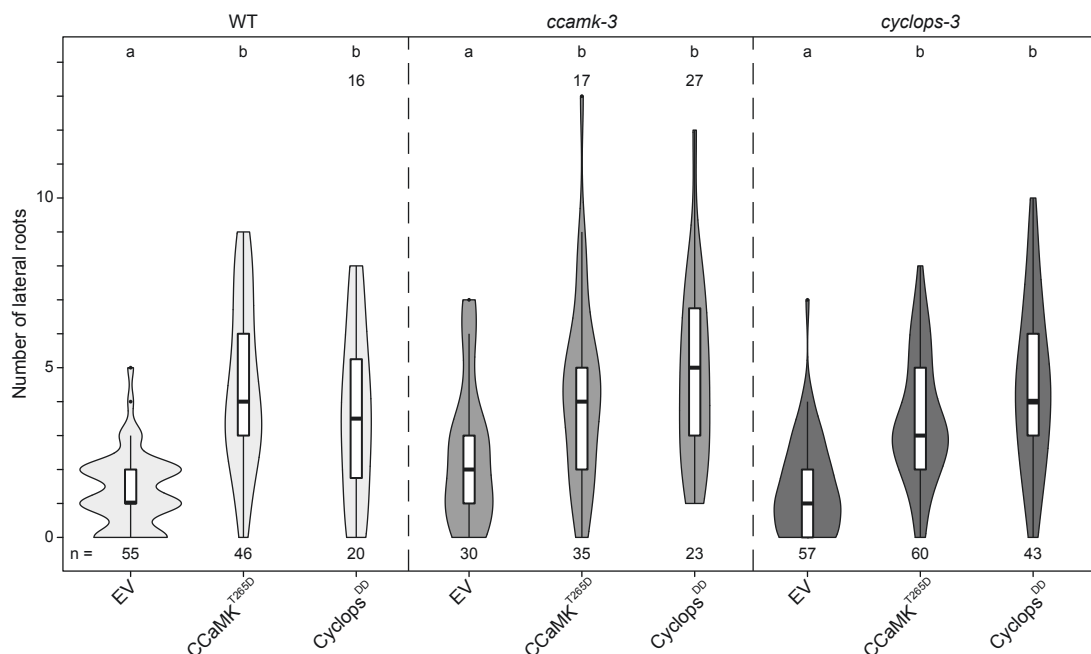


Figure 18: Stimulation of lateral root formation mediated by deregulated versions of either CCaMK or Cyclops is not dependent on Cyclops or CCaMK, respectively. Liquid cultures of *L. japonicus* WT, *ccamk-3* and *cyclops-3* roots transformed with the empty vector (EV), *Ubq_{pro}:CCaMK^{T265D}* (CCaMK^{T265D}), or *Ubq_{pro}:3xHA-Cyclops^{DD}* (Cyclops^{DD}) were generated. Violin plots represent the number of lateral roots per root system 10 dpt. Data were subjected to Kruskal-Wallis test followed by Dunn's *post-hoc* analysis; $p < 0.05$. n: number of roots analysed. Numbers above Violin plots: the value of individual data points outside of the plotting area.

6.2.5. Ectopic expression of *NIN* stimulates lateral root formation

Ectopic expression of *NIN* was found to induce the formation of enlarged bumps and malformed LRs in the absence of a symbiont in *L. japonicus* (Soyano et al., 2013). Therefore, we asked whether ectopic expression of *NIN* could stimulate the formation of LRs in root organ cultures, which are unable to support spontaneous nodule development. Ten days post inoculation in liquid medium, we observed a significant increase in the number of LRs in WT roots transformed with both *Ubq_{pro}:Myc-CCaMK^{T265D}* and *Ubq_{pro}:Myc-NIN*, in comparison to control roots transformed with the EV (Figure 19). Moreover, the non-nodulating *nin-2* mutant did not display any differences in LR density and primary root length in comparison to WT plants (Supplemental Figure 9). Taken together, these results demonstrate that ectopic expression of the transcriptional regulator *NIN* is sufficient to trigger the LR developmental program. Intriguingly, a subset of the roots ectopically expressing *NIN* overcurled and formed spirals (Figure 19B - C). This phenomenon was never observed with any of the other deregulated versions of the tested symbiosis genes and suggests a restrictive expression pattern dictated by the endogenous *NIN* promoter that does not allow root spiralling even in the presence of ectopically expressed *NIN* activators such as Cyclops^{DD}.

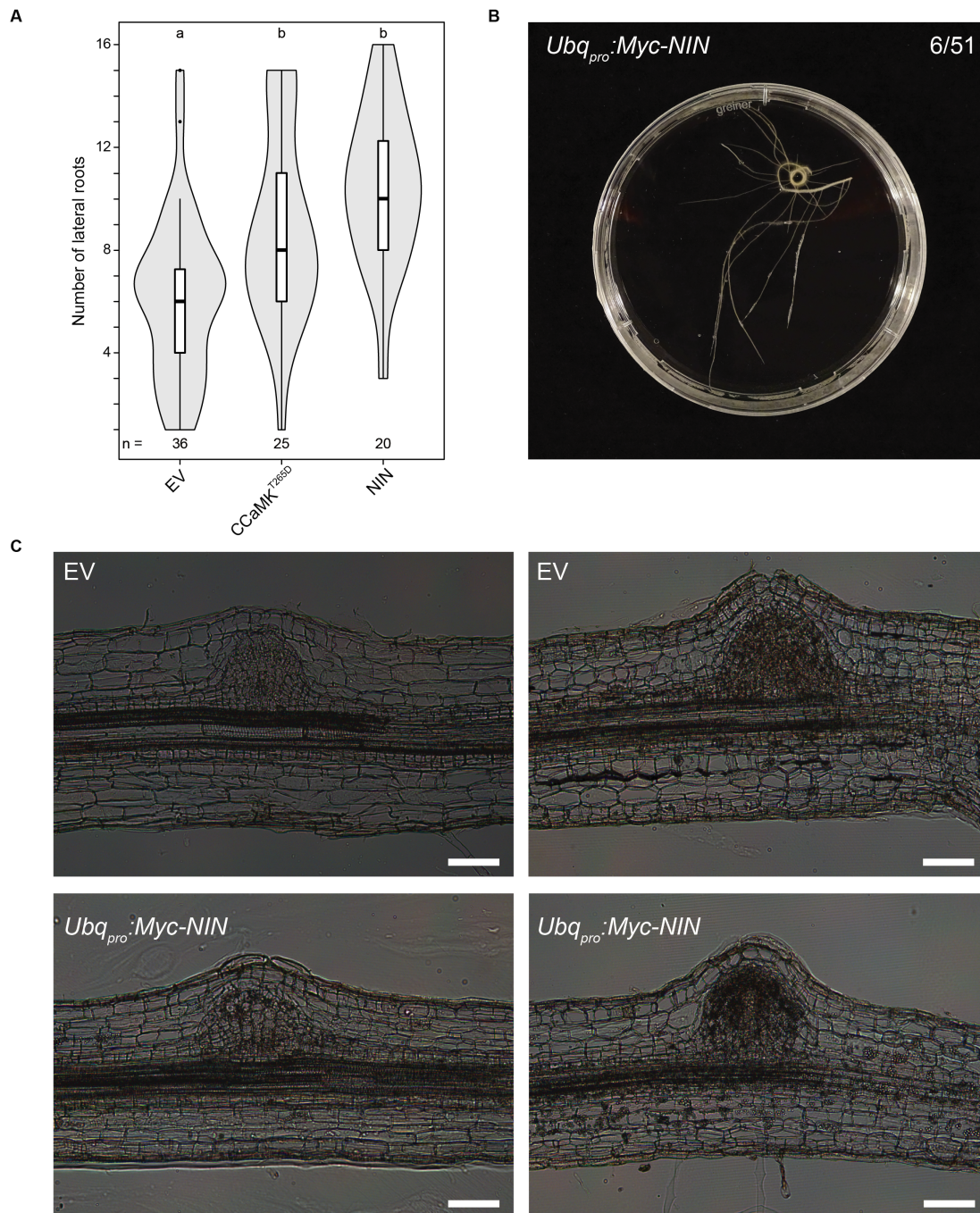


Figure 19: Ectopic expression of *NIN* stimulates lateral root formation and results in overcurling. (A) Liquid cultures of *L. japonicus* WT roots transformed with the empty vector (EV), *Ubq_{pro}:Myc-CCaMK^{T265D}* (CCaMK^{T265D}) or *Ubq_{pro}:Myc-NIN* (NIN) were generated. Violin plots represent the number of lateral roots per root system 10 dpt. Data were subjected to Kruskal-Wallis test followed by Dunn's *post-hoc* analysis; $p < 0.05$. n: number of roots analysed. (B) Representative picture of a *L. japonicus* WT overcurling root transformed with *Ubq_{pro}:Myc-NIN* 20 dpt in the MSR liquid medium. Numbers: roots exhibiting overcurling/total roots analysed. (C) Pictures of root sections from *L. japonicus* WT transformed with the empty vector (EV) or with *Ubq_{pro}:Myc-NIN* 10 dpt in MSR liquid medium. Note that the LRs formed on roots ectopically expressing *NIN* were anatomically similar to those observed on roots transformed with the empty vector. Bars, 100 μ m. The picture presented in panel (B) was taken by Martina Katharina Ried.

6.2.6. *NIN* is required for lateral root formation stimulated by auto-active CCaMK

So far, we could demonstrate that ectopic *NIN* expression results in the activation of the LR developmental program in root organ cultures and that *NIN* is required for AM fungi- or rhizobia-mediated increase in LR density in whole plants implicating the transcription factor in symbiosis as well as LR developmental signalling (Figure 13 and 19). Furthermore, *NIN* was found to be indispensable for auto-active CCaMK- and Cyclops^{DD}-mediated spontaneous nodule formation (Marsh et al., 2007; Madsen et al., 2010; Singh et al., 2014). To examine whether *NIN* is also required for auto-active CCaMK-mediated stimulation of LR formation, we ectopically expressed *CCaMK*¹⁻³¹⁴ in the *nin-2* mutant. In line with our previous observations, WT roots transformed with *Ubq_{pro}:Myc-CCaMK*¹⁻³¹⁴ formed a significantly increased number of LRs in comparison to roots transformed with the EV or with *Ubq_{pro}:Myc-CCaMK*. Intriguingly, ectopic expression of *CCaMK*¹⁻³¹⁴ in *nin-2* roots led to a reduction of the number of LRs suggesting that *NIN* might counteract a repressor of LR formation implicated in the signalling pathway activated by *CCaMK*¹⁻³¹⁴ (Figure 20). Such repressor might be the NSP1/NSP2 complex because we observed that the *nsp1-1* and *nsp2-2* mutants both formed significantly more LRs than the WT when transformed with the EV control (Figure 21) and no further increase was observed when either of the *nsp1-1* or *nsp2-2* mutants were transformed with *Ubq:CCaMK*¹⁻³¹⁴ (Figure 21). Additionally, both *nsp* mutants displayed a higher LR density than WT plants (Supplemental Figure 10). Taken together, these results indicate that *NIN* is required for *CCaMK*¹⁻³¹⁴-mediated LR induction and suggest that the *NSPs* may act as repressors of LR development, and that the stimulation by their absence cannot be further increased by *CCaMK*¹⁻³¹⁴.

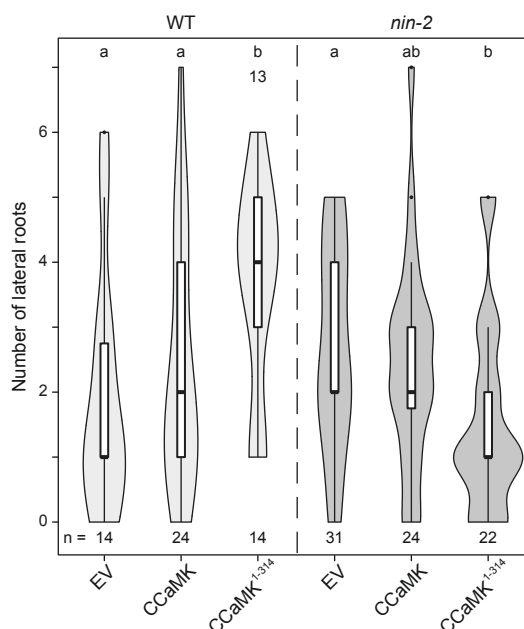


Figure 20: Stimulation of lateral root formation mediated by ectopic expression of *CCaMK*¹⁻³¹⁴ requires *NIN*. Liquid cultures of *L. japonicus* WT and *nin-2* roots transformed with the empty vector (EV), *Ubq_{pro}:Myc-CCaMK* (CCaMK) or *Ubq_{pro}:Myc-CCaMK*¹⁻³¹⁴ (*CCaMK*¹⁻³¹⁴) were generated. Violin plots represent the number of lateral roots per root system 10 dpt. Data were subjected to Kruskal-Wallis test followed by Dunn's *post-hoc* analysis; $p < 0.05$. n, number of roots analysed. Number above Violin plots: the value of an individual data point outside of the plotting area.

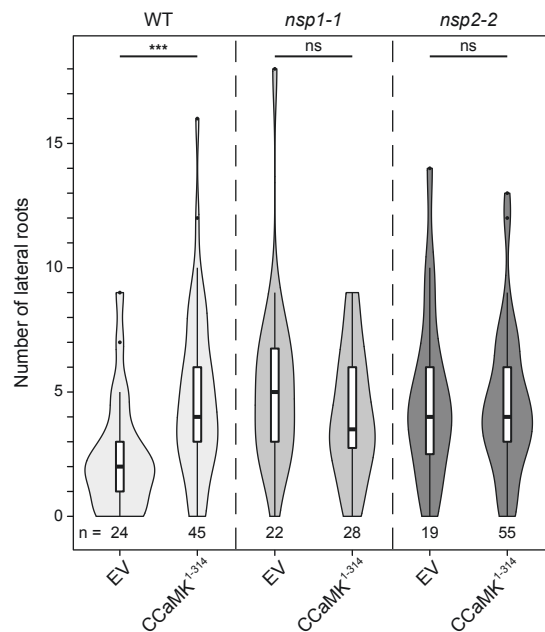


Figure 21: Stimulation of lateral root formation mediated by ectopic expression of CCaMK¹⁻³¹⁴ requires NSP1 and NSP2. Liquid cultures of *L. japonicus* WT, *nsp1-1* and *nsp2-2* roots transformed with the empty vector (EV) or *Ubg_{pro}:CCaMK¹⁻³¹⁴* (CCaMK¹⁻³¹⁴) were generated. Violin plots represent the number of lateral roots per root system 14 dpt. Data were subjected to pairwise *t*-test: **p* < 0.05; ***p* < 0.01; ****p* < 0.001. ns: not significant. n: number of roots analysed.

6.2.7. Lateral root induction mediated by auto-active CCaMK is conserved in *Dryas drummondii* but not in *Fragaria vesca*

RNS with nitrogen-fixing bacteria is confined to the FaFaCuRo clade in which the distribution of nodulating species is scattered (Soltis et al., 1995; Doyle, 2011). To examine whether the induction of LRs mediated by the activation of symbioses signalling is conserved among members of this clade, we tested the LR inducing capability of *LjCCaMK¹⁻³¹⁴* in the actinorhizal plant *Dryas drummondii*, which carries a *NIN* ortholog, and in *Fragaria vesca*, a non-nodulating member of the Rosales that lost a functional *NIN* gene (Griesmann et al., 2018). We generated composite plants with transgenic roots and observed a significant increase in the LR density of *D. drummondii* roots transformed with *Ubg_{pro}:Myc-LjCCaMK¹⁻³¹⁴* in comparison to roots transformed with the EV or with *Ubg_{pro}:Myc-CCaMK* (Figure 22A - C). By contrast, *F. vesca* roots ectopically expressing *LjCCaMK¹⁻³¹⁴* did not display any increase in LR density in comparison to control roots (Figure 22D - F). Taken together, these results indicate that the induction of LRs mediated by CCaMK¹⁻³¹⁴ is not specific to legumes (Fabales) and are consistent with the idea that *NIN* is required to mediate this developmental response in FaFaCuRo member species.

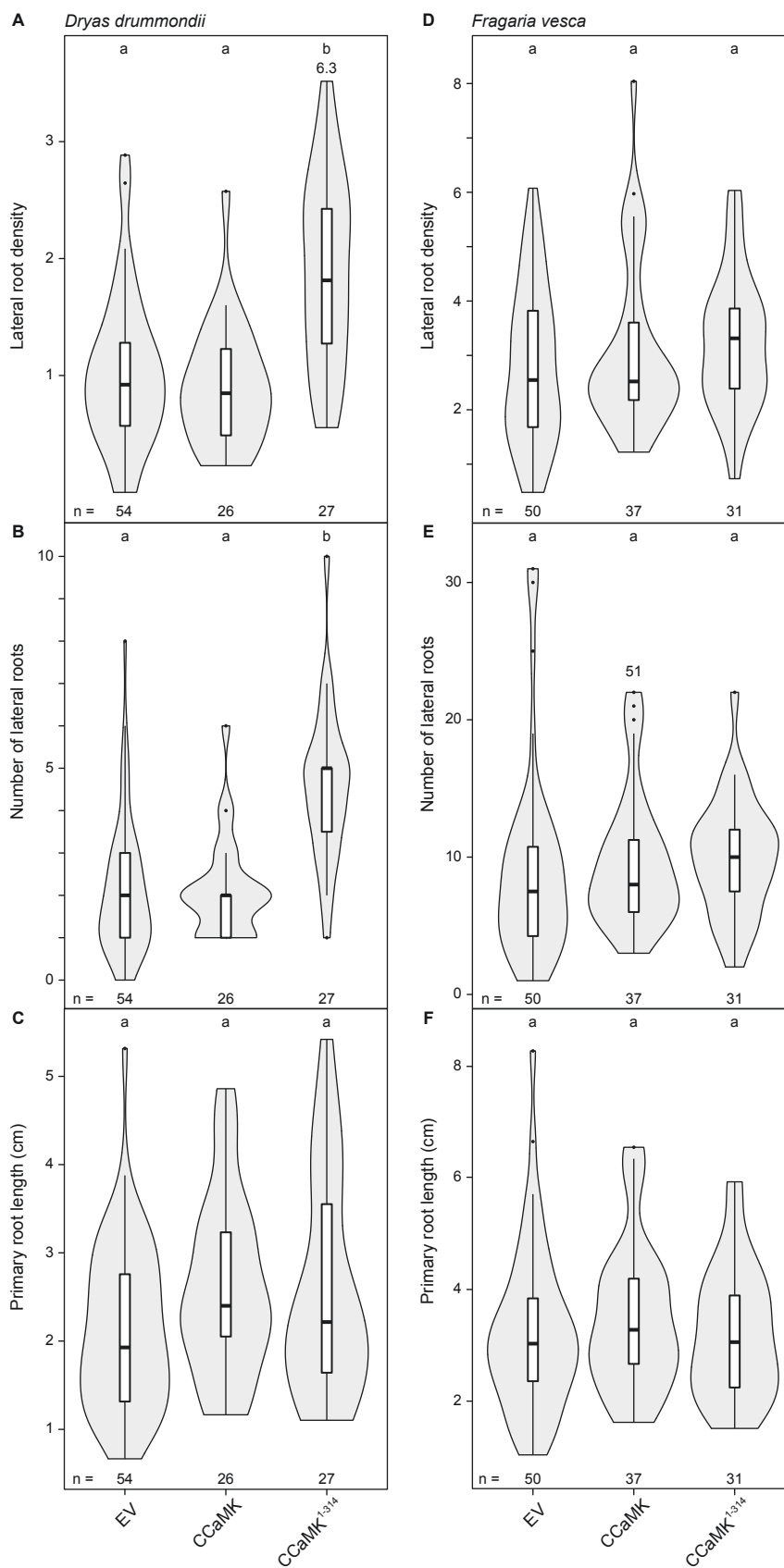


Figure 22: Ectopic expression of *LjCCaMK*¹⁻³¹⁴ stimulates lateral root formation in *Dryas drummondii* but not in *Fragaria vesca*. *D. drummondii* (A - C) and *F. vesca* (D - F) composite plants transformed with the empty vector (EV), *Ubc_{pro}:Myc-LjCCaMK* (CCaMK) or *Ubc_{pro}:Myc-LjCCaMK*¹⁻³¹⁴ (CCaMK¹⁻³¹⁴) were generated. (continuation of figure legend on the next page)

Legend Figure 22: continued

Violin plots represent the lateral root density (**A** and **D**), the number of lateral roots (**B** and **E**) and the primary root length (**C** and **F**) 65 days post *Agrobacterium rhizogenes* inoculation. Data were subjected to Kruskal-Wallis test followed by Dunn's *post-hoc* analysis; $p < 0.05$. n: number of roots analysed. Lateral root density: number of lateral roots/cm of primary root. Number above Violin plots: the value of an individual data point outside of the plotting area. The data presented in this figure were generated by Chloé Cathebras and Aline Sandré.

7. Discussion

7.1. Acquisition of *PACE* in the last common ancestor of the FaFaCuRo clade enabled the formation of infection threads in the root cortex

The mechanistic connection between *PACE* and cortical IT formation together with their congruent phylogenetic distribution strongly support the idea that the acquisition of *PACE* by the latest common ancestor of the FaFaCuRo clade enabled cortical ITs and thus laid the foundation for the evolution of present day RNS. Our findings support an evolutionary model in which an ancestral symbiotic transcription factor complex (comprising CCaMK and Cyclops), that facilitated intracellular symbiosis with AM fungi already in the earliest land plants (Delaux et al., 2014, 2015), gained control over the transcriptional regulation of the *NIN* gene by the acquisition of *PACE* (Figure 2). This genetic innovation in the last common ancestor of the FaFaCuRo clade extended the function of the ancestral CCaMK/Cyclops complex to initiate cortical IT development.

The *NIN*-like protein family underwent important evolutionary steps preceding the origin of RNS including a gene duplication leading to *NIN* and *NLP1* as closest paralogs (Liu and Bisseling, 2020). It is very likely that the *NIN* protein itself underwent changes that enabled its role in nodulation (Soyano and Hayashi, 2014), but it is from a statistical point of view likely that the *PACE* acquisition and the *NIN* enabling mutations occurred independently from each other. Because our phylogenomic analysis places the acquisition of *PACE* to the latest ancestor of the FaFaCuRo clade we conclude that *NIN* enabling mutations occurred earlier and it will be interesting to determine what these critical changes were and where they occurred phylogenetically. *NIN* genes from FaFaCuRo member species were reported to cluster together in phylogeny analyses, suggesting that sequence adaptation of *NIN* was a crucial step during the evolution of RNS (Clavijo et al., 2015). Supporting this hypothesis, *NIN* from *S. lycopersicum* cannot restore IT formation in the *L. japonicus nin-15* mutant (Rosa Elena Andrade, unpublished data) and *MtNLP1*, the closest *M. truncatula NIN* paralogue, neither restores ITs nor nodule formation in *Mtnin-1* (Liu and Bisseling, 2020). Although the loss of nitrate responsiveness of *NIN* was proposed as one of the evolutionary events necessary for the emergence of RNS, these critical amino acid changes within *NIN* that permitted its role in the establishment of RNS have not been identified so far (Suzuki et al., 2013; Liu and Bisseling, 2020).

A “young” primary cell wall characteristic for recently divided cells is considered an important prerequisite for cortical IT initiation (Parniske, 2018; Geurts et al., 2016) but cell division is not restricted to the formation of novel organs (Murray et al., 2007). It is therefore conceptually possible that the common ancestor of the FaFaCuRo clade was forming ITs in recently divided cortical cells but in the absence of root nodules. Multiple lines of evidence indicate that the diverse types of lateral organs harbouring nitrogen-fixing bacteria (“nodules”) evolved multiple times independently. Indeed, *CE*-mediated *NIN* expression

is important for nodule organogenesis in legumes, but upon searching for this regulatory element in a region of 0.1 Mb upstream and downstream of the *NIN* gene, Liu and colleagues (Liu et al., 2019c) found its presence to be restricted to legume species, indicating an evolutionary emergence independently of and significantly later than the last common ancestor (Liu et al., 2019c; Liu and Bisseling, 2020). ITs in root hairs are only found in Fabales and Fagales and therefore also considered a more recent acquisition (Parniske, 2018; Madsen et al., 2010). *CE* only in combination with *PACE* facilitates root hair ITs (Figure 6, 7 and 8; Supplementary Figure 4 and 5) and additional elements in the 3 kb promoter are necessary for nodule and cortical IT development (Figure 6, 7, 8 and 23; Supplementary Figure 4 and 5). These observations highlight the enormous complexity of concerted activity of *cis*-elements and transcription factors underlying the spatiotemporal expression control by present day *NIN* promoters in RNS-competent species (Figure 23).

Altogether, our data pinpoint the acquisition of *PACE* as a key event during the evolution of nodulation. Together with the discovery that multiple independent losses of *PACE* (Table 1) are associated with multiple losses of RNS within the FaFaCuRo clade (Griesmann et al., 2018), our data underpin the essential position of *PACE* in the evolutionary gain and loss of RNS.

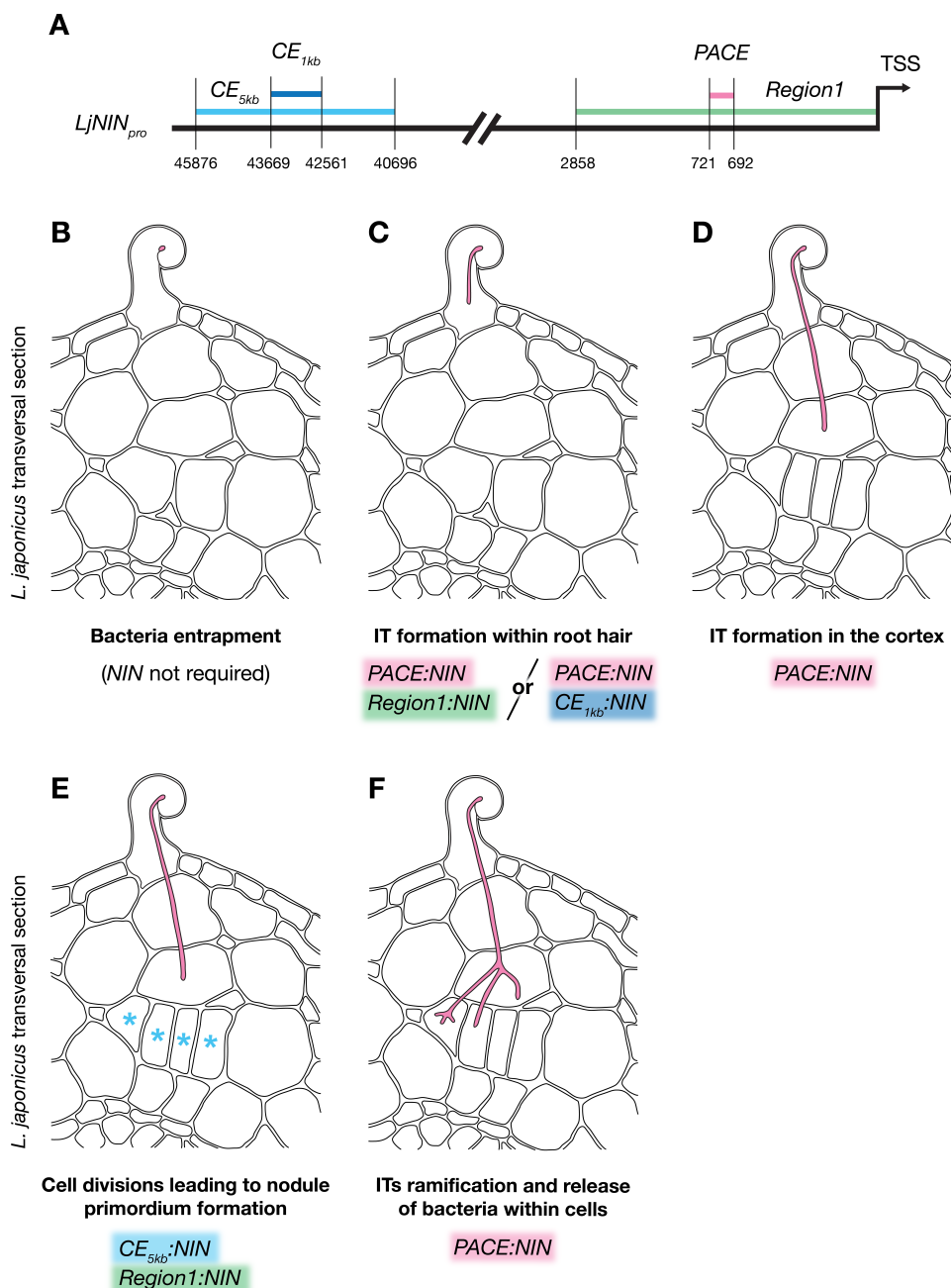


Figure 23: Cis-regulatory regions controlling *NIN* expression and enabling rhizobia infection and nodule development in *L. japonicus*. (A) Schematic representation of the *L. japonicus* *NIN* promoter and cis-regulatory regions that control *NIN* expression and enable rhizobia infection and nodule development. *CE*_{1kb} and *CE*_{5kb} regions encompass several putative cytokinin response elements (Liu et al., 2019c). *Region1* encompasses *PACE* as well as the NSP1 and IPN2 binding sites (Hirsch et al., 2009; Xiao et al., 2020). Numbers indicate the number of bases from the transcriptional start site (TSS). (B – F) Schematic illustrations of the early stages of rhizobia infection and nodule primordium formation in *L. japonicus* WT roots. The highlighted cis-regulatory regions and/or cis-regulatory element driving *NIN* expression below each stage were found to be sufficient to enable the corresponding process. (B) *NIN* is not required for root hair curling and bacteria entrapment. (C) *Region1* driving *NIN* expression is sufficient for IT formation within root hairs. Redundantly, *CE*_{1kb} in combination with *PACE* driving *NIN* expression is sufficient for IT formation within root hairs. This suggests the presence of redundant cis-regulatory element(s) within *Region1* and *CE*_{1kb} that, in combination with *PACE*, enable(s) root hair IT development. (D) *PACE* driving *NIN* expression is sufficient for IT formation in the cortex. (E) *CE*_{5kb} in combination with *Region1* driving *NIN* expression induces cell divisions (blue stars) leading to nodule primordium formation upon rhizobia inoculation. *PACE* is not required for this process. (F) *PACE* driving *NIN* expression is sufficient for ITs ramification and release of bacteria within cells upon nodule development. TSS, transcriptional start site. The drawings in this figure are based on microscopy pictures of semithin transversal sections of *L. japonicus* WT roots published by van Spronsen et al. (2001).

7.2. Activation of *NIN* induces the formation of lateral roots

7.2.1. Components of the common symbiosis pathway trigger lateral root development via the activation of *NIN*

We report a novel regulatory role of the CCaMK/Cyclops complex on the development of LRs via the activation of *NIN* (Figure 24). We established a LR induction assay and took advantage of deregulated versions of common symbiosis genes conferring spontaneous activation of symbiosis signalling and nodule development, to study their effect on the formation of LRs in *L. japonicus* (Figure 14). Root organ cultures are unable to support normal and spontaneous nodulation ((Raggio et al., 1957; Tsikou et al., 2018); this study), therefore providing a unique system in which nodule organogenesis and LR signalling pathways are uncoupled from each other. We demonstrated that LR formation is stimulated by ectopic expression of *SymRK*, *CCaMK¹⁻³¹⁴*, *CCaMK^{T265D}* and *Cyclops^{DD}* in *L. japonicus* (Figure 15A and 16; Supplementary Figure 8). A major function of *SymRK* in symbiosis is the activation of CCaMK, probably through the calcium-spiking machinery (Hayashi et al., 2010; Madsen et al., 2010). The complex formed by CCaMK and Cyclops transactivates the *NIN* promoter via direct binding of Cyclops to a palindromic sequence encompassed within the *cis*-regulatory element *PACE* and this transcriptional activation cascade was proposed to enable bacterial uptake by plant cells through the formation of cortical ITs ((Singh et al., 2014); this study). In the model emerging from our data, the expression of *NIN* driven by CCaMK/Cyclops appears to be additionally involved in the activation of the LR developmental program (Figure 24).

We observed that *CCaMK^{T265D}* and *Cyclops^{DD}* were both able to stimulate LR formation when expressed under their native promoter in absence of external stimuli (Figure 15B), therefore supporting the idea that the LR induction pathway mediated by CCaMK/Cyclops is initiated at the very early stages of the plant-fungi and rhizobium interactions. These data are in line with the observation that the NF- and MF-mediated activation of CCaMK are both sufficient to induce the formation of LRs in *M. truncatula* (Oláh et al., 2005; Maillet et al., 2011).

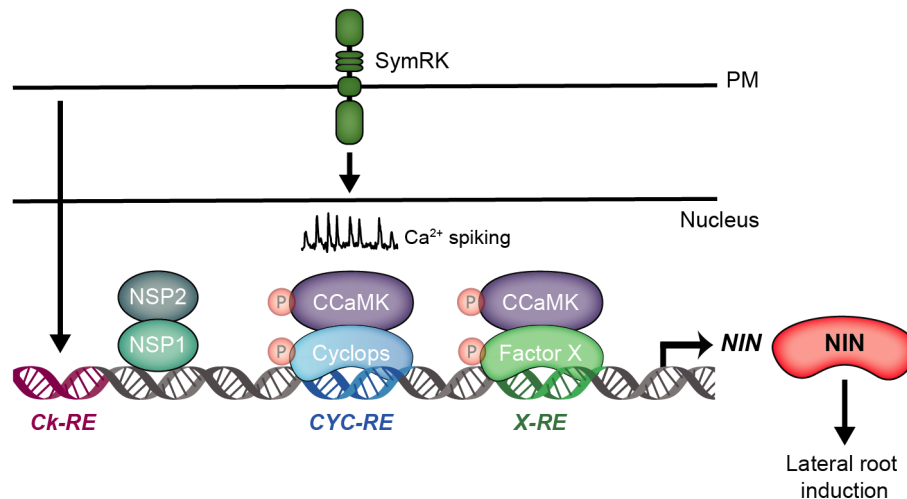


Figure 24: A model for lateral root induction by common symbiosis genes. Upon ectopic expression, SymRK stimulates the formation of LRs probably through the activation of the calcium spiking machinery. Within the nucleus, calcium spiking is conceptually decoded by CCaMK whose auto-active versions induce the formation of LRs through the activation of Cyclops or (an) unknown factor(s) (Factor X), that in turn transactivate the *NIN* promoter through identical or distinct response elements (*CYC-RE* and *X-RE*, respectively). *NIN* appears to be essential to mediate this developmental response and induces LR formation upon ectopic expression. In addition, *NSP1* and *NSP2* are required for LR induction mediated by auto-active CCaMK and were reported to bind to the *NIN* promoter as a complex (Hirsch et al., 2009). Furthermore, cytokinin accumulation in the inner root cell layers was reported to induce the activation of *NIN* through cytokinin response elements (*Ck-RE*) (Liu et al., 2019c) and might, together with CCaMK's targets and the NSPs, contribute to dictate the precise expression of this gene to trigger the LR developmental program. PM: plasma membrane.

7.2.2. Genetic redundancy in the lateral root signalling pathway mediated by auto-active CCaMK

We observed that CCaMK^{T265D} was able to stimulate LR formation in the absence of *Cyclops* revealing genetic redundancy in the LR signalling pathway at the hierarchical level of *Cyclops* (Figure 18 and 23). This *Cyclops*-independent pathway might proceed via additional CCaMK phosphorylation target(s) yet to be identified, a hypothesis previously put forward by Yano et al. (Yano et al., 2008) for the CCaMK^{T265D}-triggered nodule organogenesis in *cyclops* mutant. Several proteins have been identified to interact and be phosphorylated by CCaMK such as STF3, CIP73, NAC73 and PP45, and play a role in nodulation or abscisic acid signalling, however, their putative role in LR formation has not been reported yet (Kang et al., 2011; Zhu et al., 2016; Ni et al., 2019; Wang et al., 2021). The identification of interaction partner(s) and/or phosphorylation target(s) of CCaMK that mediate these developmental responses independently of *Cyclops* would open new avenues in our understanding of the connections between nodule organogenesis, LR and abscisic acid signalling (Bensmihen, 2015; Harris, 2015).

7.2.3. *NIN* orchestrates nodule organogenesis and lateral root formation

NIN is an essential component of the nodule organogenesis signalling pathway (Schauser et al., 1999; Marsh et al., 2007; Madsen et al., 2010; Singh et al., 2014) and its ectopic expression induces cortical cell division leading to the formation of enlarged bumps and malformed LRs in the absence of rhizobia (Soyano et al., 2013). These observations suggest that the specificity between the two programs, leading to nodule organogenesis or LR development, arises from a signal that occurs upstream of *NIN*. This might be achieved by distinct *cis*-regulatory elements within the *NIN* promoter which dictate the precise expression pattern of this transcription factor (Figure 24; (Yoro et al., 2014; Liu et al., 2019c)). In root organ culture, the ectopic expression of *NIN* led to a significant increase in LRs that were anatomically similar to those observed on roots transformed with an EV (Figure 19). These observations provide additional support for a model first proposed by Soyano and Hayashi (Soyano and Hayashi, 2014) in which *NIN* recruited the LR developmental program by targeting regulatory regions of downstream genes such as *ASL18/LBD16* to evolve root nodules ((Schiessl et al., 2019; Soyano et al., 2019, 2021); Figure 24). In addition, we observed that a subset of roots ectopically expressing *NIN* overcurled (Figure 19B), a phenomenon also reported in *M. truncatula* roots ectopically expressing *LBD16* (Schiessl et al., 2019). Root coiling phenotype is linked to defect in auxin transport (Taylor et al., 2021). It is therefore possible that the deregulation of *NIN* expression imposes an asymmetric auxin distribution in the roots growing on horizontally placed plates through the activation of *ASL18/LBD16* and/or additional unknown targets.

We found that the formation of LRs is repressed in the *nin-2* mutant ectopically expressing CCaMK¹⁻³¹⁴ (Figure 20) which led us to the hypothesis that *NIN* might counteract one or multiple repressor(s) of LR formation implicated in the signalling pathway activated by CCaMK¹⁻³¹⁴. Although the NSP1/NSP2 complex was reported to binds to the *NIN* promoter ((Hirsch et al., 2009); Figure 24), both NSPs were positioned downstream of *NIN* or in an alternative pathway in the Cyclops^{DD}-mediated activation of the nodule organogenesis signalling (Singh et al., 2014; Limpens and Bisseling, 2014). It is therefore possible that in the CCaMK¹⁻³¹⁴-mediated LR induction pathway, *NIN* regulates the activity of both NSPs (Figure 21), which, in addition, appear to also repress the formation of LRs under non-symbiotic conditions (Figure 21; Supplementary Figure 10).

7.2.4. The evolution of the *NIN* regulon

Recent studies revealed that the scattered distribution of nodulating species among the FaFaCuRo clade is a consequence of multiple independent losses or fragmentations of *NIN* and *RPG* (Arrighi et al., 2008) in plant lineages (Griesmann et al., 2018; van Velzen et al., 2018). We observed that ectopic expression of *Lj*CCaMK¹⁻³¹⁴ enhanced the formation of LRs in the nodulating species *D. drummondii* but not in the non-nodulating species *F. vesca* which has lost *NIN* (Figure 22; (Griesmann et al., 2018)). It is therefore tempting to speculate

that *NIN* is required to mediate this developmental response in FaFaCuRo member species. The recruitment of the LR developmental program by *NIN* was suggested by the identification of *NIN*-targeted *cis*-elements within *ASL18/LBD16* introns, however these binding sites are only present in legume species (Soyano et al., 2019). Our data suggest that the co-option of the LR program by *NIN* extends beyond this order. The *NIN* regulon might have differentially evolved among nodulating species and this might partially reflect the diversity observed in nodule structures (Sprent, 2007; Pawlowski and Demchenko, 2012; Svistoonoff et al., 2014).

NIN is present in species outside of the FaFaCuRo clade (Clavijo et al., 2015; Griesmann et al., 2018; Liu and Bisseling, 2020), however, it is only known to have RNS-specific functions although a possible role in AM fungal colonization in *M. truncatula* was reported (Guillotin et al., 2016) but contradicted by a recent study (Kumar et al., 2020). Here we observed that *NIN* is necessary for both AM and rhizobia-mediated LR increase thus revealing a new role of this gene not specific to RNS (Figure 13; Supplementary Figure 7). These data indicate that *NIN* might not only employ the LR program for nodule organogenesis, but also activate the LR program in a symbiotic context. In future studies, it will be interesting to investigate whether the role of *NIN* in the AM and auto-active CCaMK-mediated LR induction is conserved among non-FaFaCuRo species such as tomato. This might provide new insights into the evolution of the *NIN* regulon, which was hypothesised to be one of the drivers of the evolution of the RNS in the FaFaCuRo clade (Soyano and Hayashi, 2014).

8. Materials and Methods

8.1. Plant material, bacterial and fungal strains

Lotus japonicus ecotype Gifu B-129 wild-type (WT) (Handberg and Stougaard, 1992), *ccamk-3*, *cyclops-3*, *nin-2*, *nsp1-1*, *nsp2-2*, *snf1-1* (Perry et al., 2009) and *nin-15* (LORE1 line 30003529 (Małolepszy et al., 2016)) were used in this thesis. The *nin-15* mutant was genotyped to select plant homozygous for the LORE1 insertions by Rosa Elena Andrade. Seed bags are listed in Supplementary Table 1. Seeds from *Dryas drummondii* (DA462) were purchased from the seed producer Jelitto (Jelitto Staudensamen GmbH). Seeds from *Fragaria vesca* were obtained from the Greenhouse Laboratory Center Dürnast (GHL) of the Technical University of Munich (TUM). *Agrobacterium rhizogenes* strain AR1193 (Stougaard et al., 1987) was used to transform roots of *L. japonicus*, *D. drummondii* and *F. vesca*. *Mezorhizobium loti* MAFF 303099, *M. loti* R7A and *Rhizophagus irregularis* DAOM197118 spores (Symplanta) were used to inoculate *L. japonicus* or chive roots when stated.

8.2. Cultivation of chive and inoculation with AM spores

Spores from the AM fungus *R. irregularis* were used to inoculate *L. japonicus* roots in a chive nurse plant system. Chive seeds were surface-sterilized with 1.2 % NaClO for 2 min, rinsed 5 times with sterile deionized water and germinated in open pots (7×7×8 cm) containing *R. irregularis* spores and 200 ml of sand:vermiculite mixture (2:1). Briefly, 5000 spores were resuspended in 10 ml of a modified ¼ Hoagland's medium ((Hoagland and Arnon, 1938) 0.1 mM KH₂PO₄; 1.5 mM KNO₃; 2 mM MgSO₄·7H₂O; 2 mM K₂SO₄; 2.5 mM CaSO₄·2H₂O; 12.5 μM Fe-EDDHA; 10 μM FeSO₄·7H₂O; 11 μM Na₂EDTA; 46.2 μM H₃BO₃; 9.14 μM MnCl₂·4H₂O; 0.77 μM ZnSO₄·7H₂O; 0.32 μM CuSO₄·5H₂O; 0.1 μM Na₂MoO₄·2H₂O; 0.1 μM CoCl₂·6H₂O; pH 5.8; hereafter referred to as Hoagland's medium) and added to each pots containing 150 ml of sand:vermiculite mixture before being covered with an additional 50 ml of sand:vermiculite mixture. Fifty surface-sterilized chive seeds were germinated per pots and watered immediately with 20 ml of Hoagland's medium. The next day, seeds were watered with 10 ml of Hoagland's medium, followed by 3 times per week with 20 ml of Hoagland's medium for 4 weeks. Chive plants were then transferred to new open pots (7×7×8 cm) containing 200 ml of sand:vermiculite mixture (2:1) (2 plants per pot) and watered 3 times per week with 20 ml of Hoagland's medium for 4 additional weeks before being harvested to inoculate *L. japonicus* roots.

8.3. Cultivation of bacterial strains

The bacterial strains *M. loti* MAFF 303099 (*M. loti*), *M. loti* MAFF 303099 constitutively expressing the *Discosoma* sp. red fluorescent protein (*M. loti* DsRed, (Maekawa et al., 2009))

and *M. loti* R7A constitutively expressing the cyan fluorescent protein (*M. loti* CFP, kindly provided by David Chiasson, Saint Mary's University, Canada) were used to inoculate *L. japonicus* roots. Strains were grown in Tryptone yeast extract liquid medium (Beringer, 1974) supplemented with the appropriate antibiotics. Bacterial liquid cultures were incubated at 28 °C for about 16 to 20 h under agitation (180 rpm) and bacteria were collected by centrifugation and washed twice with a nitrogen-reduced FAB medium (500 µM MgSO₄·7H₂O; 250 µM KH₂PO₄; 250 µM KCl; 250 µM CaCl₂·2H₂O; 100 µM KNO₃; 25 µM Fe-EDDHA; 50 µM H₃BO₃; 25 µM MnSO₄·H₂O; 10 µM ZnSO₄·7H₂O; 0.5 µM Na₂MoO₄·2H₂O; 0.2 µM CuSO₄·5H₂O; 0.2 µM CoCl₂·6H₂O; pH 5.7) and resuspended in the same medium.

8.4. *Lotus japonicus* growth conditions, symbiotic inoculations and root organ liquid cultures

L. japonicus seeds were scarified and surface-sterilized as described (Gossmann et al., 2012) before germination on ½ Gamborg's B5 medium ((Gamborg et al., 1968) Figure 3 – 11; Supplementary Figure 3 - 6) or deionized water (Figure 12 – 21; Supplementary Figure 7 - 10) solidified with 0.8 % Bacto™ agar in square plates (12 x 12 x 1.7 cm). Plates were kept in dark for three days before transferring to light condition in a Panasonic growth cabinet (MLR-352H-PE) at 24 °C under a 16 h/8 h light/dark regime (50 µmol·m⁻²·s⁻¹). Six-days-old seedlings were (1) subject to hairy root transformation as described (Charpentier et al., 2008) (Figure 3, 4, 5, 6, 7, 8, 9, 10, 11, 15, 16, 18, 19, 20, 21 and Supplementary Figure 3, 4, 5, 6 and 8); or (2) transferred to Weck jars (SKU 745 or 743; J.Weck GmbH u. Co. KG) containing 300 ml of sand:vermiculite mixture (2:1) and 20 ml of nitrogen-reduced FAB medium containing *M. loti* DsRed (OD₆₀₀ = 0.01) (Figure 4C).

For *in vivo* promoter expression analysis (Figure 3), transgenic roots expressing a kanamycin-resistance gene were kept on square plates supplemented with kanamycin (25 µg/ml) 10 days after *A. rhizogenes* inoculation. Plants with transformed roots were kept nitrogen-reduced FAB medium solidified with 0.8 % Bacto™ agar in square plates for 1 week before transferring to a growth chamber at 24 °C under a 16 h/8 h light/dark regime (275 µmol·m⁻²·s⁻¹) in Weck jars (SKU 745 or 743) containing 300 ml of sand:vermiculite mixture (2:1) and 30 ml of nitrogen-reduced FAB medium containing *M. loti* DsRed (Figure 4, 5, 6, 7, 8, 9, 10, 11) or *M. loti* R7A CFP (Figure 3) set to a final optical density at 600 nm (OD₆₀₀) of 0.05. For Supplementary Figure 3 and 6, plants were grown in Weck jars (SKU 745 or 743) containing 300 ml of sand:vermiculite mixture (2:1) and 60 ml of nitrogen-reduced FAB medium containing *M. loti* DsRed or MAFF 303099 *lacZ* (*M. loti lacZ*) (OD₆₀₀ = 0.01).

For root organ liquid cultures, plants with emerging transformed roots were transferred to Fåhraeus medium (0.9 mM CaCl₂; 0.5 mM MgSO₄·7H₂O; 0.73 mM KH₂PO₄; 1.05 mM Na₂HPO₄; 20.4 µM C₆H₅FeO₇; 48.5 µM H₃BO₃; 10 µM MnSO₄·4H₂O; 1 µM ZnSO₄·7H₂O; 0.5 µM CuSO₄·5H₂O; 0.5 µM CoCl₂; 1 µM NaMoO₄·2H₂O; pH 6.5; hereafter referred to as FP medium) supplemented with 0.1 µM of the ethylene biosynthesis inhibitor L-α-(2-

aminoethoxyvinyl)-glycine and solidified with 1 % agar (Kalys, cat. no. HP696) in square plates two weeks post *A. rhizogenes* inoculation and kept on FP plates for two additional weeks. Primary root tips of 1.5 cm length were cut off and transferred to round Petri dishes (8.5 cm diameter) sealed with micropore tape (3M™ Health Care, cat. no. 1530-0) containing 18 ml of modified Strullu-Romand liquid medium ((Declerck et al., 1998); 0.73 mM Ca(NO₃)₂; 0.50 mM CaSO₄; 3 mM MgSO₄·7H₂O; 0.87 mM KCl; 30.13 μM KH₂PO₄; 2.03 mM NaFe-EDTA; 10.98 μM MnSO₄·4H₂O; 0.97 μM ZnSO₄·7H₂O; 29.92 μM H₃BO₃; 0.88 μM CuSO₄·5H₂O; 10.71 nM N₂MoO₄·2H₂O; 27.51 nM (NH₄)₆Mo₇O₂₄·4H₂O; 4.11 mM C₉H₁₇NO₅; 4.09 nM C₁₀H₁₆N₂O₃S; 8.12 μM C₆H₅NO₂; 5.32 μM C₈H₁₁NO₃; 3.77 μM C₁₂H₁₇N₄OS; 0.30 μM C₆₃H₈₉CoN₁₄O₁₄P; 29.21 mM C₁₂H₂₂O₁₁; hereafter referred to as MSR medium) and grown at 22 °C in the dark (Figure 15, 16, 18, 19, 20 and 21; Supplementary Figure 8). Number of emerged LR_s were scored every 10 days post transfer (dpt) to MSR medium. Sectioning was performed on transformed roots 10 dpt to MSR medium (Figure 19C). Roots were embedded in 6% low-melting agarose and sliced into 50 μm thick sections using a vibrating-blade microtome (Leica VT1000 S).

8.5. Phenotypic analysis and quantification of infection events

Infected and non-infected nodules were discriminated by the presence and absence of a *DsRed* signal (representing *M. loti DsRed*) detected or not detected inside of the nodules, respectively. Presence or absence of bacteria was later confirmed by examination of sections of representative nodules. Infection threads (ITs) and *M. loti* entrapments in root hairs were detected by their *DsRed* fluorescence (for microscope settings see Supplementary Table 2). For phenotypic analysis of *nin-15* (Figure 4), quantification was performed 21 days after inoculation (dpi) with *M. loti DsRed* as follows: (1) the total number of nodules (including infected and non-infected) was determined under white light illumination (WLI); (2) the number of infected nodules and root hair ITs were counted as described above.

For complementation experiments of *nin-2* and *nin-15* (Figure 5, 6, 7, 8, 9, 10 and 11; Supplementary Figure 4 and 5), quantifications and sectioning were performed 21 or 35 dpi with *M. loti DsRed* with the microscope settings listed in Supplementary Table 2 in the following order: (1) transgenic roots were identified by GFP fluorescence-emanating nuclei with a GFP filter; (2) infected nodules were counted as described above; (3) the total number of nodules (including infected and non-infected ones) was then determined under WLI; (4) the number of non-infected nodules was calculated by subtracting the number of infected nodules from the total number of nodules. To quantify infection events in root hairs, the number of bacterial entrapment and ITs in root hairs were counted on a 0.5 cm root piece for each transgenic root system, excised from a region where bacterial accumulation was detected by *DsRed* fluorescence. Sectioning was performed on non-infected and infected nodules and the presence/absence of ITs and symbiosomes in cortical cells was examined. Nodule primordia and nodules were embedded in 6% low-melting agarose and sliced into 40 - 50 μm thick sections using a vibrating-blade microtome (Leica VT1000 S).

8.6. Phenotypic analysis and quantification of primary root length and lateral root numbers under sterile conditions and symbiotic treatments

For phenotypic analyses, 7 days old seedlings were treated in the following ways:

(1) Lateral root number, primary root length and shoot dry weight under sterile conditions

Seedlings were transferred to sterile Weck jars (SKU 745, J.WECK GmbH u. Co. KG) containing 300 ml of dry sand:vermiculite mixture (2:1) and 20 ml of Hoagland's medium (1.5 mM KNO₃; pH 5.8) (Figure 4E and 17; Supplementary Figures 9 and 10). Weck jars were placed in a growth chamber at 24 °C under a 16 h/8 h light/dark regime (275 μmol.m⁻².s⁻¹). Seedlings were harvested 28 days (Figure 4E) or 30 days (Figure 17; Supplementary Figures 9 and 10) post germination and scanned at 800 dots per inch with a scanner (Epson V700). Emerged LRs were scored and the primary root length was measured for each plant with the ImageJ software (<https://fiji.sc>). Shoot dry weight was measured after drying the shoot at 60 °C for 1 h (Figure 4E).

(2) Lateral root number and primary root length upon rhizobia inoculation

Seedlings were transferred to open pots (7×7×8 cm) containing 200 ml of sand:vermiculite mixture (2:1) and watered with 40 ml of nitrogen-reduced FAB medium either without (mock treatment), or with *M. loti* MAFF 303099 set to a final OD₆₀₀ of 0.05 (*M. loti* treatment) immediately after transfer to pots, followed by 20 ml of nitrogen-reduced FAB medium every 2 days (Figures 12 and 13; Supplementary Figure 7). Open pots were placed in a growth chamber at 24 °C under a 16 h/8 h light/dark regime (275 μmol.m⁻².s⁻¹). Plants were harvested 10 days post inoculation and scanned at 800 dots per inch with a scanner (Epson V700). Emerged LRs were scored and the primary root length was measured for each plant with ImageJ.

(3) Lateral root number and primary root length upon AM inoculation

Seedlings were transferred to open pots (7×7×8 cm) containing 200 ml of sand:vermiculite mixture (2:1) and either 0.5 g of non-inoculated chive root pieces (mock treatment) or 0.5 g of chive root pieces inoculated with *R. irregularis* for 8 weeks (*R. irregularis* treatment) (Figures 12 and 13; Supplementary Figure 7). Seedlings were watered with 40 ml of Hoagland's medium (9 mM KNO₃; pH 5.8) immediately after transfer to pots, followed by 20 ml of Hoagland's medium (9 mM KNO₃; pH 5.8) every 2 days. Open pots were placed in a growth chamber at 24 °C under a 16 h/8 h light/dark regime (178 μmol.m⁻².s⁻¹). Plants were harvested 10 days post treatment and scanned at 800 dots per inch with a scanner (Epson V700). Emerged LRs were scored and the primary root length was measured for each plant with ImageJ.

8.7. Promoter activity analysis

For promoter activity analyses with fluorescent reporters (Figure 3), transgenic root systems were harvested 10 - 14 dpi. Nodule primordia with bacterial infection at stage 3 or

4 (see section 6.1.2 for stage description) were selected by locating the CFP signal (*M. loti* R7A CFP) via rapid (around 10 seconds) Z-stack analysis with the confocal light scanning microscope (Supplementary Table 2). Nodule primordia were embedded in 6% low-melting agarose, sliced into 40 - 50 μm thick sections using a vibrating-blade microtome (Leica VT1000 S) and imaged as described in Supplementary Table 2.

8.8. *Dryas drummondii* and *Fragaria vesca* growth conditions and root transformation

Seeds of *D. drummondii* were germinated as described in (Billault-Penneteau et al., 2019). Seeds of *F. vesca* were transferred to spin columns and treated for 5 min with concentrated H_2SO_4 . Columns were spun in Eppendorf tubes for 30 seconds at 20,000 g to separate the H_2SO_4 from the seed, rinsed 5 times with sterile deionized water and incubated at 4 °C for 5 h under agitation. Seeds were germinated on deionized water solidified with 0.8 % Bacto™ agar (Becton Dickinson and Co.) in square plates and placed in a Panasonic growth chamber at 22 °C under a 16 h/8 h light/dark regime (50 $\mu\text{mol.m}^{-2}.\text{s}^{-1}$).

D. drummondii hairy root transformation was performed as described in (Billault-Penneteau et al., 2019). Transgenic hairy roots in *F. vesca* were induced by *A. rhizogenes* strain AR1193 (Stougaard et al., 1987). Transformation was performed by cutting 12 days old *F. vesca* seedlings on filter paper soaked with bacterial suspension. Seedlings were kept in the dark at 18 °C for 3 days and then placed in a Panasonic growth chamber at 22°C under a 16 h light/8 h dark regime (50 $\mu\text{mol.m}^{-2}.\text{s}^{-1}$). *D. drummondii* *A. rhizogenes*-transformed composite plants were grown on Hoagland's medium (1 mM KNO_3 ; pH 5.8) solidified with 0.4 % Gelrite™ (Duchefa) in square plates. *F. vesca* *A. rhizogenes*-transformed composite plants were grown on Gamborg's B5 medium (Gamborg et al., 1968) solidified with 0.8 % Bacto™ agar (Becton Dickinson and Co.) in square plates for three days and then transferred to Gamborg's B5 medium supplemented with 300 $\mu\text{g.l}^{-1}$ of cefotaxime. Thirty days post cutting, *F. vesca* composite plants were transferred to Hoagland's medium (1 mM KNO_3 ; pH 5.8) solidified with 0.4 % Gelrite™ (Duchefa). Forty-five and forty-two days post cutting, *D. drummondii* and *F. vesca* composite plants, respectively, were transferred to sterile Weck jars (SKU 745, J.WECK GmbH u. Co. KG) containing 300 g of clay pebbles (Leca) and 50 ml of Hoagland's medium (100 μM KNO_3 ; 250 μM KH_2PO_4 ; pH 5.8) (Figure 22). Twenty and twenty-three days after transfer to the Weck jars, *D. drummondii* and *F. vesca* composite plants, respectively, were harvested and scanned at 800 dots per inch with a scanner (Epson V700). Emerged LR's were scored and the primary root length was measured for each plant with ImageJ.

8.9. Cloning and DNA constructs

A detailed description of constructs and a list of oligonucleotides can be found in Supplementary Table 3 and Supplementary Table 4, respectively. Constructs were generated with the Golden Gate cloning system (Binder et al., 2014) and the Invitrogen's GATEWAY™ cloning system. For the construction of promoter:*NIN* fusions for complementation experiments (Figure 5, 6, 7, 8, 9, 10 and 11; Supplementary Figure 4 and 5), the *NIN* genomic sequence without the 5' and 3'UTRs served as a cloning module. A 3 kb region of the *L. japonicus* *NIN* promoter plus the 244 bp *NIN* 5'UTR was cloned from *L. japonicus* Gifu and used for complementation experiments (Figure 4, 5, 6, 7, 8 and 9; Supplementary Figure 4 and 5), dual luciferase assays (Supplementary Figure 1), fluorimetric GUS assay (Supplementary Figure 2) and promoter activity analysis (Figure 3; Supplementary Figure 3). For all the other versions of the *L. japonicus* *NIN* promoter tested (Figure 3, 4, 5, 6, 7, 8, 9, 10 and 11; Supplementary Figure 2, 3, 4, 5 and 6), the *LjNIN* minimal promoter (98 bp (Singh et al., 2014)) plus the *LjNIN* 5'UTR was fused to 3' end of the promoter. A 472 bp region containing multiple cytokinin response elements and highly conserved in eight legume species was identified 5' of the *NIN* transcriptional start site by Liu et al. (Liu et al., 2019c). We used this conserved region of 472 bp from *L. japonicus* and added flanking regions (192 bp upstream and 366 bp downstream; 2399 bp upstream and 2231 bp downstream, respectively) to obtain cytokinin element-containing regions of 1 kb and 5 kb (*CE_{1kb}* and *CE_{5kb}*, respectively). The *Solanum lycopersicum* gene ID Solyc01g112190.2.1 was identified as the closest homologue of *LjNIN* gene based on phylogenetic analysis (Griesmann et al., 2018), and is referred to as *SININ*. A 3 kb region of the *SININ* promoter plus the 238 bp *SININ* 5'UTR was cloned from *S. lycopersicum* cv. "MoneyMaker" and *PACE* or *mPACE* (Supplementary Figure 2A) was inserted 184 bp upstream of the *SININ* 5'UTR and used for complementation experiments (Figure 10 and 11), dual luciferase assays (Supplementary Figure 1) and fluorimetric GUS assay (Supplementary Figure 2).

8.10. Imaging

Microscope and scanner settings as well as parameters for image acquisition are listed in Supplementary Table 2.

8.11. Data visualization and statistical analysis

Statistical analyses and data visualization were performed with RStudio 1.1.383 (RStudio Inc.). Boxplots were used to display data in Figure 4, 6, 7, 9, 10 and 11 and Supplementary Figure 1, 3 and 4 (thick black or white lines: median; box: interquartile range; whiskers: lowest and highest data point within 1.5 interquartile range (IQR); black filled circles, data

points inside 1.5 IQR; white filled circles, data points outside 1.5 IQR of the upper/lower quartile). Violin plots were used to display data in Figure 12, 13, 14, 15, 16, 17 18, 19, 20, 21 and 22 and Supplementary Figure 7, 8, 9 and 10 (outline of the violin plots, probability of the kernel density; thick black lines, median; box, interquartile range; whiskers, lowest and highest data point within 1.5 IQR; black filled circles, data points outside 1.5 IQR of the upper/lower quartile. The R package “beeswarm” with the method “center” was used to plot the individual data points for the boxplots (<http://CRAN.R-project.org/package=beeswarm>). The R package “ggplot2” was used to generate the violin plots (<https://cran.r-project.org/web/packages/ggplot2/index.html>). The R package “agricolae” was used to perform ANOVA statistical analysis with *post hoc* Tukey and statistical results were displayed in small letters where different letters indicated statistical significance (<https://cran.rproject.org/web/packages/agricolae/index.html>). Tests applied are stated in the figure legend.

9. References

- Ané, J.M. et al. (2004). *Medicago truncatula* DMI1 required for bacterial and fungal symbioses in legumes. *Science* **303**: 1364–1367.
- Arrighi, J.F., Godfroy, O., De Billy, F., Saurat, O., Jauneau, A., and Gough, C. (2008). The RPG gene of *Medicago truncatula* controls *Rhizobium*-directed polar growth during infection. *Proc. Natl. Acad. Sci. U. S. A.* **105**: 9817–9822.
- Bago, B., Pfeffer, P., and Shachar-hill, Y. (2000). Carbon metabolism and transport in arbuscular mycorrhizas. *Plant Physiol.* **124**: 949–957.
- Banba, M., Gutjahr, C., Miyao, A., Hirochika, H., Paszkowski, U., Kouchi, H., and Imaizumi-Anraku, H. (2008). Divergence of evolutionary ways among common sym genes: CASTOR and CCaMK show functional conservation between two symbiosis systems and constitute the root of a common signaling pathway. *Plant Cell Physiol.* **49**: 1659–1671.
- Bell, C.D., Soltis, D.E., and Soltis, P.S. (2010). The age and diversification of the angiosperms re-revisited. *Am. J. Bot.* **97**: 1296–1303.
- Bensmihen, S. (2015). Hormonal control of lateral root and nodule development in legumes. *Plants* **4**: 523–547.
- Beringer, J.E. (1974). R factor transfer in *Rhizobium leguminosarum*. *J. Gen. Microbiol.* **84**: 188–198.
- Billault-Penneteau, B., Sandré, A., Folgmann, J., Parniske, M., and Pawlowski, K. (2019). *Dryas* as a model for studying the root symbioses of the rosaceae. *Front. Plant Sci.* **10**: 1–13.
- Binder, A., Lambert, J., Morbitzer, R., Popp, C., Ott, T., Lahaye, T., and Parniske, M. (2014). A modular plasmid assembly kit for multigene expression, gene silencing and silencing rescue in plants. *PLoS One* **9**.
- Bonaldi, K., Gargani, D., Prin, Y., Fardoux, J., Gully, D., Nouwen, N., Goormachtig, S., and Giraud, E. (2011). Nodulation of *Aeschynomene afraspera* and *A. indica* by photosynthetic *Bradyrhizobium* Sp. strain ORS285: the Nod-dependent versus the Nod-independent symbiotic interaction. *Mol. Plant-Microbe Interact.* **24**: 1359–1371.
- Bravo, A., Brands, M., Wewer, V., Dörmann, P., and Harrison, M.J. (2017). Arbuscular mycorrhiza-specific enzymes FatM and RAM2 fine-tune lipid biosynthesis to promote development of arbuscular mycorrhiza. *New Phytol.* **214**: 1631–1645.
- Breakspear, A., Liu, C., Roy, S., Stacey, N., Rogers, C., Trick, M., Morieri, G., Mysore, K.S., Wen, J., Oldroyd, G.E.D., Downie, J.A., and Murray, J.D. (2014). The root hair “infectome” of *Medicago truncatula* uncovers changes in cell cycle genes and reveals a requirement for auxin signaling in rhizobial infection. *Plant Cell* **26**: 4680–4701.
- Bright, L.J., Liang, Y., Mitchell, D.M., and Harris, J.M. (2005). The *LATD* gene of *Medicago truncatula* is required for both nodule and root development. *Mol. Plant-Microbe Interact.* **18**: 521–532.
- Broghammer, A. et al. (2012). Legume receptors perceive the rhizobial lipochitin oligosaccharide signal molecules by direct binding. *Proc. Natl. Acad. Sci. U. S. A.* **109**: 13859–13864.
- Van Brussel, A.A.N., Bakhuizen, R., Van Spronsen, P.C., Spaink, H.P., Tak, T., Lugtenberg, B.J.J., and Kijne, J.W. (1992). Induction of pre-infection thread structures in the leguminous host plant by mitogenic lipo-oligosaccharides of rhizobium. *Science* **257**: 70–72.

- Bu, F., Rutten, L., Roswanjaya, Y.P., Kulikova, O., Rodriguez-Franco, M., Ott, T., Bisseling, T., van Zeijl, A., and Geurts, R.** (2020). Mutant analysis in the nonlegume *Parasponia andersonii* identifies NIN and NF-YA1 transcription factors as a core genetic network in nitrogen-fixing nodule symbioses. *New Phytol.* **226**: 541–554.
- Buecker, C. and Wysocka, J.** (2012). Enhancers as information integration hubs in development: lessons from genomics. *Trends Genet.* **28**: 276–284.
- Capoen, W., Sun, J., Wysham, D., Otegui, M.S., Venkateshwaran, M., Hirsch, S., Miwa, H., Downie, J.A., Morris, R.J., Ané, J.M., and Oldroyd, G.E.D.** (2011). Nuclear membranes control symbiotic calcium signaling of legumes. *Proc. Natl. Acad. Sci. U. S. A.* **108**: 14348–14353.
- Carbonnel, S. and Gutjahr, C.** (2014). Control of arbuscular mycorrhiza development by nutrient signals. *Front. Plant Sci.* **5**: 1–5.
- Caretti, G., Salsi, V., Vecchi, C., Imbriano, C., and Mantovani, R.** (2003). Dynamic recruitment of NF-Y and histone acetyltransferases on cell-cycle promoters. *J. Biol. Chem.* **278**: 30435–30440.
- Carvalho, T.L.G., Balsemão-Pires, E., Saraiva, R.M., Ferreira, P.C.G., and Hemerly, A.S.** (2014). Nitrogen signalling in plant interactions with associative and endophytic diazotrophic bacteria. *J. Exp. Bot.* **65**: 5631–5642.
- Catalano, C.M., Czymmek, K.J., Gann, J.G., and Sherrier, D.J.** (2007). *Medicago truncatula* syntaxin SYP132 defines the symbiosome membrane and infection droplet membrane in root nodules. *Planta* **225**: 541–550.
- Catoira, R., Galera, C., De Billy, F., Penmetsa, R. V., Journet, E.P., Maillet, F., Rosenberg, C., Cook, D., Gough, C., and Denarie, J.** (2000). Four genes of *Medicago truncatula* controlling components of a Nod factor transduction pathway. *Plant Cell* **12**: 1647–1665.
- Cerri, M.R. et al.** (2017). The *ERN1* transcription factor gene is a target of the CCaMK/CYCLOPS complex and controls rhizobial infection in *Lotus japonicus*. *New Phytol.* **215**: 323–337.
- Chabaud, M., Genre, A., Sieberer, B.J., Faccio, A., Fournier, J., Novero, M., Barker, D.G., and Bonfante, P.** (2011). Arbuscular mycorrhizal hyphopodia and germinated spore exudates trigger Ca²⁺ spiking in the legume and nonlegume root epidermis. *New Phytol.* **189**: 347–355.
- Chakraborty, S., Valdés-López, O., Stonoha-Arther, C., and Ané, J.-M.** (2022). Transcription factors controlling the rhizobium–legume symbiosis: integrating infection, organogenesis and the abiotic environment. *Plant Cell Physiol.* **00**: 1–18.
- Chardin, C., Girin, T., Roudier, F., Meyer, C., and Krapp, A.** (2014). The plant RWP-RK transcription factors: key regulators of nitrogen responses and of gametophyte development. *J. Exp. Bot.* **65**: 5577–5587.
- Charpentier, M.** (2018). Calcium signals in the plant nucleus: origin and function. *J. Exp. Bot.* **69**: 4165–4173.
- Charpentier, M., Bredemeier, R., Wanner, G., Takeda, N., Schleiff, E., and Parniske, M.** (2008). *Lotus japonicus* Castor and Pollux are ion channels essential for perinuclear calcium spiking in legume root endosymbiosis. *Plant Cell* **20**: 3467–3479.
- Charpentier, M. and Oldroyd, G.** (2010). How close are we to nitrogen-fixing cereals? *Curr. Opin. Plant Biol.* **13**: 556–564.
- Charpentier, M., Sun, J., Martins, T.V., Radhakrishnan, G. V, Findlay, K., Soumpourou, E., Thouin, J., Véry, A., Sanders, D., Morris, R.J., and Oldroyd, G.E.D.** (2016). Nuclear-localized cyclic nucleotide-gated channels mediate symbiotic calcium

- oscillations. *Science* **352**: 1102–5.
- Chaulagain, D. and Frugoli, J.** (2021). The regulation of nodule number in legumes is a balance of three signal transduction pathways. *Int. J. Mol. Sci.* **22**: 1–14.
- Chen, C., Ané, J.M., and Zhu, H.** (2008a). OsIPD3, an ortholog of the *Medicago truncatula* DMI3 interacting protein IPD3, is required for mycorrhizal symbiosis in rice. *New Phytol.* **180**: 311–315.
- Chen, C., Gao, M., Liu, J., and Zhu, H.** (2007). Fungal symbiosis in rice requires an ortholog of a legume common symbiosis gene encoding a Ca²⁺/calmodulin-dependent protein kinase. *Plant Physiol.* **145**: 1619–1628.
- Chen, Y.F., Wang, Y., and Wu, W.H.** (2008b). Membrane transporters for nitrogen, phosphate and potassium uptake in plants. *J. Integr. Plant Biol.* **50**: 835–848.
- Choudhury, S.R. and Pandey, S.** (2015). Phosphorylation-dependent regulation of G-protein cycle during nodule formation in soybean. *Plant Cell* **27**: 3260–3276.
- Clavijo, F. et al.** (2015). The *Casuarina* *NIN* gene is transcriptionally activated throughout *Frankia* root infection as well as in response to bacterial diffusible signals. *New Phytol.* **208**: 887–903.
- Colebatch, G., Desbrosses, G., Ott, T., Krusell, L., Montanari, O., Kloska, S., Kopka, J., and Udvardi, M.K.** (2004). Global changes in transcription orchestrate metabolic differentiation during symbiotic nitrogen fixation in *Lotus japonicus*. *Plant J.* **39**: 487–512.
- Combiér, J.P., De Billy, F., Gamas, P., Niebel, A., and Rivas, S.** (2008). Trans-regulation of the expression of the transcription factor *MtHAP2-1* by a uORF controls root nodule development. *Genes Dev.* **22**: 1549–1559.
- Coronado, C., Zuanazzi, J.A.S., Sallaud, C., Quirion, J.C., Esnault, R., Husson, H.P., Kondorosi, A., and Ratet, P.** (1995). Alfalfa root flavonoid production is nitrogen regulated. *Plant Physiol.* **108**: 533–542.
- Couzigou, J.M. et al.** (2012). *NODULE ROOT* and *COCHLEATA* maintain nodule development and are legume orthologs of Arabidopsis *BLADE-ON-PETIOLE* genes. *Plant Cell* **24**: 4498–4510.
- D’Haeze, W., Gao, M., De Rycke, R., Van Montagu, M., Engler, G., and Holsters, M.** (1998). Roles for azorhizobial nod factors and surface polysaccharides in intercellular invasion and nodule penetration, respectively. *Mol. Plant-Microbe Interact.* **11**: 999–1008.
- Das, D., Paries, M., Hobecker, K., Gigl, M., Dawid, C., Lam, H.M., Zhang, J., Chen, M., and Gutjahr, C.** (2022). PHOSPHATE STARVATION RESPONSE transcription factors enable arbuscular mycorrhiza symbiosis. *Nat. Commun.* **13**.
- Das, D.R., Horváth, B., Kundu, A., Kaló, P., and DasGupta, M.** (2019). Functional conservation of CYCLOPS in crack entry legume *Arachis hypogaea*. *Plant Sci.* **281**: 232–241.
- Deakin, W.J. and Broughton, W.J.** (2009). Symbiotic use of pathogenic strategies: rhizobial protein secretion systems. *Nat. Rev. Microbiol.* **7**: 312–320.
- Declerck, S., Strullu, D.G., and Plenchette, C.** (1998). Monoxenic culture of the intraradical forms of *Glomus* sp. isolated from a tropical ecosystem: a proposed methodology for germplasm collection. *Mycologia* **90**: 579–585.
- Delaux, P.M. et al.** (2015). Algal ancestor of land plants was preadapted for symbiosis. *Proc. Natl. Acad. Sci. U. S. A.* **112**: 13390–13395.
- Delaux, P.M., Varala, K., Edger, P.P., Coruzzi, G.M., Pires, J.C., and Ané, J.M.** (2014). Comparative phylogenomics uncovers the impact of symbiotic associations on host

- genome evolution. *PLoS Genet.* **10**.
- Diaz, R.J. and Rosenberg, R.** (2008). Spreading dead zones and consequences for marine ecosystems. *Science* **321**: 926–929.
- Dong, W. et al.** (2021). An SHR–SCR module specifies legume cortical cell fate to enable nodulation. *Nature* **589**: 586–590.
- Doyle, J.J.** (2016). Chasing unicorns: nodulation origins and the paradox of novelty. *Am. J. Bot.* **103**: 1865–1868.
- Doyle, J.J.** (2011). Phylogenetic perspectives on the origins of nodulation. *Mol. Plant-Microbe Interact.* **24**: 1289–1295.
- Ehrhardt, D.W., Morrey Atkinson, E., and Long, S.R.** (1992). Depolarization of alfalfa root hair membrane potential by *Rhizobium meliloti* nod factors. *Science* **256**: 998–1000.
- Ehrhardt, D.W., Wais, R., and Long, S.R.** (1996). Calcium spiking in plant root hairs responding to rhizobium modulation signals. *Cell* **85**: 673–681.
- Erisman, J.W., Galloway, J.N., Seitzinger, S., Bleeker, A., Dise, N.B., Roxana Petrescu, A.M., Leach, A.M., and de Vries, W.** (2013). Consequences of human modification of the global nitrogen cycle. *Philos. Trans. R. Soc. B Biol. Sci.* **368**.
- Erisman, J.W., Sutton, M.A., Galloway, J., Klimont, Z., and Winiwarter, W.** (2008). How a century of ammonia synthesis changed the world. *Nat. Geosci.* **1**: 636–639.
- Esseling, J.J., Lhuissier, F.G.P., and Emons, A.M.C.** (2003). Nod factor-induced root hair curling: continuous polar growth towards the point of nod factor application. *Plant Physiol.* **132**: 1982–1988.
- Fabre, S., Gully, D., Poitout, A., Patrel, D., Arrighi, J.F., Giraud, E., Czernic, P., and Cartieaux, F.** (2015). Nod factor-independent nodulation in *Aeschynomene evenia* required the common plant-microbe symbiotic toolkit. *Plant Physiol.* **169**: 2654–2664.
- De Faria, S.M., Hay, G.T., and Sprent, J.I.** (1988). Entry of rhizobia into roots of *Mimosa scabrella* Benth occurs between epidermal cells. *Microbiology* **134**: 2291–2296.
- Feng, J., Lee, T., Schiessl, K., and Oldroyd, G.E.D.** (2021). Processing of NODULE INCEPTION controls the transition to nitrogen fixation in root nodules. *Science* **374**: 629–632.
- Ferraioli, S., Täte, R., Rogato, A., Chiurazzi, M., and Patriarca, E.J.** (2004). Development of ectopic roots from abortive nodule primordia. *Mol. Plant-Microbe Interact.* **17**: 1043–1050.
- Fliegmann, J. and Bono, J.J.** (2015). Lipo-chitooligosaccharidic nodulation factors and their perception by plant receptors. *Glycoconj. J.* **32**: 455–464.
- Fortin, J.A., Bécard, G., Declerck, S., Dalpé, Y., St-Arnaud, M., Coughlan, A.P., and Piché, Y.** (2002). Arbuscular mycorrhiza on root-organ cultures. *Can. J. Bot.* **80**: 1–20.
- Fournier, J. et al.** (2018). Cell remodeling and subtilase gene expression in the actinorhizal plant *Discaria trinervis* highlight host orchestration of intercellular *Frankia* colonization. *New Phytol.* **219**: 1018–1030.
- Fournier, J., Teillet, A., Chabaud, M., Ivanov, S., Genre, A., Limpens, E., Carvalho-Niebel, F. De, and Barker, D.G.** (2015). Remodeling of the infection chamber before infection thread formation reveals a two-step mechanism for rhizobial entry into the host legume root hair. *Plant Physiol.* **167**: 1233–1242.
- Fournier, J., Timmers, A.C.J., Sieberer, B.J., Jauneau, A., Chabaud, M., and Barker, D.G.** (2008). Mechanism of infection thread elongation in root hairs of *Medicago truncatula* and dynamic interplay with associated rhizobial colonization. *Plant Physiol.* **148**: 1985–1995.
- Gage, D.J.** (2002). Analysis of infection thread development using Gfp- and DsRed-

- expressing *Sinorhizobium meliloti*. J. Bacteriol. **184**: 7042–7046.
- Gamborg, O.L., Miller, R.A., and Ojima, K.** (1968). Nutrient requirements of suspension cultures of soybean root cells. Exp. Cell Res. **50**: 151–158.
- Gauthier-Coles, C., White, R.G., and Mathesius, U.** (2019). Nodulating legumes are distinguished by a sensitivity to cytokinin in the root cortex leading to pseudonodule development. Front. Plant Sci. **9**: 1–14.
- Genre, A., Chabaud, M., Balzergue, C., Puech-Pagès, V., Novero, M., Rey, T., Fournier, J., Rochange, S., Bécard, G., Bonfante, P., and Barker, D.G.** (2013). Short-chain chitin oligomers from arbuscular mycorrhizal fungi trigger nuclear Ca²⁺ spiking in *Medicago truncatula* roots and their production is enhanced by strigolactone. New Phytol. **198**: 190–202.
- Genre, A., Chabaud, M., Faccio, A., Barker, D.G., and Bonfante, P.** (2008). Prepenetration apparatus assembly precedes and predicts the colonization patterns of arbuscular mycorrhizal fungi within the root cortex of both *Medicago truncatula* and *Daucus carota*. Plant Cell **20**: 1407–1420.
- Genre, A., Chabaud, M., Timmers, T., Bonfante, P., and Barker, D.G.** (2005). Arbuscular mycorrhizal fungi elicit a novel intracellular apparatus in *Medicago truncatula* root epidermal cells before infection. Plant Cell **17**: 3489–3499.
- Geurts, R., Xiao, T.T., and Reinhold-Hurek, B.** (2016). What does it take to evolve a nitrogen-fixing endosymbiosis? Trends Plant Sci. **21**: 199–208.
- Gherbi, H., Markmann, K., Svistoonoff, S., Estevan, J., Autran, D., Giczey, G., Auguy, F., Péret, B., Laplaze, L., Franche, C., Parniske, M., and Bogusz, D.** (2008). SymRK defines a common genetic basis for plant root endosymbioses with arbuscular mycorrhiza fungi, rhizobia, and *Frankia* bacteria. Proc. Natl. Acad. Sci. U. S. A. **105**: 4928–4932.
- Gianinazzi, S., Gollotte, A., Binet, M.N., van Tuinen, D., Redecker, D., and Wipf, D.** (2010). Agroecology: the key role of arbuscular mycorrhizas in ecosystem services. Mycorrhiza **20**: 519–530.
- Gleason, C., Chaudhuri, S., Yang, T., Muñoz, A., Poovaiah, B.W., and Oldroyd, G.E.D.** (2006). Nodulation independent of rhizobia induced by a calcium-activated kinase lacking autoinhibition. Nature **441**: 1149–1152.
- Godfroy, O., Debellé, F., Timmers, T., and Rosenberg, C.** (2006). A rice calcium- and calmodulin-dependent protein kinase restores nodulation to a legume mutant. Mol. Plant-Microbe Interact. **19**: 495–501.
- Goh, T. et al.** (2019). Lateral root initiation requires the sequential induction of transcription factors LBD16 and PUCHI in *Arabidopsis thaliana*. New Phytol. **224**: 749–760.
- Goh, T., Joi, S., Mimura, T., and Fukaki, H.** (2012). The establishment of asymmetry in *Arabidopsis* lateral root founder cells is regulated by LBD16/ASL18 and related LBD/ASL proteins. Development **139**: 883–893.
- Gonzalez-Rizzo, S., Crespi, M., and Frugier, F.** (2006). The *Medicago truncatula* CRE1 cytokinin receptor regulates lateral root development and early symbiotic interaction with *Sinorhizobium meliloti*. Plant Cell **18**: 2680–2693.
- Gossmann, J.A., Markmann, K., Brachmann, A., Rose, L.E., and Parniske, M.** (2012). Polymorphic infection and organogenesis patterns induced by a *Rhizobium leguminosarum* isolate from *Lotus* root nodules are determined by the host genotype. New Phytol. **196**: 561–573.
- Granqvist, E., Sun, J., Op den Camp, R., Pujic, P., Hill, L., Normand, P., Morris, R.J., Downie, J.A., Geurts, R., and Oldroyd, G.E.D.** (2015). Bacterial-induced calcium

- oscillations are common to nitrogen-fixing associations of nodulating legumes and nonlegumes. *New Phytol.* **207**: 551–558.
- Griesmann, M. et al.** (2018). Phylogenomics reveals multiple losses of the nitrogen-fixing root nodule symbiosis. *Science* **13**.
- Groth, M., Takeda, N., Perry, J., Uchid, H., Dräxl, S., Brachmann, A., Sato, S., Tabata, S., Kawaguchi, M., Wang, T.L., and Parniske, M.** (2010). *NENA*, a *Lotus japonicus* homolog of *Sec13*, is required for rhizodermal infection by arbuscular mycorrhizal fungi and rhizobia but dispensable for cortical endosymbiotic development. *Plant Cell* **22**: 2509–2526.
- Guan, D. et al.** (2013). Rhizobial infection is associated with the development of peripheral vasculature in nodules of *Medicago truncatula*. *Plant Physiol.* **162**: 107–115.
- Guillot, B., Couzigou, J.M., and Combier, J.P.** (2016). NIN is involved in the regulation of arbuscular mycorrhizal symbiosis. *Front. Plant Sci.* **7**: 1–7.
- Gutjahr, C., Banba, M., Croset, V., An, K., Miyao, A., An, G., Hirochika, H., Imaizumi-Anraku, H., and Paszkowski, U.** (2008). Arbuscular mycorrhiza-specific signaling in rice transcends the common symbiosis signaling pathway. *Plant Cell* **20**: 2989–3005.
- Gutjahr, C., Casieri, L., and Paszkowski, U.** (2009a). *Glomus intraradices* induces changes in root system architecture of rice independently of common symbiosis signaling. *New Phytol.* **182**: 829–837.
- Gutjahr, C., Novero, M., Guether, M., Montanari, O., Udvardi, M., and Bonfante, P.** (2009b). Presymbiotic factors released by the arbuscular mycorrhizal fungus *Gigaspora margarita* induce starch accumulation in *Lotus japonicus* roots. *New Phytol.* **183**: 53–61.
- Gutjahr, C. and Parniske, M.** (2013). Cell and developmental biology of arbuscular mycorrhiza symbiosis. *Annu. Rev. Cell Dev. Biol.* **29**: 593–617.
- Gutjahr, C. and Paszkowski, U.** (2013). Multiple control levels of root system remodeling in arbuscular mycorrhizal symbiosis. *Front. Plant Sci.* **4**: 1–8.
- Handberg, K. and Stougaard, J.** (1992). *Lotus japonicus*, an autogamous, diploid legume species for classical and molecular genetics. *Plant J.* **2**: 487–496.
- Harris, J.M.** (2015). Abscisic acid: hidden architect of root system structure. *Plants* **4**: 548–572.
- Harrison, M.J. and Ivanov, S.** (2017). Exocytosis for endosymbiosis: membrane trafficking pathways for development of symbiotic membrane compartments. *Curr. Opin. Plant Biol.* **38**: 101–108.
- Hayashi, T., Banba, M., Shimoda, Y., Kouchi, H., Hayashi, M., and Imaizumi-Anraku, H.** (2010). A dominant function of CCaMK in intracellular accommodation of bacterial and fungal endosymbionts. *Plant J.* **63**: 141–154.
- Heckmann, A.B., Lombardo, F., Miwa, H., Perry, J.A., Bunnewell, S., Parniske, M., Wang, T.L., and Downie, J.A.** (2006). *Lotus japonicus* nodulation requires two GRAS domain regulators, one of which is functionally conserved in a non-legume. *Plant Physiol.* **142**: 1739–1750.
- Heckmann, A.B., Sandal, N., Bek, A.S., Madsen, L.H., Jurkiewicz, A., Nielsen, M.W., Tirichine, L., and Stougaard, J.** (2011). Cytokinin induction of root nodule primordia in *Lotus japonicus* is regulated by a mechanism operating in the root cortex. *Mol. Plant-Microbe Interact.* **24**: 1385–1395.
- Heidstra, R., Geurts, R., Franssen, H., Spaink, H.P., Van Kammen, A., and Bisseling, T.** (1994). Root hair deformation activity of nodulation factors and their fate on *Vicia sativa*. *Plant Physiol.* **105**: 787–797.
- Helber, N., Wippel, K., Sauer, N., Schaarschmidt, S., Hause, B., and Requena, N.** (2011).

- A versatile monosaccharide transporter that operates in the arbuscular mycorrhizal fungus *Glomus* sp is crucial for the symbiotic relationship with plants. *Plant Cell* **23**: 3812–3823.
- Herendeen, P.S., Magallon-Puebla, S., Lupia, R., Crane, P.R., and Kobylinska, J.** (1999). A preliminary conspectus of the allon flora from the late cretaceous (Late Santonian) of central Georgia, U.S.A. *Ann. Missouri Bot. Gard.* **86**: 407–471.
- Herrbach, V., Chirinos, X., Rengel, D., Agbevenou, K., Vincent, R., Pateyron, S., Huguet, S., Balzergue, S., Pasha, A., Provart, N., Gough, C., and Bensmihen, S.** (2017). Nod factors potentiate auxin signaling for transcriptional regulation and lateral root formation in *Medicago truncatula*. *J. Exp. Bot.* **68**: 569–583.
- Herrbach, V., Remblière, C., Gough, C., and Bensmihen, S.** (2014). Lateral root formation and patterning in *Medicago truncatula*. *J. Plant Physiol.* **171**: 301–310.
- Hirsch, A.M. and Larue, T.A.** (1997). Is the legume nodule a modified root or stem or an organ sui generis? *CRC. Crit. Rev. Plant Sci.* **16**: 361–392.
- Hirsch, S., Kim, J., Muñoz, A., Heckmann, A.B., Downie, J.A., and Oldroyd, G.E.D.** (2009). GRAS proteins form a DNA binding complex to induce gene expression during nodulation signaling in *Medicago truncatula*. *Plant Cell* **21**: 545–557.
- Hoagland, D.R. and Arnon, D.I.** (1938). The water-culture method for growing plants without soil. Circular California Agricultural Experiment Station 347, ed. 2, Berkeley: University of California.
- Hoffman, B.M., Lukoyanov, D., Yang, Z.Y., Dean, D.R., and Seefeldt, L.C.** (2014). Mechanism of nitrogen fixation by nitrogenase: The next stage. *Chem. Rev.* **114**: 4041–4062.
- Horváth, B. et al.** (2011). *Medicago truncatula* *IPD3* is a member of the common symbiotic signaling pathway required for rhizobial and mycorrhizal symbioses. *Mol. Plant-Microbe Interact.* **24**: 1345–1358.
- Huisman, R., Hontelez, J., Mysore, K.S., Wen, J., Bisseling, T., and Limpens, E.** (2016). A symbiosis-dedicated SYNTAXIN OF PLANTS 13II isoform controls the formation of a stable host-microbe interface in symbiosis. *New Phytol.* **211**: 1338–1351.
- Imaizumi-Anraku, H. et al.** (2005). Plastid proteins crucial for symbiotic fungal and bacterial entry into plant roots. *Nature* **433**: 527–531.
- Ivanov, S., Fedorova, E.E., Limpens, E., De Mita, S., Genre, A., Bonfante, P., and Bisseling, T.** (2012). *Rhizobium*-legume symbiosis shares an exocytotic pathway required for arbuscule formation. *Proc. Natl. Acad. Sci. U. S. A.* **109**: 8316–8321.
- Javot, H., Pumplin, N., and Harrison, M.J.** (2007). Phosphate in the arbuscular mycorrhizal symbiosis: transport properties and regulatory roles. *Plant, Cell Environ.* **30**: 310–322.
- Jiang, Y., Wang, W., Xie, Q., Liu, N., Liu, L., Wang, D., Zhang, X., Yang, C., Chen, X., Tang, D., and Wang, E.** (2017). Plants transfer lipids to sustain colonization by mutualistic mycorrhizal and parasitic fungi. *Science* **356**: 1172–1173.
- Jin, Y., Liu, H., Luo, D., Yu, N., Dong, W., Wang, C., Zhang, X., Dai, H., Yang, J., and Wang, E.** (2016). DELLA proteins are common components of symbiotic rhizobial and mycorrhizal signalling pathways. *Nat. Commun.* **7**.
- Joner, E.J., Ravnskov, S., and Jakobsen, I.** (2000). Arbuscular mycorrhizal phosphate transport under monoxenic conditions using radio-labelled inorganic and organic phosphate. *Biotechnol. Lett.* **22**: 1705–1708.
- Journet, E.P., El-Gachtouli, N., Vernoud, V., De Billy, F., Pichon, M., Dedieu, A., Arnould, C., Morandi, D., Barker, D.G., and Gianinazzi-Pearson, V.** (2001). *Medicago truncatula* *ENOD11*: a novel RPRP-encoding early nodulin gene expressed during

- mycorrhization in arbuscule-containing cells. *Mol. Plant-Microbe Interact.* **14**: 737–748.
- Kakouridis, A., Hagen, J.A., Kan, M.P., Mambelli, S., Feldman, L.J., Herman, D.J., Weber, P.K., Pett-Ridge, J., and Firestone, M.K.** (2022). Routes to roots: direct evidence of water transport by arbuscular mycorrhizal fungi to host plants.
- Kaló, P. et al.** (2005). Nodulation signaling in legumes requires NSP2, a member of the GRAS family of transcriptional regulators. *Science* **308**: 1786–1789.
- Kanamori, N. et al.** (2006). A nucleoporin is required for induction of Ca²⁺ spiking in legume nodule development and essential for rhizobial and fungal symbiosis. *Proc. Natl. Acad. Sci. U. S. A.* **103**: 359–364.
- Kang, H., Hong, Z., and Zhang, Z.** (2013). A MYB transcription factor interacts with NSP2 and is involved in nodulation in *Lotus japonicus*. *Biol. Nitrogen Fixat.* **2–2**: 599–607.
- Kang, H., Zhu, H., Chu, X., Yang, Z., Yuan, S., Yu, D., Wang, C., Hong, Z., and Zhang, Z.** (2011). A novel interaction between CCaMK and a protein containing the scythe_N ubiquitin-like domain in *Lotus japonicus*. *Plant Physiol.* **155**: 1312–1324.
- Kawaharada, Y. et al.** (2015). Receptor-mediated exopolysaccharide perception controls bacterial infection. *Nature* **523**: 308–312.
- Kawaharada, Y., Nielsen, M.W., Kelly, S., James, E.K., Andersen, K.R., Rasmussen, S.R., Füchtbauer, W., Madsen, L.H., Heckmann, A.B., Radutoiu, S., and Stougaard, J.** (2017). Differential regulation of the Epr3 receptor coordinates membrane-restricted rhizobial colonization of root nodule primordia. *Nat. Commun.* **8**.
- Kevei, Z. et al.** (2007). 3-Hydroxy-3-methylglutaryl coenzyme A reductase1 interacts with NORK and is crucial for nodulation in *Medicago truncatula*. *Plant Cell* **19**: 3974–3989.
- Keymer, A. et al.** (2017). Lipid transfer from plants to arbuscular mycorrhiza fungi. *Elife* **6**: 1–33.
- Kim, S., Zeng, W., Bernard, S., Liao, J., Venkateshwaran, M., Ane, J.M., and Jiang, Y.** (2019). Ca²⁺-regulated Ca²⁺ channels with an RCK gating ring control plant symbiotic associations. *Nat. Commun.* **10**: 1–12.
- Kistner, C. and Parniske, M.** (2002). Evolution of signal transduction in intracellular symbiosis. *Trends Plant Sci.* **7**: 511–518.
- Kistner, C., Winzer, T., Pitzschke, A., Mulder, L., Sato, S., Kaneko, T., Tabata, S., Sandal, N., Stougaard, J., Webb, K.J., Szczyglowski, K., and Parniske, M.** (2005). Seven *Lotus japonicus* genes required for transcriptional reprogramming of the root during fungal and bacterial symbiosis. *Plant Cell* **17**: 2217–2229.
- Konishi, M. and Yanagisawa, S.** (2013). Arabidopsis NIN-like transcription factors have a central role in nitrate signalling. *Nat. Commun.* **4**.
- Korasick, D.A., Chatterjee, S., Tonelli, M., Dashti, H., Lee, S.G., Westfall, C.S., Fulton, D.B., Andreotti, A.H., Amarasinghe, G.K., Strader, L.C., and Jez, J.M.** (2015). Defining a two-pronged structural model for PB1 (Phox/Bem1p) domain interaction in plant auxin responses. *J. Biol. Chem.* **290**: 12868–12878.
- Kosuta, S., Chabaud, M., Lougnon, G., Gough, C., Dénarié, J., Barker, D.G., and Bécard, G.** (2003). A diffusible factor from arbuscular mycorrhizal fungi induces symbiosis-specific *MtENOD11* expression in roots of *Medicago truncatula*. *Plant Physiol.* **131**: 952–962.
- Kosuta, S., Hazledine, S., Sun, J., Miwa, H., Morris, R.J., Downie, J.A., and Oldroyd, G.E.D.** (2008). Differential and chaotic calcium signatures in the symbiosis signaling pathway of legumes. *Proc. Natl. Acad. Sci. U. S. A.* **105**: 9823–9828.
- Kuhn, H., Küster, H., and Requena, N.** (2010). Membrane steroid-binding protein 1 induced by a diffusible fungal signal is critical for mycorrhization in *Medicago*

- truncatula*. *New Phytol.* **185**: 716–733.
- Kumar, A., Cousins, D.R., Liu, C.W., Xu, P., and Murray, J.D.** (2020). Nodule inception is not required for arbuscular mycorrhizal colonization of *Medicago truncatula*. *Plants* **9**: 1–9.
- Kvon, E.Z. et al.** (2016). Progressive loss of function in a limb enhancer during snake evolution. *Cell* **167**: 633–642.
- Laffont, C., Ivanovici, A., Gautrat, P., Brault, M., Djordjevic, M.A., and Frugier, F.** (2020). The NIN transcription factor coordinates CEP and CLE signaling peptides that regulate nodulation antagonistically. *Nat. Commun.* **11**: 1–13.
- Laporte, P., Lepage, A., Fournier, J., Catrice, O., Moreau, S., Jardinaud, M.F., Mun, J.H., Larrainzar, E., Cook, D.R., Gamas, P., and Niebel, A.** (2014). The CCAAT box-binding transcription factor NF-YA1 controls rhizobial infection. *J. Exp. Bot.* **65**: 481–494.
- Lévy, J. et al.** (2004). A putative Ca²⁺ and calmodulin-dependent protein kinase required for bacterial and fungal symbioses. *Science* **303**: 1361–1364.
- Li, H.L., Wang, W., Mortimer, P.E., Li, R.Q., Li, D.Z., Hyde, K.D., Xu, J.C., Soltis, D.E., and Chen, Z.D.** (2015). Large-scale phylogenetic analyses reveal multiple gains of actinorhizal nitrogen-fixing symbioses in angiosperms associated with climate change. *Sci. Rep.* **5**: 1–8.
- Li, X. et al.** (2019). Atypical receptor kinase RINRK1 required for rhizobial infection but not nodule development in *Lotus japonicus*. *Plant Physiol.* **181**: 804–816.
- Limpens, E. and Bisseling, T.** (2014). CYCLOPS: a new vision on rhizobium-induced nodule organogenesis. *Cell Host Microbe* **15**: 127–129.
- Liu, C.W. et al.** (2019a). A protein complex required for polar growth of rhizobial infection threads. *Nat. Commun.* **10**: 1–17.
- Liu, C.W. et al.** (2019b). NIN acts as a network hub controlling a growth module required for rhizobial infection. *Plant Physiol.* **179**: 1704–1722.
- Liu, C.W. and Murray, J.D.** (2016). The role of flavonoids in nodulation host-range specificity: an update. *Plants* **5**: 4045–4053.
- Liu, J. and Bisseling, T.** (2020). Evolution of NIN and NIN-like genes in relation to nodule symbiosis. *Genes (Basel)*. **11**: 1–15.
- Liu, J., Rasing, M., Zeng, T., Klein, J., Kulikova, O., and Bisseling, T.** (2021). NIN is essential for development of symbiosomes, suppression of defence and premature senescence in *Medicago truncatula* nodules.
- Liu, J., Rutten, L., Limpens, E., Van Der Molen, T., Van Velzen, R., Chen, R., Chen, Y., Geurts, R., Kohlen, W., Kulikova, O., and Bisseling, T.** (2019c). A remote *cis*-regulatory region is required for *NIN* expression in the pericycle to initiate nodule primordium formation in *Medicago truncatula*. *Plant Cell* **31**: 68–83.
- Luginbuehl, L.H., Menard, G.N., Kurup, S., Van Erp, H., Radhakrishnan, G. V., Breakspear, A., Oldroyd, G.E.D., and Eastmond, P.J.** (2017). Fatty acids in arbuscular mycorrhizal fungi are synthesized by the host plant. *Science* **356**: 1175–1178.
- Madsen, E.B., Madsen, L.H., Radutoiu, S., Olbryt, M., Rakwaska, M., Szczyglowski, K., Sato, S., Kaneko, T., Tabata, S., Sandal, N., and Stougaard, J.** (2003). A receptor kinase gene of the LysM type is involved in legume perception of rhizobial signals. *Nature* **425**: 637–640.
- Madsen, L.H., Tirichine, L., Jurkiewicz, A., Sullivan, J.T., Heckmann, A.B., Bek, A.S., Ronson, C.W., James, E.K., and Stougaard, J.** (2010). The molecular network governing nodule organogenesis and infection in the model legume *Lotus japonicus*. *Nat. Commun.* **1**.

- Maekawa, T., Kusakabe, M., Shimoda, Y., Sato, S., Tabata, S., Murooka, Y., and Hayashi, M. (2008). Polyubiquitin promoter-based binary vectors for overexpression and gene silencing in *Lotus japonicus*. *Mol. Plant-Microbe Interact.* **21**: 375–382.
- Maekawa, T., Maekawa-Yoshikawa, M., Takeda, N., Imaizumi-Anraku, H., Murooka, Y., and Hayashi, M. (2009). Gibberellin controls the nodulation signaling pathway in *Lotus japonicus*. *Plant J.* **58**: 183–194.
- Magne, K., George, J., Berbel Tornero, A., Broquet, B., Madueño, F., Andersen, S.U., and Ratet, P. (2018). *Lotus japonicus* *NOOT-BOP-COCH-LIKE1* is essential for nodule, nectary, leaf and flower development. *Plant J.* **94**: 880–894.
- Magori, S. and Kawaguchi, M. (2009). Long-distance control of nodulation: molecules and models. *Mol. Cells* **27**: 129–134.
- Maillet, F. et al. (2011). Fungal lipochitooligosaccharide symbiotic signals in arbuscular mycorrhiza. *Nature* **469**: 58–64.
- Malolepszy, A. et al. (2016). The *LORE1* insertion mutant resource. *Plant J.* **88**: 306–317.
- Marchive, C., Roudier, F., Castaings, L., Bréhaut, V., Blondet, E., Colot, V., Meyer, C., and Krapp, A. (2013). Nuclear retention of the transcription factor NLP7 orchestrates the early response to nitrate in plants. *Nat. Commun.* **4**: 1–9.
- Markmann, K., Giczey, G., and Parniske, M. (2008). Functional adaptation of a plant receptor-kinase paved the way for the evolution of intracellular root symbioses with bacteria. *PLoS Biol.* **6**: 0497–0506.
- Markmann, K. and Parniske, M. (2009). Evolution of root endosymbiosis with bacteria: how novel are nodules? *Trends Plant Sci.* **14**: 77–86.
- Marsh, J.F., Rakocevic, A., Mitra, R.M., Brocard, L., Sun, J., Eschstruth, A., Long, S.R., Schultze, M., Ratet, P., and Oldroyd, G.E.D. (2007). *Medicago truncatula* *NIN* is essential for rhizobial-independent nodule organogenesis induced by autoactive calcium/calmodulin-dependent protein kinase. *Plant Physiol.* **144**: 324–335.
- Miller, J.B., Pratap, A., Miyahara, A., Zhou, L., Bornemann, S., Morris, R.J., and Oldroyd, G.E.D. (2013). Calcium/calmodulin-dependent protein kinase is negatively and positively regulated by calcium, providing a mechanism for decoding calcium responses during symbiosis signaling. *Plant Cell* **25**: 5053–5066.
- Mitra, R.M., Gleason, C.A., Edwards, A., Hadfield, J., Downie, J.A., Oldroyd, G.E.D., and Long, S.R. (2004). A Ca²⁺/calmodulin-dependent protein kinase required for symbiotic nodule development: gene identification by transcript-based cloning. *Proc. Natl. Acad. Sci. U. S. A.* **101**: 4701–4705.
- Mukherjee, A. and Ané, J.M. (2011). Germinating spore exudates from arbuscular mycorrhizal fungi: molecular and developmental responses in plants and their regulation by ethylene. *Mol. Plant-Microbe Interact.* **24**: 260–270.
- Murray, J.D. et al. (2011). *Vapyrin*, a gene essential for intracellular progression of arbuscular mycorrhizal symbiosis, is also essential for infection by rhizobia in the nodule symbiosis of *Medicago truncatula*. *Plant J.* **65**: 244–252.
- Murray, J.D., Karas, B.J., Sato, S., Tabata, S., Amyot, L., and Szczyglowski, K. (2007). A cytokinin perception mutant colonized by *Rhizobium* in the absence of nodule organogenesis. *Science* **305**: 101–104.
- Navazio, L., Moscatiello, R., Genre, A., Novero, M., Baldan, B., Bonfante, P., and Mariani, P. (2007). A diffusible signal from arbuscular mycorrhizal fungi elicits a transient cytosolic calcium elevation in host plant cells. *Plant Physiol.* **144**: 673–681.
- Ni, L. et al. (2019). Abscisic acid inhibits rice protein phosphatase PP45 via H₂O₂ and relieves repression of the Ca²⁺/CaM-dependent protein kinase DMI3. *Plant Cell* **31**:

- 128–152.
- Nishida, H., Tanaka, S., Handa, Y., Ito, M., Sakamoto, Y., Matsunaga, S., Betsuyaku, S., Miura, K., Soyano, T., Kawaguchi, M., and Suzaki, T. (2018). A NIN-LIKE PROTEIN mediates nitrate-induced control of root nodule symbiosis in *Lotus japonicus*. *Nat. Commun.* **9**.
- Oláh, B., Brière, C., Bécard, G., Dénarié, J., and Gough, C. (2005). Nod factors and a diffusible factor from arbuscular mycorrhizal fungi stimulate lateral root formation in *Medicago truncatula* via the DMI1/DMI2 signalling pathway. *Plant J.* **44**: 195–207.
- Oldroyd, G., Murray, J., Poole, P., and JA, D. (2011). The rules of engagement in the legume-rhizobial symbiosis. *Annu Rev Genet* **45**: 119–144.
- Oldroyd, G.E.D. (2013). Speak, friend, and enter: signalling systems that promote beneficial symbiotic associations in plants. *Nat. Rev. Microbiol.* **11**: 252–263.
- Oldroyd, G.E.D. and Long, S.R. (2003). Identification and characterization of *Nodulation Signaling Pathway 2*, a gene of *Medicago truncatula* involved in nod factor signaling. *Plant Physiol.* **131**: 1027–1032.
- Ortu, G., Balestrini, R., Pereira, P.A., Becker, J.D., Küster, H., and Bonfante, P. (2012). Plant genes related to gibberellin biosynthesis and signaling are differentially regulated during the early stages of AM fungal interactions. *Mol. Plant* **5**: 951–954.
- Ott, T., Van Dongen, J.T., Günther, C., Krusell, L., Desbrosses, G., Vigeolas, H., Bock, V., Czechowski, T., Geigenberger, P., and Udvardi, M.K. (2005). Symbiotic leghemoglobins are crucial for nitrogen fixation in legume root nodules but not for general plant growth and development. *Curr. Biol.* **15**: 531–535.
- Ovchinnikova, E. et al. (2011). IPD3 controls the formation of nitrogen-fixing symbiosomes in pea and *Medicago* spp. *Mol. Plant-Microbe Interact.* **24**: 1333–1344.
- Pan, H., Oztas, O., Zhang, X., Wu, X., Stonoha, C., Wang, E., Wang, B., and Wang, D. (2016). A symbiotic SNARE protein generated by alternative termination of transcription. *Nat. Plants* **2**: 1–5.
- Pankievicz, V.C.S., Irving, T.B., Maia, L.G.S., and Ané, J.M. (2019). Are we there yet? The long walk towards the development of efficient symbiotic associations between nitrogen-fixing bacteria and non-leguminous crops. *BMC Biol.* **17**: 1–17.
- Parniske, M. (2008). Arbuscular mycorrhiza: the mother of plant root endosymbioses. *Nat. Rev. Microbiol.* **6**: 763–775.
- Parniske, M. (2000). Intracellular accommodation of microbes by plants: a common developmental program for symbiosis and disease? *Curr Opin Plant Biol* **3**: 320–328.
- Parniske, M. (2018). Uptake of bacteria into living plant cells, the unifying and distinct feature of the nitrogen-fixing root nodule symbiosis. *Curr. Opin. Plant Biol.* **44**: 164–174.
- Pawlowski, K. and Demchenko, K.N. (2012). The diversity of actinorhizal symbiosis. *Protoplasma* **249**: 967–979.
- Peck, M.C., Fisher, R.F., and Long, S.R. (2006). Diverse flavonoids stimulate NodD1 binding to *nod* gene promoters in *Sinorhizobium meliloti*. *J. Bacteriol.* **188**: 5417–5427.
- Perrine-Walker, F.M., Lartaud, M., Kouchi, H., and Ridge, R.W. (2014). Microtubule array formation during root hair infection thread initiation and elongation in the *Mesorhizobium-Lotus* symbiosis. *Protoplasma* **251**: 1099–1111.
- Perry, J., Brachmann, A., Welham, T., Binder, A., Charpentier, M., Groth, M., Haage, K., Markmann, K., Wang, T.L., and Parniske, M. (2009). TILLING in *Lotus japonicus* identified large allelic series for symbiosis genes and revealed a bias in functionally defective ethyl methanesulfonate alleles toward glycine replacements. *Plant Physiol.*

- 151: 1281–1291.
- Pfeffer, P.E., Douds, D.D., Bécard, G., and Shachar-Hill, Y.** (1999). Carbon uptake and the metabolism and transport of lipids in an arbuscular mycorrhiza. *Plant Physiol.* **120**: 587–598.
- Pimprikar, P., Carbonnel, S., Paries, M., Katzer, K., Klingl, V., Bohmer, M.J., Karl, L., Floss, D.S., Harrison, M.J., Parniske, M., and Gutjahr, C.** (2016). A CCaMK-CYCLOPS-DELLA complex activates transcription of *RAM1* to regulate arbuscule branching. *Curr. Biol.* **26**: 987–998.
- Poole, P., Ramachandran, V., and Terpolilli, J.** (2018). Rhizobia: from saprophytes to endosymbionts. *Nat. Rev. Microbiol.* **16**: 291–303.
- Poovaiah, B.W., Du, L., Wang, H., and Yang, T.** (2013). Recent advances in calcium/calmodulin-mediated signaling with an emphasis on plant-microbe interactions. *Plant Physiol.* **163**: 531–542.
- Popp, C. and Ott, T.** (2011). Regulation of signal transduction and bacterial infection during root nodule symbiosis. *Curr. Opin. Plant Biol.* **14**: 458–467.
- Pumplin, N., Mondo, S.J., Topp, S., Starker, C.G., Gantt, J.S., and Harrison, M.J.** (2010). *Medicago truncatula* Vapyrin is a novel protein required for arbuscular mycorrhizal symbiosis. *Plant J.* **61**: 482–494.
- Qiu, L., Lin, J.S., Xu, J., Sato, S., Parniske, M., Wang, T.L., Downie, J.A., and Xie, F.** (2015). SCARN a novel class of SCAR protein that is required for root-hair infection during legume nodulation. *PLoS Genet.* **11**: 1–27.
- Radhakrishnan, G. V. et al.** (2020). An ancestral signalling pathway is conserved in intracellular symbioses-forming plant lineages. *Nat. Plants* **6**: 280–289.
- Radutoiu, S., Madsen, L.H., Madsen, E.B., Felle, H.H., Umehara, Y., Grønlund, M., Sato, S., Nakamura, Y., Tabata, S., Sandal, N., and Stougaard, J.** (2003). Plant recognition of symbiotic bacteria requires two LysM receptor-like kinases. *Nature* **425**: 585–592.
- Radutoiu, S., Madsen, L.H., Madsen, E.B., Jurkiewicz, A., Fukai, E., Quistgaard, E.M.H., Albrektsen, A.S., James, E.K., Thirup, S., and Stougaard, J.** (2007). LysM domains mediate lipochitin-oligosaccharide recognition and Nfr genes extend the symbiotic host range. *EMBO J.* **26**: 3923–3935.
- Raggio, M., Raggio, N., and Torrey, J.G.** (1957). The nodulation of isolated leguminous roots. *Am. J. Bot.* **44**: 325.
- Ramachandiran, S., Takezawa, D., Wang, W., and Poovaiah, B.W.** (1997). Functional domains of plant chimeric calcium/calmodulin-dependent protein kinase: regulation by autoinhibitory and visinin-like domains. *J. Biochem.* **121**: 984–990.
- Redecker, D., Kodner, R., and Graham, L.E.** (2000). Glomalean fungi from the Ordovician. *Science* (80-.). **289**: 1920–1921.
- Remy, W., Taylort, T.N., Hass, H., and Kerp, H.** (1994). Four hundred-million-year-old vesicular arbuscular mycorrhizae. *Proc. Natl. Acad. Sci. USA* **91**: 11841–11843.
- Ried, M.K., Antolín-Llovera, M., and Parniske, M.** (2014). Spontaneous symbiotic reprogramming of plant roots triggered by receptor-like kinases. *Elife* **3**: 1–17.
- Roy, S., Liu, W., Nandety, R.S., Crook, A., Mysore, K.S., Pislariu, C.I., Frugoli, J., Dickstein, R., and Udvardi, M.K.** (2020). Celebrating 20 years of genetic discoveries in legume nodulation and symbiotic nitrogen fixation. *Plant Cell* **32**: 15–41.
- Rush, T.A. et al.** (2020). Lipo-chitooligosaccharides as regulatory signals of fungal growth and development. *Nat. Commun.* **11**.
- Saito, K. et al.** (2007). Nucleoporin85 is required for calcium spiking, fungal and bacterial symbioses, and seed production in *Lotus japonicus*. *Plant Cell* **19**: 610–624.

- Sathyanarayanan, P. V., Cremo, C.R., and Poovaiah, B.W.** (2000). Plant chimeric Ca²⁺/calmodulin-dependent protein kinase. *J. Biol. Chem.* **275**: 30417–30422.
- Schachtman, D.P., Reid, R.J., and Ayling, S.M.** (1998). Phosphorus uptake by plants: from soil to cell. *Plant Physiol.* **116**: 447–453.
- Schauser, L., Roussis, A., Stiller, J., and Stougaard, J.** (1999). A plant regulator controlling development of symbiotic root nodules. *Nature* **402**: 191–195.
- Schauser, L., Wieloch, W., and Stougaard, J.** (2005). Evolution of NIN-like proteins in *Arabidopsis*, rice, and *Lotus japonicus*. *J. Mol. Evol.* **60**: 229–237.
- Schiessl, K. et al.** (2019). NODULE INCEPTION recruits the lateral root developmental program for symbiotic nodule organogenesis in *Medicago truncatula*. *Curr. Biol.* **29**: 3657–3668.e5.
- Shachar-Hill, Y., Pfeffer, P.E., Douds, D., Osman, S.F., Doner, L.W., and Ratcliffe, R.G.** (1995). Partitioning of intermediary carbon metabolism in vesicular-arbuscular mycorrhizal leek. *Plant Physiol.* **108**: 7–15.
- Shen, D., Xiao, T.T., van Velzen, R., Kulikova, O., Gong, X., Geurts, R., Pawlowski, K., and Bisseling, T.** (2020). A homeotic mutation changes legume nodule ontogeny into actinorhizal-type ontogeny. *Plant Cell* **32**: 1868–1885.
- Shen, J., Yuan, L., Zhang, J., Li, H., Bai, Z., Chen, X., Zhang, W., and Zhang, F.** (2011). Phosphorus dynamics: from soil to plant. *Plant Physiol.* **156**: 997–1005.
- Sieberer, B.J., Chabaud, M., Timmers, A.C., Monin, A., Fournier, J., and Barker, D.G.** (2009). A nuclear-targetedameleon demonstrates intranuclear Ca²⁺ spiking in *Medicago truncatula* root hairs in response to rhizobial nodulation factors. *Plant Physiol.* **151**: 1197–1206.
- Sieberer, B.J., Timmers, A.C.J., and Emons, A.M.C.** (2005). Nod factors alter the microtubule cytoskeleton in *Medicago truncatula* root hairs to allow root hair reorientation. *Mol. Plant-Microbe Interact.* **18**: 1195–1204.
- Singh, S., Katzer, K., Lambert, J., Cerri, M., and Parniske, M.** (2014). CYCLOPS, A DNA-binding transcriptional activator, orchestrates symbiotic root nodule development. *Cell Host Microbe* **15**: 139–152.
- Singh, S. and Parniske, M.** (2012). Activation of calcium- and calmodulin-dependent protein kinase (CCaMK), the central regulator of plant root endosymbiosis. *Curr. Opin. Plant Biol.* **15**: 444–453.
- Smit, P., Raedts, J., Portyanko, V., Debellé, F., Gough, C., Bisseling, T., and Geurts, R.** (2005). NSP1 of the GRAS protein family is essential for rhizobial nod factor-induced transcription. *Science* **308**: 1789–1791.
- Soltis, D.E., Soltis, P.S., Morgant, D.R., Swensent, S.M., Mullin, B.C., Dowdi, J.M., and Peter, G.M.** (1995). Chloroplast gene sequence data suggest a single origin of the predisposition for symbiotic nitrogen fixation in angiosperms. *Proc. Natl. Acad. Sci. USA* **92**: 2647–2651.
- Soyano, T. and Hayashi, M.** (2014). Transcriptional networks leading to symbiotic nodule organogenesis. *Curr. Opin. Plant Biol.* **20**: 146–154.
- Soyano, T., Hirakawa, H., Sato, S., Hayashi, M., and Kawaguchi, M.** (2014). NODULE INCEPTION creates a long-distance negative feedback loop involved in homeostatic regulation of nodule organ production. *Proc. Natl. Acad. Sci. U. S. A.* **111**: 14607–14612.
- Soyano, T., Kouchi, H., Hirota, A., and Hayashi, M.** (2013). NODULE INCEPTION directly targets *NF-Y* subunit genes to regulate essential processes of root nodule development in *Lotus japonicus*. *PLoS Genet.* **9**.
- Soyano, T., Liu, M., Kawaguchi, M., and Hayashi, M.** (2021). Leguminous nodule

- symbiosis involves recruitment of factors contributing to lateral root development. *Curr. Opin. Plant Biol.* **59**: 1–8.
- Soyano, T., Shimoda, Y., Kawaguchi, M., and Hayashi, M.** (2019). A shared gene drives lateral root development and root nodule symbiosis pathways in *Lotus*. *Science* **366**: 1021–1023.
- Sprent, J.I.** (2007). Evolving ideas of legume evolution and diversity: a taxonomic perspective on the occurrence of nodulation. *New Phytol.* **174**: 11–25.
- Van Spronsen, P.C., Grønlund, M., Bras, C.P., Spaink, H.P., and Kijne, J.W.** (2001). Cell biological changes of outer cortical root cells in early determinate nodulation. *Mol. Plant-Microbe Interact.* **14**: 839–847.
- Stougaard, J., Abildsten, D., and Marcker, K.A.** (1987). System for transformation of plants. *Mol. Gen. Genet.* **207**: 251–255.
- Stracke, S., Kistner, C., Yoshida, S., Mulder, L., Sato, S., Kaneko, T., Tabata, S., Sandal, N., Stougaard, J., Szczyglowski, K., and Parniske, M.** (2002). A plant receptor-like kinase required for both bacterial and fungal symbiosis. *Nature* **417**: 959–962.
- Sun, J. et al.** (2015). Activation of symbiosis signaling by arbuscular mycorrhizal fungi in legumes and rice. *Plant Cell* **27**: 823–838.
- Suzuki, W., Konishi, M., and Yanagisawa, S.** (2013). The evolutionary events necessary for the emergence of symbiotic nitrogen fixation in legumes may involve a loss of nitrate responsiveness of the NIN transcription factor. *Plant Signal. Behav.* **8**: e25975.
- Svistoonoff, S., Hocher, V., and Gherbi, H.** (2014). Actinorhizal root nodule symbioses: what is signalling telling on the origins of nodulation? *Curr. Opin. Plant Biol.* **20**: 11–18.
- Svistoonoff, S., Laplaze, L., Auguy, F., Runions, J., Duponnois, R., Haseloff, J., Franche, C., and Bogusz, D.** (2003). *cg12* expression is specifically linked to infection of root hairs and cortical cells during *Casuarina glauca* and *Allocasuarina verticillata* actinorhizal nodule development. *Mol. Plant-Microbe Interact.* **16**: 600–607.
- Takeda, N., Maekawa, T., and Hayashi, M.** (2012). Nuclear-localized and deregulated calcium- and calmodulin-dependent protein kinase activates rhizobial and mycorrhizal responses in *Lotus japonicus*. *Plant Cell* **24**: 810–822.
- Tanaka, K., Cho, S.H., Lee, H., Pham, A.Q., Batek, J.M., Cui, S., Qiu, J., Khan, S.M., Joshi, T., Zhang, Z.J., Xu, D., and Stacey, G.** (2015). Effect of lipo-chitooligosaccharide on early growth of C4 grass seedlings. *J. Exp. Bot.* **66**: 5727–5738.
- Taylor, I., Lehner, K., McCaskey, E., Nirmal, N., Ozkan-Aydin, Y., Murray-Cooper, M., Jain, R., Hawkes, E.W., Ronald, P.C., Goldman, D.I., and Benfey, P.N.** (2021). Mechanism and function of root circumnutation. *Proc. Natl. Acad. Sci. U. S. A.* **118**: 1–10.
- Thamdrup, B.** (2012). New pathways and processes in the global nitrogen cycle. *Annu. Rev. Ecol. Evol. Syst.* **43**: 407–428.
- Timmers, A.C.J., Auriac, M.C., and Truchet, G.** (1999). Refined analysis of early symbiotic steps of the *Rhizobium-Medicago* interaction in relationship with microtubular cytoskeleton rearrangements. *Development* **126**: 3617–3628.
- Tirichine, L. et al.** (2006). Deregulation of a Ca²⁺/calmodulin-dependent kinase leads to spontaneous nodule development. *Nature* **441**: 1153–1156.
- Tirichine, L., Sandal, N., Madsen, L.H., Radutoiu, S., Albrektsen, A.S., Sato, S., Asamizu, E., Tabata, S., and Stougaard, J.** (2007). A gain-of-function mutation in a cytokinin receptor triggers spontaneous root nodule organogenesis. *Science* **315**: 104–107.
- Truchet, G., Roche, P., Lerouge, P., Vasse, J., Camut, S., de Billy, F., Promé, J.-C., and**

- Dénarié, J. (1991). Sulphated lipo-oligosaccharide signals of *Rhizobium meliloti* elicit root nodule organogenesis in alfalfa. *Nature* **368**: 444–446.
- Tsikou, D., Yan, Z., Holt, D.B., Abel, N.B., Reid, D.E., Madsen, L.H., Bhasin, H., Sexauer, M., Stougaard, J., and Markmann, K. (2018). Systemic control of legume susceptibility to rhizobial infection by a mobile microRNA. *Science* **6907**: 1–8.
- van Velzen, R. et al. (2018). Comparative genomics of the nonlegume *Parasponia* reveals insights into evolution of nitrogen-fixing rhizobium symbioses. *Proc. Natl. Acad. Sci.* **115**: E4700–E4709.
- van Velzen, R., Doyle, J.J., and Geurts, R. (2019). A resurrected scenario: single gain and massive loss of nitrogen-fixing nodulation. *Trends Plant Sci.* **24**: 49–57.
- Venkateshwaran, M., Jayaraman, D., Chabaud, M., Genre, A., Balloon, A.J., Maeda, J., Forshey, K., Den Os, D., Kwiecien, N.W., Coon, J.J., Barker, D.G., and Ané, J.M. (2015). A role for the mevalonate pathway in early plant symbiotic signaling. *Proc. Natl. Acad. Sci. U. S. A.* **112**: 9781–9786.
- Vernié, T., Kim, J., Frances, L., Ding, Y., Sun, J., Guan, D., Niebel, A., Gifford, M.L., de Carvalho-Niebel, F., and Oldroyd, G.E.D. (2015). The NIN transcription factor coordinates diverse nodulation programs in different tissues of the *Medicago truncatula* root. *Plant Cell* **27**: 3410–3424.
- Wais, R.J., Galera, C., Oldroyd, G., Catoira, R., Penmetsa, R.V., Cook, D., Gough, C., Dénarié, J., and Long, S.R. (2000). Genetic analysis of calcium spiking responses in nodulation mutants of *Medicago truncatula*. *Proc. Natl. Acad. Sci. U. S. A.* **97**: 13407–13412.
- Walan, P., Davidsson, S., Johansson, S., and Höök, M. (2014). Phosphate rock production and depletion: regional disaggregated modeling and global implications. *Resour. Conserv. Recycl.* **93**: 178–187.
- Wang, H., Moore, M.J., Soltis, P.S., Bell, C.D., Brockington, S.F., Alexandre, R., Davis, C.C., Latvis, M., Manchester, S.R., and Soltis, D.E. (2009). Rosid radiation and the rapid rise of angiosperm-dominated forests. *Proc. Natl. Acad. Sci. U. S. A.* **106**: 3853–3858.
- Wang, T., Guo, J., Peng, Y., Lyu, X., Liu, B., Sun, S., and Wang, X. (2021). Light-induced mobile factors from shoots regulate rhizobium-triggered soybean root nodulation. *Science* **374**: 65–71.
- Werner, G.D.A., Cornwell, W.K., Sprent, J.I., Kattge, J., and Kiers, E.T. (2014). A single evolutionary innovation drives the deep evolution of symbiotic N₂-fixation in angiosperms. *Nat. Commun.* **5**: 1–9.
- White, J., Prell, J., James, E.K., and Poole, P. (2007). Nutrient sharing between symbionts. *Plant Physiol.* **144**: 604–614.
- Wittkopp, P. and Kalay, G. (2011). *Cis*-regulatory elements: molecular mechanisms and evolutionary processes underlying divergence. *Nat Rev Genet* **13**: 59–69.
- Wopereis, J., Pajuelo, E., Dazzo, F.B., Jiang, Q., Gresshoff, P.M., De Bruijn, F.J., Stougaard, J., and Szczyglowski, K. (2000). Short root mutant of *Lotus japonicus* with a dramatically altered symbiotic phenotype. *Plant J.* **23**: 97–114.
- Xiao, A., Yu, H., Fan, Y., Kang, H., Ren, Y., Huang, X., Gao, X., Wang, C., Zhang, Z., Zhu, H., and Cao, Y. (2020). Transcriptional regulation of *NIN* expression by IPN2 is required for root nodule symbiosis in *Lotus japonicus*. *New Phytol.* **227**: 513–528.
- Xiao, T.T., Schilderink, S., Moling, S., Deinum, E.E., Kondorosi, E., Franssen, H., Kulikova, O., Niebel, A., and Bisseling, T. (2014). Fate map of *Medicago truncatula* root nodules. *Dev.* **141**: 3517–3528.

- Xiao, T.T., van Velzen, R., Kulikova, O., Franken, C., and Bisseling, T.** (2019). Lateral root formation involving cell division in both pericycle, cortex and endodermis is a common and ancestral trait in seed plants. *Dev.* **146**: 1–5.
- Xie, F., Murray, J.D., Kim, J., Heckmann, A.B., Edwards, A., Oldroyd, G.E.D., and Downie, J.A.** (2012). Legume pectate lyase required for root infection by rhizobia. *Proc. Natl. Acad. Sci. U. S. A.* **109**: 633–638.
- Yano, K. et al.** (2008). CYCLOPS, a mediator of symbiotic intracellular accommodation. *Proc. Natl. Acad. Sci. U. S. A.* **105**: 20540–20545.
- Yokota, K. et al.** (2009). Rearrangement of actin cytoskeleton mediates invasion of *Lotus japonicus* roots by *Mesorhizobium loti*. *Plant Cell* **21**: 267–284.
- Yoon, H.J., Hossain, M.S., Held, M., Hou, H., Kehl, M., Tromas, A., Sato, S., Tabata, S., Andersen, S.U., Stougaard, J., Ross, L., and Szczyglowski, K.** (2014). *Lotus japonicus* *SUNERGOS1* encodes a predicted subunit A of a DNA topoisomerase VI that is required for nodule differentiation and accommodation of rhizobial infection. *Plant J.* **78**: 811–821.
- Yoro, E., Suzaki, T., Toyokura, K., Miyazawa, H., Fukaki, H., and Kawaguchi, M.** (2014). A positive regulator of nodule organogenesis, *NODULE INCEPTION*, acts as a negative regulator of rhizobial infection in *Lotus japonicus*. *Plant Physiol.* **165**: 747–758.
- Zhu, H., Chen, T., Zhu, M., Fang, Q., Kang, H., Hong, Z., and Zhang, Z.** (2008). A novel ARID DNA-binding protein interacts with SymRK and is expressed during early nodule development in *Lotus japonicus*. *Plant Physiol.* **148**: 337–347.
- Zhu, Y., Yan, J., Liu, W., Liu, L., Sheng, Y., Sun, Y., Li, Y., Scheller, H.V., Jiang, M., Hou, X., Ni, L., and Zhang, A.** (2016). Phosphorylation of a NAC transcription factor by a calcium/calmodulin-dependent protein kinase regulates abscisic acid-induced antioxidant defense in maize. *Plant Physiol.* **171**: 1651–1664.

10. List of Figures and Table

Figure 1	Overview of the symbiotic signal transduction in plant root cells	16
Figure 2	Acquisition of <i>PACE</i> was a key step in the evolution of RNS	29
Figure 3	<i>PACE</i> drives the expression of <i>NIN</i> during IT development in the cortex	31
Figure 4	<i>L. japonicus nin-15</i> mutant phenotype	32
Figure 5	<i>PACE</i> is necessary for bacterial infection and functionally conserved across the FaFaCuRo clade	34
Figure 6	The <i>CYC-box</i> and flanking sequences of <i>PACE</i> are required for the full restoration of the bacterial infection process in the <i>L. japonicus nin-2</i> mutant	36
Figure 7	The <i>CYC-box</i> and flanking sequences of <i>PACE</i> are required for the full restoration of the bacterial infection process but are dispensable for the nodule organogenesis process in the <i>L. japonicus nin-2</i> mutant	38
Figure 8	The <i>CYC-box</i> and flanking sequences of <i>PACE</i> are required for the full restoration of the bacterial infection process but are dispensable for the nodule organogenesis process in the <i>L. japonicus nin-2</i> mutant	40
Figure 9	<i>PACEs</i> from FaFaCuRo species are functionally equivalent in restoring bacterial infection in the <i>L. japonicus nin-15</i> mutant	42
Figure 10	<i>PACE</i> enables IT formation in the cortex	46
Figure 11	<i>PACE</i> alone or in the context of the <i>S. lycopersicum NIN</i> promoter (a species outside of the FaFaCuRo clade) enables IT formation in the cortex	48
Figure 12	<i>Rhizophagus irregularis</i> and <i>Mesorhizobium loti</i> impact root system architecture in <i>L. japonicus</i>	50
Figure 13	<i>Rhizophagus irregularis</i> and <i>Mesorhizobium loti</i> -mediated increase in lateral root density requires <i>NIN</i>	52
Figure 14	Schematic illustration of the experimental setup for the cultivation of root organ liquid cultures	53
Figure 15	Expression of deregulated versions of <i>SymRK</i> , <i>CCaMK</i> or <i>Cyclops</i> stimulates lateral root formation	54
Figure 16	Expression of a phosphomimetic version of <i>Cyclops</i> but not its phosphoablative version stimulates lateral root formation	55
Figure 17	Deregulation of <i>CCaMK</i> in the <i>snf1-1</i> mutant stimulates lateral root formation	55

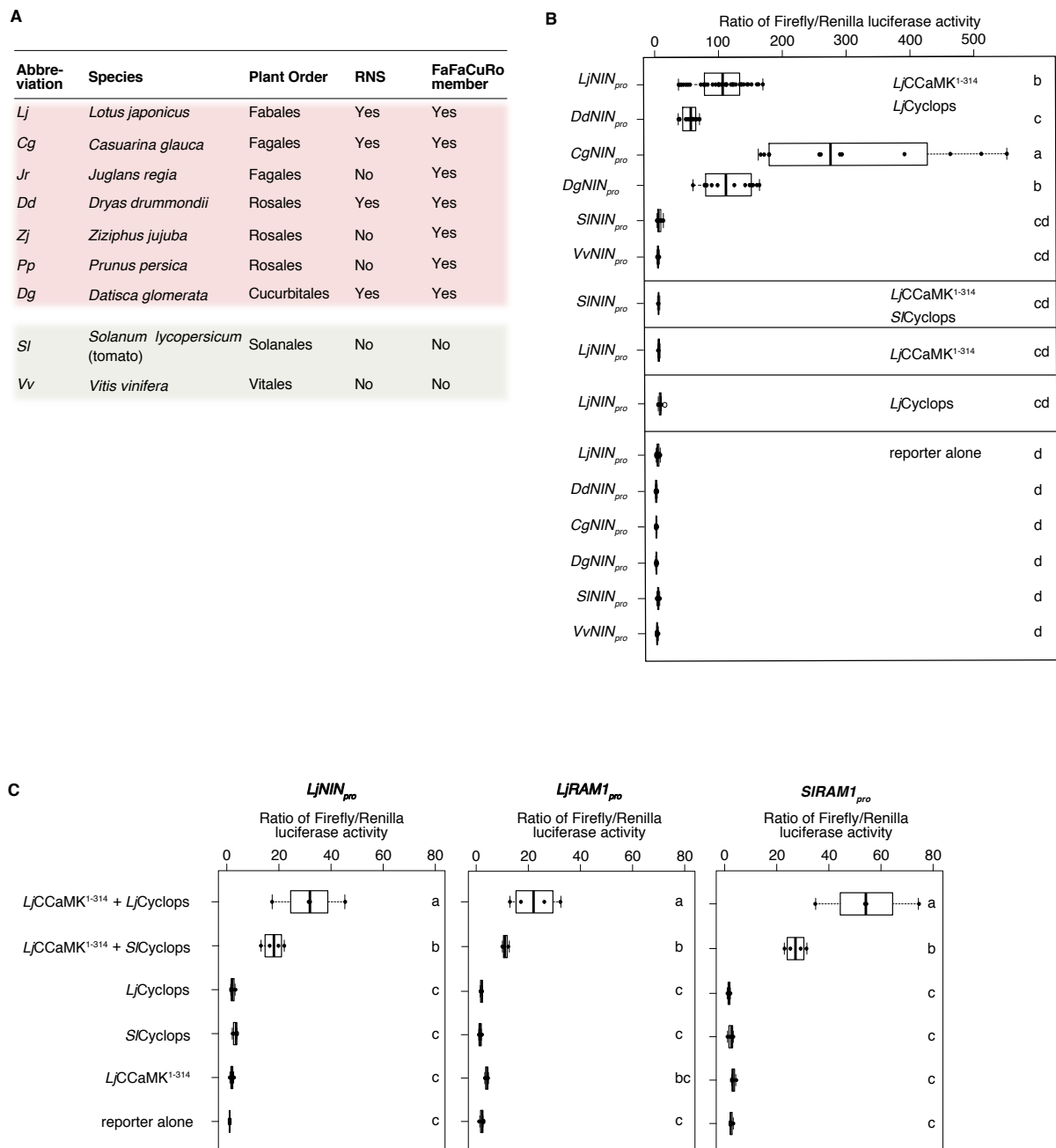
Figure 18	Stimulation of lateral root formation mediated by deregulated versions of either CCaMK or Cyclops is not dependent on <i>Cyclops</i> or CCaMK, respectively	56
Figure 19	Ectopic expression of <i>NIN</i> stimulates lateral root formation and results in overcurling	58
Figure 20	Stimulation of lateral root formation mediated by ectopic expression of CCaMK ¹⁻³¹⁴ requires <i>NIN</i>	59
Figure 21	Stimulation of lateral root formation mediated by ectopic expression of CCaMK ¹⁻³¹⁴ requires <i>NSP1</i> and <i>NSP2</i>	60
Figure 22	Ectopic expression of <i>LjCCaMK</i> ¹⁻³¹⁴ stimulates lateral root formation in <i>Dryas drummondii</i> but not in <i>Fragaria vesca</i>	61
Figure 23	<i>Cis</i> -regulatory regions controlling <i>NIN</i> expression and enabling rhizobia infection and nodule development in <i>L. japonicus</i>	65
Figure 24	A model for lateral root induction by common symbiosis genes	67
Table 1	Status of <i>PACE</i> and <i>NIN</i> in non-nodulating FaFaCuRo species	44

11. Supplementary Figures and Tables

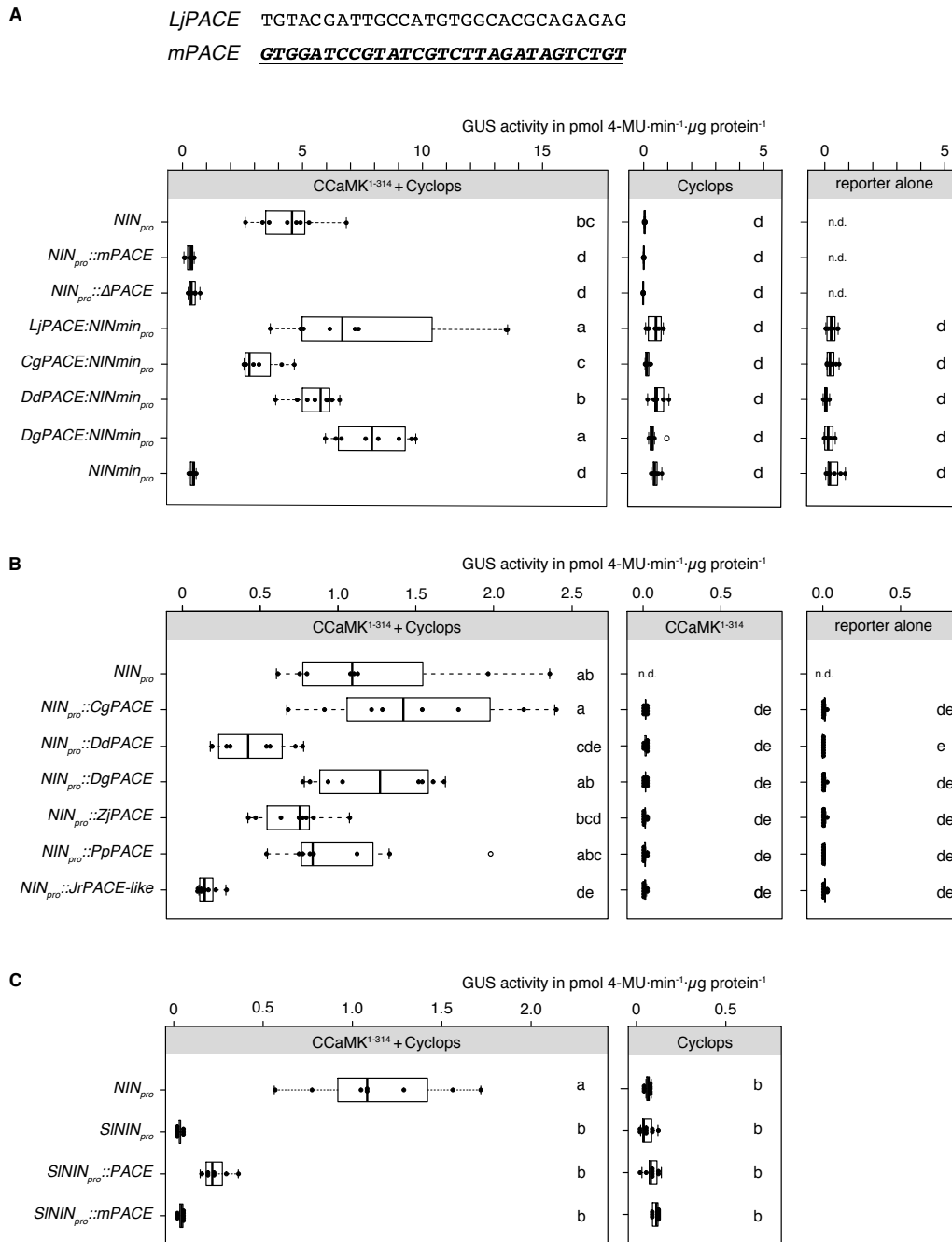
11.1. List of Supplementary Figures and Supplementary Tables

Supplementary Figure 1	Transcriptional activation of <i>NIN promoter:Firefly luciferase</i> reporter gene by CCaMK ¹⁻³¹⁴ /Cyclops is restricted to <i>NIN</i> promoters from species of the FaFaCuRo clade	98
Supplementary Figure 2	<i>PACE</i> sequence variants from species across the FaFaCuRo clade were able to functionally replace <i>L. japonicus PACE</i> in a <i>LjNIN_{pro}:GUS</i> reporter fusion	99
Supplementary Figure 3	Spatio-temporal <i>GUS</i> expression driven by <i>PACE</i> and the <i>NIN</i> promoter in <i>L. japonicus</i> roots during the bacterial infection process	100
Supplementary Figure 4	The <i>CYC-box</i> and flanking sequences of <i>PACE</i> are required for the full restoration of the bacterial infection process in the <i>L. japonicus nin-2</i> mutant	102
Supplementary Figure 5	The <i>CYC-box</i> and flanking sequences of <i>PACE</i> are required for the full restoration of the bacterial infection process in the <i>L. japonicus nin-2</i> mutant	103
Supplementary Figure 6	Spatio-temporal <i>GUS</i> expression driven by <i>PACE</i> variants in <i>L. japonicus</i> roots during the bacterial infection process	104
Supplementary Figure 7	<i>Rhizophagus irregularis</i> and <i>Mesorhizobium loti</i> -mediated increase in lateral root density requires <i>NIN</i>	105
Supplementary Figure 8	Time-course of lateral root formation stimulated by the expression of deregulated versions of SymRK, CCaMK or Cyclops	106
Supplementary Figure 9	Mutation of <i>NIN</i> does not affect primary root length or lateral root formation	107
Supplementary Figure 10	Mutation of <i>NSP1</i> or <i>NSP2</i> stimulates lateral root formation and affects primary root length	108
Supplementary Table 1	Seed bags and bacterial strains used in this study	109
Supplementary Table 2	Microscope/scanner settings and image analysis used in this study	111
Supplementary Table 3	Plasmids used in this study	112
Supplementary Table 4	Name and sequences of primers used in this study	116

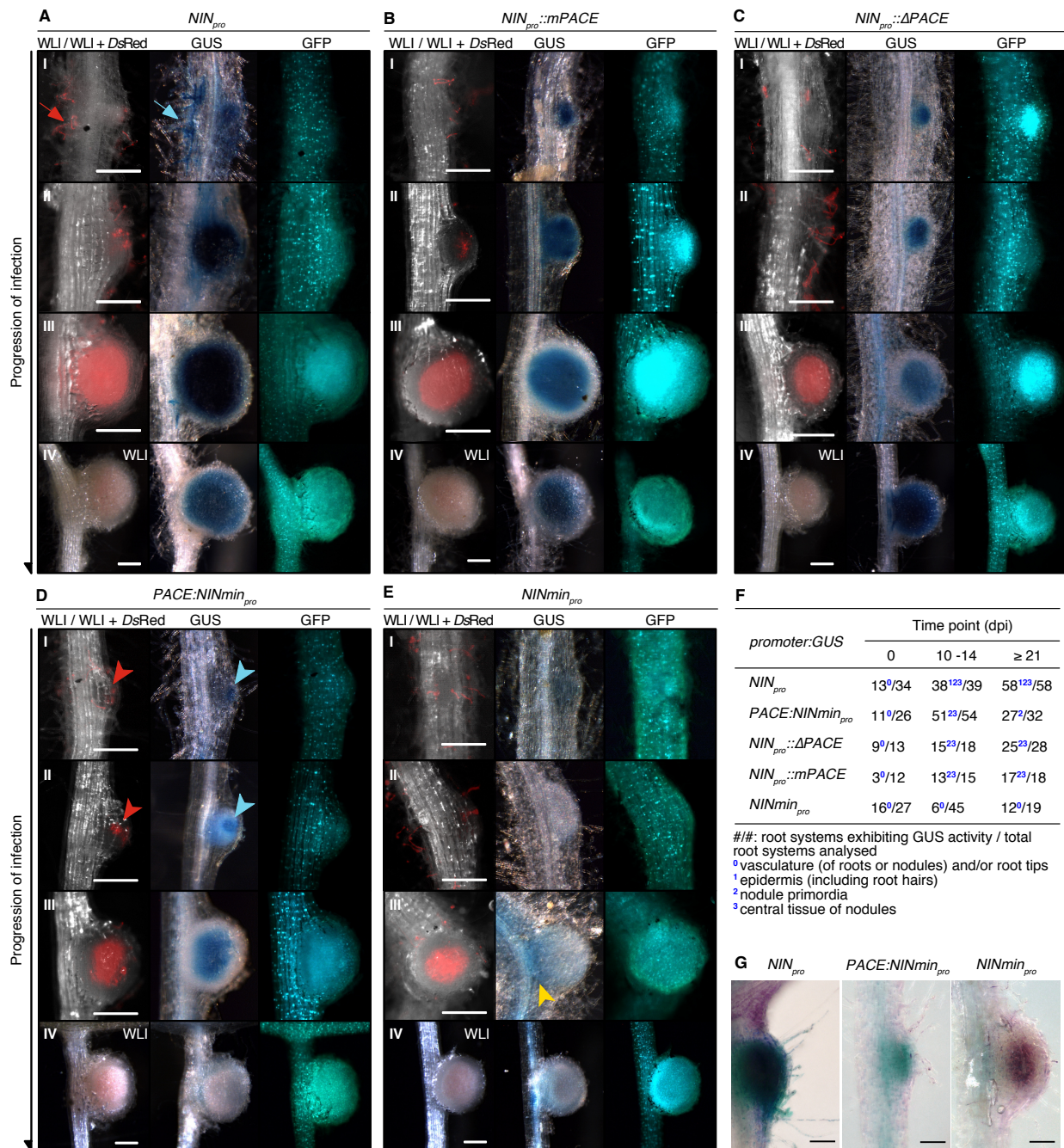
11.2. Supplementary Figures



Supplementary Figure 1: Transcriptional activation of *NIN promoter:Firefly luciferase reporter gene* by *CCaMK¹⁻³¹⁴/Cyclops* is restricted to *NIN* promoters from species of the FaFaCuRo clade. *Nicotiana benthamiana* leaf cells were transformed with T-DNAs carrying a *Firefly luciferase* reporter gene driven by either of the indicated promoters in tandem with the *AtACT2_{pro}:Renilla luciferase* reporter fusion that provides a quantitative internal standard. (A) List of species within the FaFaCuRo clade (light red shade) and outside (light grey shade) and abbreviations. (B) Reporter gene activation by *L. japonicus* *CCaMK¹⁻³¹⁴/Cyclops* via *NIN* promoters (*NIN_{pro}*) originating from listed species. (C) Comparison of the transactivation potential of *Cyclops* versions from *L. japonicus* and *S. lycopersicum*. Note that the expression of the *Firefly luciferase* reporter gene driven by *LjNIN_{pro}*, the *RAM1* promoters from *L. japonicus* and *S. lycopersicum* (*LjRAM1_{pro}* and *SIRAM1_{pro}*, respectively) was induced in the presence of *CCaMK¹⁻³¹⁴/Cyclops* regardless of the origin of *Cyclops*. In contrast, the transactivation failed with the *SININ* promoter (panel (A)). The applied statistical method was ANOVA with *post hoc* Tukey: (B), $F_{14,214} = 71.07$, $p < 2 \times 10^{-16}$; (C), plots from left to right: $F_{5,18} = 20.58$, $p = 7.14 \times 10^{-7}$; $F_{5,18} = 25.38$, $p = 1.45 \times 10^{-7}$ and $F_{5,18} = 40.49$, $p = 3.55 \times 10^{-9}$, respectively. Different small letters indicate significant differences. The data presented in this figure were generated by Ksenia Vondenhoff.



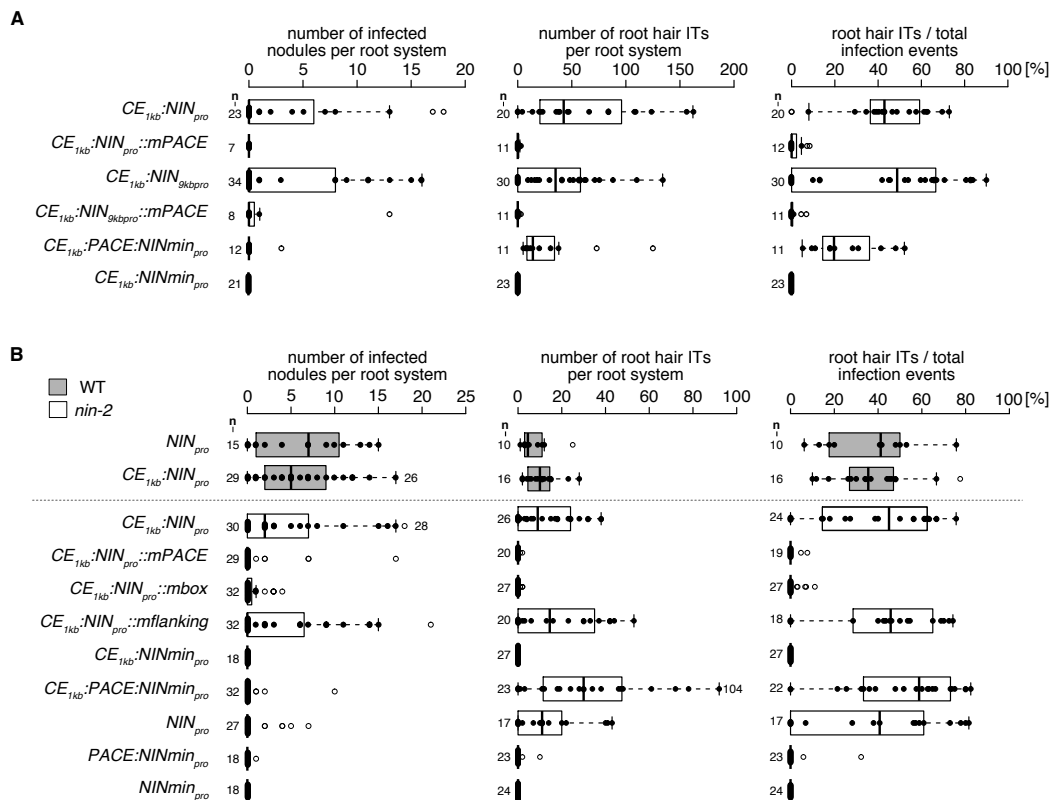
Supplementary Figure 2: PACE sequence variants from species across the FaFaCuRo clade were able to functionally replace *L. japonicus* PACE in a *LjNIN_{pro}:GUS* reporter fusion. *N. benthamiana* leaf cells were transformed with T-DNAs carrying a *GUS* reporter gene driven by either of the indicated promoters: (A) the *L. japonicus* *NIN* promoter (*NIN_{pro}*), the *LjNIN* promoter with *PACE* mutated or deleted (*NIN_{pro}::mPACE* and *NIN_{pro}::ΔPACE*, respectively), or *PACE* sequence variants from the nodulating FaFaCuRo species fused to the *LjNIN* minimal promoter (*NIN_{min}_{pro}*); (B) chimeric promoters where *LjPACE* in the *LjNIN* promoter was replaced with either one of the *PACE* variants from species tested in (A) or from non-nodulating FaFaCuRo species including the *Juglans regia* *PACE*-like motif (*JrPACE-like*); (C) the *S. lycopersicum* *NIN* promoter (*SININ_{pro}*), the *SININ* promoter with *LjPACE* (*SININ_{pro}::PACE*) or *mPACE* (*SININ_{pro}::mPACE*) inserted. For species abbreviations see **Supplementary Figure 1**. Note in (A) that the deletion or mutation of *PACE* in *LjNIN* promoter resulted in a drastic reduction in reporter gene expression and in (C) insertion of *LjPACE* but not *mPACE* into the *S. lycopersicum* promoter confers transactivation by CCaMK¹⁻³¹⁴/Cyclops. The applied statistical method was ANOVA with *post hoc* Tukey: (A) $F_{20,144} = 51.38$, $p < 2 \times 10^{-16}$; (B), $F_{18,166} = 149.1$, $p < 2 \times 10^{-16}$; (C) $F_{7,62} = 30.5$, $p = 7.02 \times 10^{-7}$. Different small letters indicate significant difference. n.d., not determined. The data presented in this figure were generated by Xiaoyun Gong.



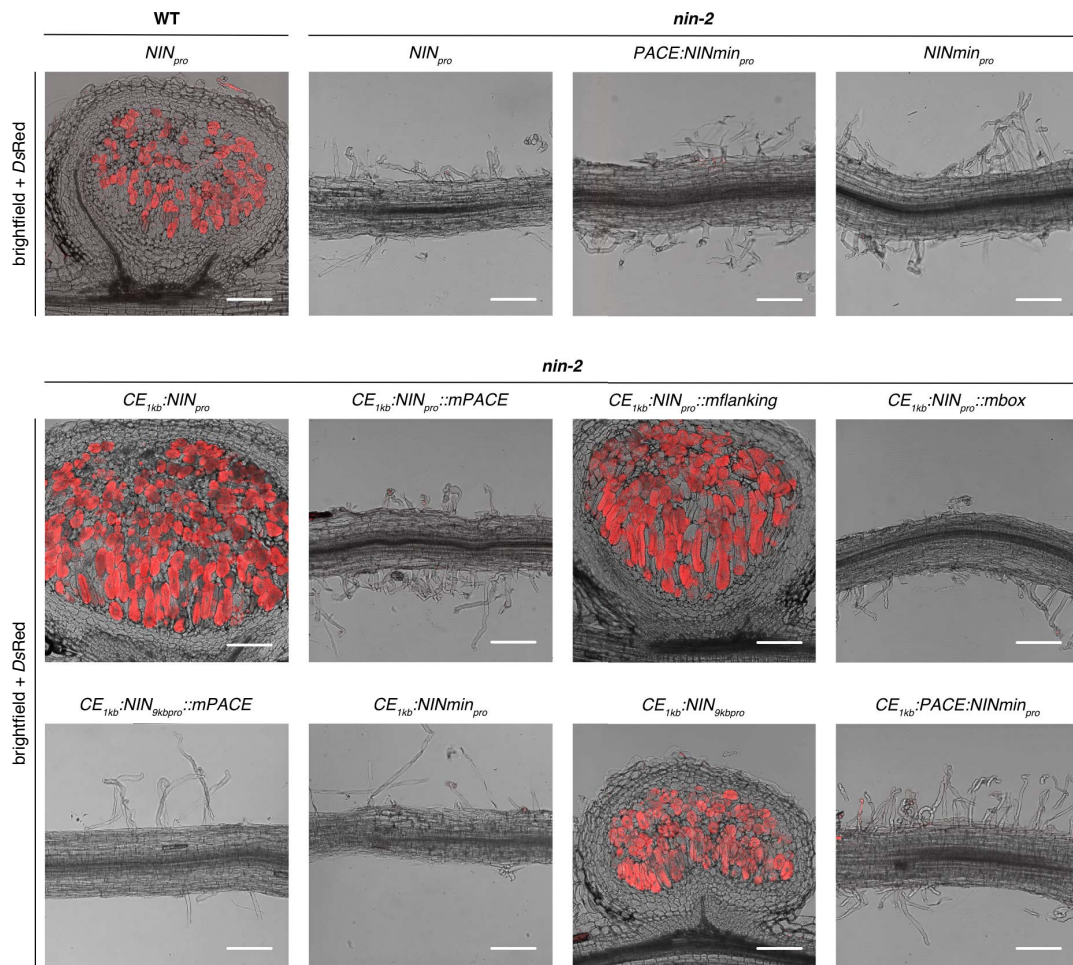
Supplementary Figure 3: Spatio-temporal GUS expression driven by PACE and the NIN promoter in *L. japonicus* roots during the bacterial infection process. *L. japonicus* wild-type hairy roots were transformed with T-DNAs carrying a *Ubg10_{pro}::NLS-GFP* transformation marker together with a *GUS* reporter gene driven by either of the indicated promoters: (A) the 3 kb *LjNIN* promoter (*NIN_{pro}*); the *LjNIN* promoter with PACE (B) mutated (*LjNIN_{pro}::mPACE*) or (C) deleted (*NIN_{pro}::ΔPACE*); (D) PACE fused to the *LjNIN* minimal promoter (*PACE:NIN_{min}_{pro}*) or (E) the *LjNIN* minimal promoter (*NIN_{min}_{pro}*). The progression of bacterial infection was determined by the *DsRed* signal 10 - 14 days post inoculation (dpi) with *M. loti* *DsRed*. Nodules undergoing different stages of infection (panels I to IV) were stained with X-Gluc to reveal the *GUS* expression pattern. Note the overlapping bacterial invasion zone and *PACE:NIN_{min}_{pro}::GUS* expression in early infection stages (red and blue arrowheads in (D)) as well as the differences between *PACE:NIN_{min}_{pro}::GUS* and the much broader *NIN_{pro}::GUS* expression at that stage (red and blue arrows in (A)). Red arrow and arrowheads: *M. loti* *DsRed*. Blue arrow and arrowheads: *GUS* activity in root hairs bearing ITs and nodule primordia, respectively. The *NIN_{min}_{pro}::GUS* fusion gave only rarely detectable signal, and if so in the vasculature (yellow arrowhead in (E)). (continuation of figure legend on the next page)

Legend Supplementary Figure 3: continued

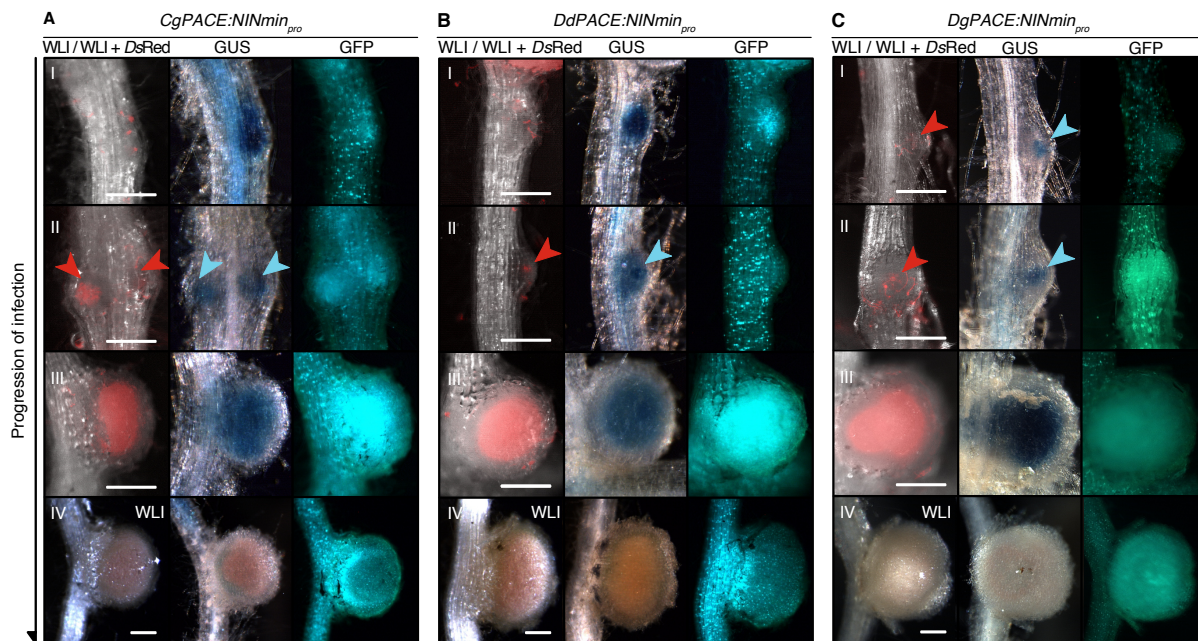
Only pictures taken under white light illumination (WLI) are displayed for nodules in panel VI to reveal the pink colour of leghemoglobin, characteristic for mature and fully infected nodules. Note that *PACE:NIN_{minpro}:GUS* expression was absent at this stage, whereas the *NIN_{pro}:GUS* resulted in strong blue staining in the nodule regardless of the presence of *PACE* (compare panel IV in **(D)** and **(A - C)**). **(F)** Quantification of transgenic root systems exhibiting *GUS* expression in different cell types and tissues exemplarily displayed in **(A - E)**. **(G)** *PACE* drove *GUS* reporter gene expression in the central tissue of primordia and nodules, but was not sufficient for expression in root hairs. Transgenic roots carrying promoter:*GUS* fusions same as in **(A, D and E)** were inoculated with *M. loti lacZ* and dual-stained with X-Gluc and Magenta-Gal. Purple: *M. loti lacZ*. Blue: *GUS* activity. Note the co-existence of blue and purple staining in root hairs on roots transformed by *NIN_{pro}:GUS*, but not that transformed by *PACE:NIN_{minpro}:GUS*. Bars, 250 μ m. The data presented in this figure were generated by Xiaoyun Gong.



Supplementary Figure 4: The *CYC*-box and flanking sequences of *PACE* are required for the full restoration of the bacterial infection process in the *L. japonicus nin-2* mutant. Roots were from a subset of plants from the same experiment depicted in Figure 6 but analysed 35 dpi with *M. loti DsRed*. (A - B) Boxplots displaying the number of root hair ITs or infected nodules and the percentage of root hair ITs among total infection events (sum of bacterial entrappings and ITs). Each dot represents one transgenic *nin-2* root system or root piece. *L. japonicus* WT roots transformed with *NIN_{pro}:NIN* or *CE_{1kb}:NIN_{pro}:NIN* were included as controls. Note that the results follow the same trend as those obtained 21 dpi with *M. loti DsRed* (Figure 6). n: number of transgenic root systems or root pieces analysed. Numbers above the boxplots: the value of individual data points outside of the plotting area. The data presented in this figure were generated by Chloé Cathebras and Xiaoyun Gong.



Supplementary Figure 5: The *CYC-box* and flanking sequences of *PACE* are required for the full restoration of the bacterial infection process in the *L. japonicus nin-2* mutant. Pictures of nodule sections or roots from *L. japonicus nin-2* roots 35 dpi with *M. loti* DsRed from the same experiments depicted in **Supplementary Figure 4**. Upper left corner: a nodule section from a *L. japonicus* WT root transformed with $NIN_{pro}:NIN$ was included for comparison. Bars, 100 μ m.

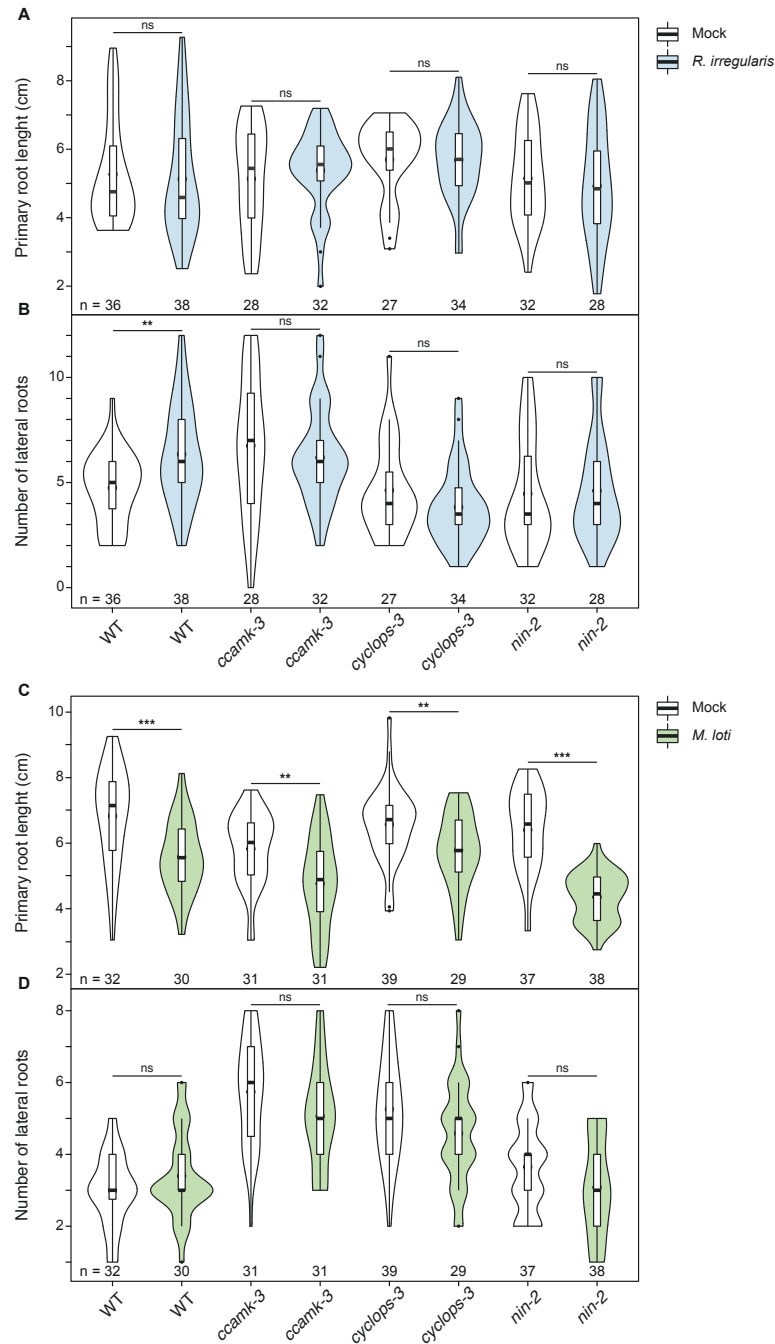


D

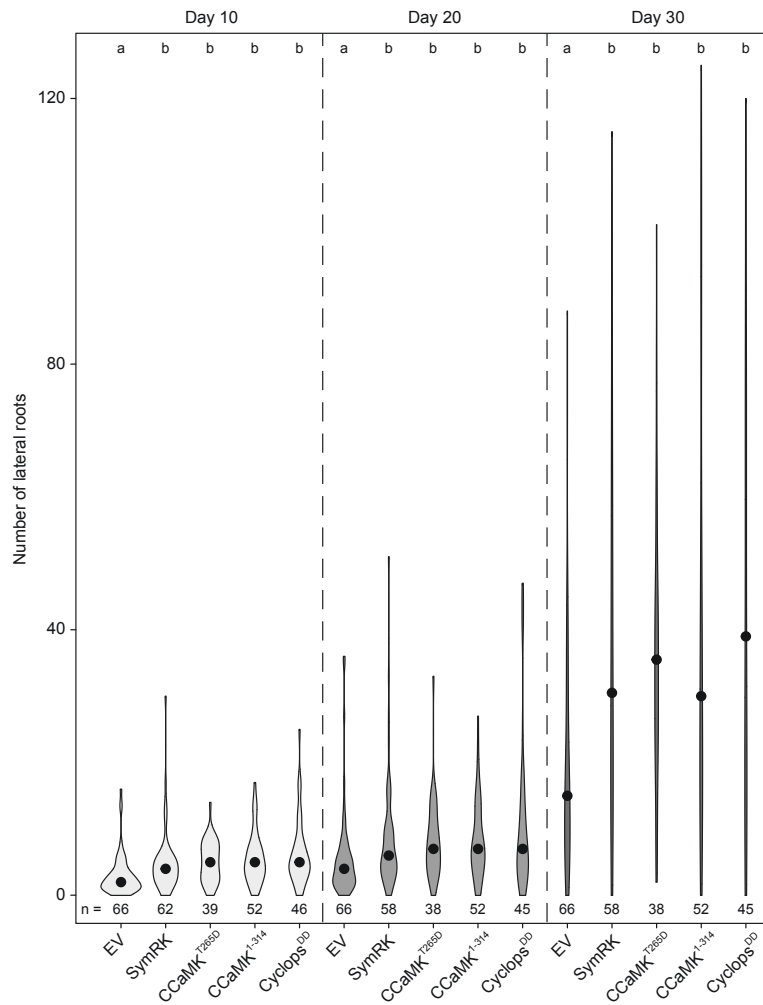
promoter:GUS	Time point (dpi)		
	0	10-14	≥ 21
<i>CgPACE:NINmin_{pro}</i>	7 ⁰ /7	14 ²³ /19	15 ² /20
<i>DdPACE:NINmin_{pro}</i>	8 ⁰ /8	15 ²³ /18	17 ² /22
<i>DgPACE:NINmin_{pro}</i>	n.d.	35 ²³ /46	28 ² /38

##: root systems exhibiting GUS activity / total root systems analysed
⁰ vasculature (of roots or nodules) and/or root tips
¹ epidermis (including root hairs)
² nodule primordia
³ central tissue of nodules

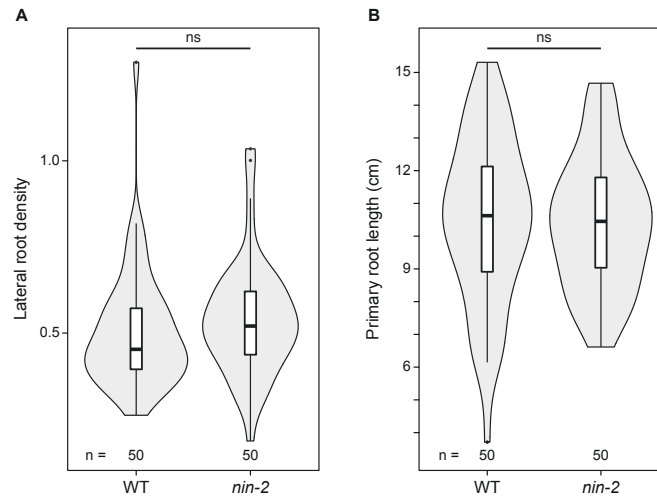
Supplementary Figure 6: Spatio-temporal GUS expression driven by PACE variants in *L. japonicus* roots during the bacterial infection process. *L. japonicus* WT roots were transformed with T-DNAs carrying a *Ubq10_{pro}:NLS-GFP* transformation marker together with a *GUS* reporter gene driven by either of the *PACE* variants from nodulating FaFaCuRo species fused to the *LjNIN* minimal promoter (*NINmin_{pro}*). For species abbreviations see Supplementary Figure 1. Note the overlapping bacterial invasion zone and *PACE:NINmin_{pro}:GUS* expression in early infection stages (red and blue arrowheads in (A - C)). Red arrowheads: *M. loti* DsRed. Blue arrowheads: GUS activity in nodule primordia. Only pictures taken under white light illumination (WLI) are displayed for nodules in panel VI to reveal the pink colour of leghemoglobin, characteristic for mature and fully infected nodules. Note that like *LjPACE*, the *PACE* variants-driven *GUS* expressions were absent at this stage (panel IV in (A - C) and panel IV in **Supplementary Figure 3D**). (D) Quantification of transgenic root systems exhibiting *GUS* expression in different cell types and tissues exemplarily displayed in (A - C). n.d.: not determined. Bars, 250 μm. The data presented in this figure were generated by Xiaoyun Gong.



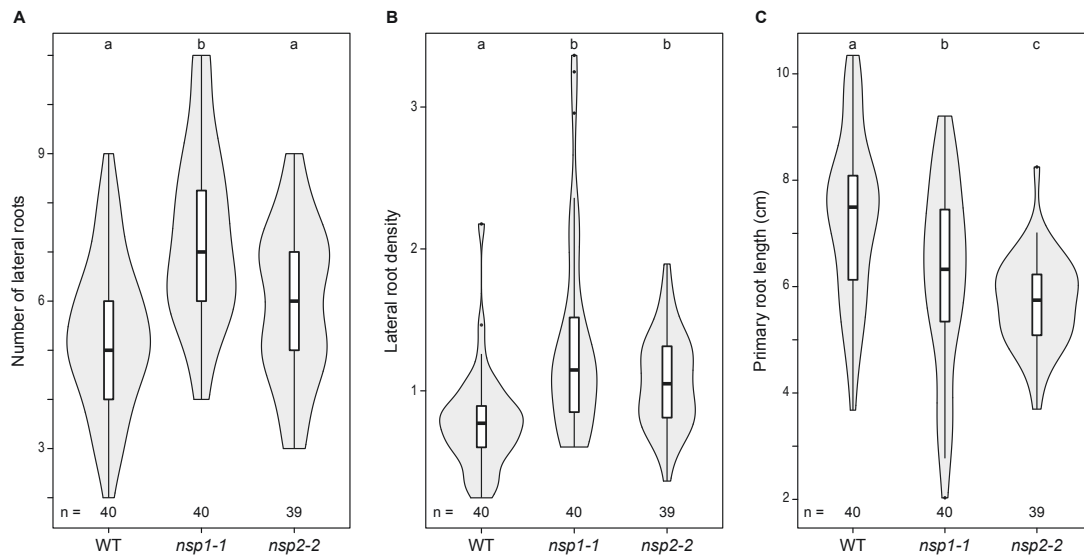
Supplementary Figure 7: *Rhizophagus irregularis* and *Mesorhizobium loti*-mediated increase in lateral root density requires *NIN* (related to Figure 13). Violin plots represent the primary root length (A and C) and the number of lateral roots (B and D) of *L. japonicus* WT, *ccamk-3*, *cyclops-3* and *nin-2* plants inoculated for 10 days with *R. irregularis* (A and B) or *M. loti* (C and D). Data were subjected to pairwise t-test: * $p < 0.05$; ** $p < 0.01$; *** $p < 0.001$. ns: not significant. n: number of plants analysed.



Supplementary Figure 8: Time-course of lateral root formation stimulated by the expression of deregulated versions of SymRK, CCaMK or Cyclops (related to **Figure 15**). Liquid culture of *L. japonicus* WT roots transformed with the empty vector (EV), *Ubq_{pro}:SymRK-mOrange* (SymRK), *Ubq_{pro}:CCaMK^{T265D}* (CCaMK^{T265D}), *Ubq_{pro}:CCaMK¹⁻³¹⁴* (CCaMK¹⁻³¹⁴) or *Ubq_{pro}:3xHA-Cyclops^{DD}* (Cyclops^{DD}) were generated. Violin plots represent the number of lateral roots per root system 10, 20 and 30 days post incubation in the MSR liquid medium. Dots represent the median. Data were subjected to Kruskal-Wallis test followed by Dunn's post-hoc analysis; $p < 0.05$. n: number of roots analysed.



Supplementary Figure 9: Mutation of *NIN* does not affect primary root length or lateral root formation. Violin plots represent the lateral root density (A) and primary root length (B) of 30 days old *L. japonicus* WT and *nin-2* plants. Data were subjected to pairwise t-test: * $p < 0.05$; ** $p < 0.01$; *** $p < 0.001$. ns: not significant. n: number of plants analysed. Lateral root density: number of lateral roots/cm of primary root.



Supplementary Figure 10: Mutation of *NSP1* or *NSP2* stimulates lateral root formation and affects primary root length. Violin plots represent the number of lateral roots (**A**), lateral root density (**B**) and primary root length (**C**) of 30 days old *L. japonicus* WT, *nsp1-1* and *nsp2-2* plants. Data were subjected to Kruskal-Wallis test followed by Dunn's post-hoc analysis; $p < 0.05$. n: number of plants analysed. Lateral root density: number of lateral roots/cm of primary root.

11.3. Supplementary Tables

Supplementary Table 1: Seed bags and bacterial strains used in this study. n.a.: not applicable; dpi: days post inoculation; dpt: days post transfer to MSR medium; dpg: days post germination.

Figures	<i>Lotus japonicus</i> seeds		Symbiont	Timepoint
	Plant genotype	Seed bag no.		
Figure 3	Gifu WT	93057	<i>M. loti</i> CFP	10 to 14 dpi
	Gifu WT	93058		
	Gifu WT	110892		
	Gifu WT	111197		
Figure 4	Gifu WT	87902	<i>M. loti</i> Ds Red	21 dpi
	<i>nin-15</i>	92685		
	Segregating F2	92688		
	<i>nin-15</i>	111638		
Figure 5	<i>nin-15</i>	111285	<i>M. loti</i> Ds Red	21 dpi
	<i>nin-15</i>	111284		
	<i>nin-15</i>	111281		
	<i>nin-15</i>	111292		
	<i>nin-2</i>	113308		
	<i>nin-2</i>	112037		
	<i>nin-2</i>	112040		
	<i>nin-2</i>	12029		
Figure 6 and 8A	<i>nin-2</i>	112031	<i>M. loti</i> Ds Red	21 dpi
		90651		
		90652		
		90654		
		90655		
		90649		
		90650		
		112037		
		112040		
	12029			
Gifu WT	112031			
Figure 7 and 8B	<i>nin-2</i>	113308		
	Gifu WT	111221		
Figure 9	<i>nin-15</i>	Same as Figure 5		
Figure 10	<i>nin-15</i>	111278		
		111638		
		111281		
		111286		
		111293		
		111292		
Figure 11	<i>nin-15</i>	111285		
		111636		
Figure 11	<i>nin-15</i>	same as Figure 10		
Supplementary Figure 3	Gifu WT	92673	<i>M. loti</i> Ds Red (A-F); <i>M. loti lacZ</i> (G)	0 to 21 dpi
Supplementary Figure 4 and 5	<i>nin-2</i>	Same as Figure 6 and 8A	<i>M. loti</i> Ds Red	35 dpi
	Gifu WT	Same as Figure 6 and 8A		
Supplementary Figure 6	Gifu WT	111268		0 to 21 dpi

Supplementary Table 1. Continued.

Figures	<i>Lotus japonicus</i> seeds		Symbiont	Timepoint
	Plant genotype	Seed bag no.		
Figure 12A - B	Gifu WT	93069	<i>R. irregularis</i>	10 dpi
Figure 12C - D	Gifu WT	112169	<i>M. loti</i>	10 dpi
Figure 13A and Supplementary Figure 7	Gifu WT	115682	<i>R. irregularis</i>	10 dpi
	<i>ccamk-3</i>	111316		
	<i>cyclops-3</i>	91863		
	<i>nin-2</i>	113304		
Figure 13B and Supplementary Figure 7	Gifu WT	93066	<i>M. loti</i>	10 dpi
	<i>ccamk-3</i>	111317		
	<i>cyclops-3</i>	91236		
	<i>nin-2</i>	114769		
Figure 15A and Supplementary Figure 8	Gifu WT	72310	n.a.	10, 20, 30 dpt
Figure 15B	Gifu WT	92142		10 dpt
Figure 16	Gifu WT	92134		30 dpg
Figure 17	Gifu WT	69343		10 dpt
	<i>snf1-1</i>	90791		
Figure 18	Gifu WT	92132		14 dpt
	<i>ccamk-3</i>	70931		
	<i>cyclops-3</i>	91224		
Figure 19	Gifu WT	111241		30 dpg
Figure 20	Gifu WT	111243		
Figure 21	<i>nin-2</i>	112042		10 dpt
	Gifu WT	70218		
	<i>nsp1-1</i>	91865		
Supplementary Figure 9	<i>nsp2-2</i>	91406		14 dpt
	Gifu WT	111225		
Supplementary Figure 10	<i>nin-2</i>	112029		30 dpg
	Gifu WT	112055		
	<i>nsp1-1</i>	91866		
	<i>nsp2-2</i>	91408		

Supplementary Table 2: Microscope/scanner settings and image analysis used in this study.

Figures	Microscope/Scanner	Light source	Objective	Filter	Camera/detector	Fluorochrome imaged	Displayed colour in Figures	Image processing	Acquisition mode
Figure 3	Leica TCS SP5	Diode laser, 405 nm	HXC IRAPO L 25x/0.95 W	Wavelength window from 440 to 500 nm	Hamamatsu PMT	GFP	Cyan	Fiji ImageJ - maximal projections of a Z-stack	Sequential mode
Figure 3	Leica TCS SP5	Argon laser, 514 nm	HXC IRAPO L 25x/0.95 W	Wavelength window from 525 to 555 nm	Hamamatsu PMT	YFP	Green	Fiji ImageJ - maximal projections of a Z-stack	Sequential mode
Figure 3	Leica TCS SP5	Diode pumped solid state laser, 561 nm	HXC IRAPO L 25x/0.95 W	Wavelength window from 580 to 640 nm	Hamamatsu PMT	mCherry	Red	Fiji ImageJ - maximal projections of a Z-stack	Sequential mode
Figure 4C (root hair pictures only), 5 and 10	Leica DM6B	Leica CTR6 LED	HPX PL FLUOTAR L 40X/0.60 CORR	none	Leica DFC 9000GT	not applicable	not applicable	Fiji ImageJ - maximal projections of a Z-stack	-
Figure 4C (root hair pictures only), 5 and 10	Leica DM6B	SOLA-SMIL LED3, 365 nm	HPX PL FLUOTAR L 40X/0.60 CORR	Leica M3: excitation filter BP 546/12, suppression filter BP 600/40	Leica DFC 9000GT	Ds Red	Red	Fiji ImageJ - maximal projections of a Z-stack	-
Figure 4C (module section pictures only), 5, 8, 10 and 11; Supplementary Figure 5	Leica TCS SP5	Argon laser, 514 nm	Leica HXC PL APO CS 20X/0.7 IMM CORR CS	Wavelength window from 559 to 633 nm	Hamamatsu PMT	Ds Red	Red	Fiji ImageJ - maximal projections of a Z-stack	Sequential mode
Supplementary Figure 3A - E and 6	Leica MZ16 FA	Schott KL 1500-Z	PLANAPO 1.0x	none	Leica DFC 300FX	not applicable	not applicable	Fiji ImageJ	-
Supplementary Figure 3A - E and 6	Leica MZ16 FA	Lumencor LED3, 390-680 nm	PLANAPO 1.0x	Leica GFP3: excitation filter BP 470/40, suppression filter BP 525/50	Leica DFC 300FX	GFP	Green	Fiji ImageJ	-
Supplementary Figure 3A - E and 6	Leica MZ16 FA	Lumencor LED3, 390-680 nm	PLANAPO 1.0x	Leica DSR: excitation filter BP 545/50, suppression filter BP 620/60	Leica DFC 300FX	Ds Red	Red	Fiji ImageJ	-
Supplementary Figure 3G	Keyence VHX-6000	Keyence inbuild light source Full ring	VH-Z5T Z5-20 x20 x200	none	Keyence VHX-6020	not applicable	not applicable	Fiji ImageJ	-
Figure 4C, 6, 7 and 9	Leica M165FC	Leica MEB127	PLANAPO 1.0x	none	Leica DFC 450C	not applicable	not applicable	Fiji ImageJ	-
Figure 4C, 6, 7 and 9	Leica M165FC	Lumencor LED3, 390-680 nm	PLANAPO 1.0x	Leica GFP3: excitation filter BP 470/40, suppression filter BP 525/50	Leica DFC 450C	GFP	Green	Fiji ImageJ	-
Figure 4C, 6, 7 and 9	Leica M165FC	Lumencor LED3, 390-680 nm	PLANAPO 1.0x	Leica DSR: excitation filter BP 545/50, suppression filter BP 620/60	Leica DFC 450C	Ds Red	Red	Fiji ImageJ	-
Figure 4A, D, G	Epson V700 DIN A4	not applicable	not applicable	not applicable	not applicable	not applicable	not applicable	Fiji ImageJ	not applicable
Figure 19D	Leica DM6B	Leica CTR6 LED	HP PL FLUOTAR 10X/0.30	none	Leica DMC 2900	not applicable	not applicable	Fiji ImageJ	-

Supplementary Table 3: Plasmids used in this study. Constructs labelled with “GW” were generated with the GATEWAY cloning system (Invitrogen). LI, LII and LIII plasmids were generated with the Golden Gate cloning system (Binder et al., 2014) and LIII plasmids were used for *Lotus japonicus* hairy root transformation. Plasmids with a reference number (ref no.) containing CC, XG or RA were generated by Chloé Cathebras, Xiaoyun Gong and Rosa Elena Andrade, respectively.

Name	Reference
<i>Ubq_{pro}</i> :GW-GFP (GW)	(Maekawa et al., 2008)
<i>Ubq_{pro}</i> :SymRK-mOrange (GW)	(Antolín-Llovera et al., 2014)
<i>Ubq_{pro}</i> :CCaMK ^{T265D} (GW)	(Singh et al., 2014)
<i>Ubq_{pro}</i> :CCaMK ¹⁻³¹⁴ (GW)	(Takeda et al., 2012)
<i>Ubq_{pro}</i> :3xHA-Cyclops ^{DD} (GW)	(Singh et al., 2014)
<i>Ubq_{pro}</i> :3xHA-Cyclops ^{AA} (GW)	(Singh et al., 2014)

Supplementary Table 3. Continued.

LI ref.no.	Name	Restriction enzyme	Plasmid construction		Backbone	Comments
			Golden Gate mod. used for assembly			
KGp1	U.A-B. <i>UjWmv₁₀₀</i> (8 kb)	SfuI	<i>UjWmv₁₀₀</i> amplified with oligos XG23 & XG24		U(BB01)	PCR fragment was amplified using <i>UjWmv₁₀₀</i> (2 kb) (Pp14) as template. The <i>AW</i> minimal promoter (<i>UjWmv₁₀₀</i>) consists of 38 bp 5' of the <i>AW</i> transcriptional start site as defined in Singh et al. (2014)
KGp4	U.A-B. <i>UjPACE</i> (<i>UjWmv₁₀₀</i>)	BspI	<i>UjPACE</i> annealed with oligos XG32 & XG33	<i>UjWmv₁₀₀</i> (XGp1)	U(BB03)	Two PCR fragments were amplified using <i>UjWmv₁₀₀</i> (2 kb) (Pp14) as template
KGp5	U.A-B. <i>UjPACE</i> (<i>UjWmv₁₀₀</i>)	BspI	<i>UjPACE</i> annealed with oligos XG74 & XG75	<i>UjWmv₁₀₀</i> (XGp1)	U(BB03)	Two PCR fragments were amplified using <i>UjWmv₁₀₀</i> (2 kb) (Pp14) as template
KGp6	U.A-B. <i>UjPACE</i> (<i>UjWmv₁₀₀</i>)	BspI	<i>UjPACE</i> annealed with oligos XG81 & XG82	<i>UjWmv₁₀₀</i> (XGp1)	U(BB03)	Two PCR fragments were amplified using <i>UjWmv₁₀₀</i> (2 kb) (Pp14) as template
PPA130	U.A-B. <i>UjPACE</i> (<i>UjWmv₁₀₀</i>)	BspI	<i>UjPACE</i> annealed with oligos XG83 & XG84	<i>UjWmv₁₀₀</i> (XGp1)	U(BB03)	Two PCR fragments were amplified using <i>UjWmv₁₀₀</i> (2 kb) (Pp14) as template
PPA131	U.A-B. <i>UjPACE</i> (<i>UjWmv₁₀₀</i>)	BspI	Fragment 1 amplified with primers BA114 and RA124	Fragment 2 amplified with primers XG167 and XG168	U(BB03)	Two PCR fragments were amplified using <i>UjWmv₁₀₀</i> (2 kb) (Pp14) as template
PPA132	U.A-B. <i>UjPACE</i> (<i>UjWmv₁₀₀</i>)	BspI	Fragment 1 amplified with primers BA114 and RA126	Fragment 2 amplified with primers XG167 and XG168	U(BB03)	Two PCR fragments were amplified using <i>UjWmv₁₀₀</i> (2 kb) (Pp14) as template
PPA133	U.A-B. <i>UjPACE</i> (<i>UjWmv₁₀₀</i>)	BspI	Fragment 1 amplified with primers BA114 and RA126	Fragment 2 amplified with primers XG167 and XG168	U(BB03)	Two PCR fragments were amplified using <i>UjWmv₁₀₀</i> (2 kb) (Pp14) as template
KGp134	U.A-B. <i>UjPACE</i> (<i>UjWmv₁₀₀</i>)	BspI	Fragment 1 amplified with primers BA114 and XG105	Fragment 2 amplified with primers XG106 and RA117	U(BB03)	Two PCR fragments were amplified using <i>UjWmv₁₀₀</i> (2 kb) (Pp14) as template
KGp135	U.A-B. <i>UjPACE</i> (<i>UjWmv₁₀₀</i>)	BspI	Fragment 1 amplified with primers BA114 and XG107	Fragment 2 amplified with primers XG106 and RA117	U(BB03)	Two PCR fragments were amplified using <i>UjWmv₁₀₀</i> (2 kb) (Pp14) as template
KGp136	U.A-B. <i>UjPACE</i> (<i>UjWmv₁₀₀</i>)	BspI	Fragment 1 amplified with primers BA114 and XG109	Fragment 2 amplified with primers XG106 and RA117	U(BB03)	Two PCR fragments were amplified using <i>UjWmv₁₀₀</i> (2 kb) (Pp14) as template
PPA116	U.A-B. <i>UjPACE</i> (<i>UjWmv₁₀₀</i>)	BspI	Fragment 1 amplified with primers BA114 and RA118	Fragment 2 amplified with primers RA119 and RA117	U(BB03)	Two PCR fragments were amplified using <i>UjWmv₁₀₀</i> (2 kb) (Pp14) as template
PPA117	U.A-B. <i>UjPACE</i> (<i>UjWmv₁₀₀</i>)	BspI	Fragment 1 amplified with primers BA114 and RA118	Fragment 2 amplified with primers RA119 and RA117	U(BB03)	Two PCR fragments were amplified using <i>UjWmv₁₀₀</i> (2 kb) (Pp14) as template
PPA118	U.A-B. <i>UjPACE</i> (<i>UjWmv₁₀₀</i>)	BspI	Fragment 1 amplified with primers BA114 and RA118	Fragment 2 amplified with primers RA119 and RA117	U(BB03)	Two PCR fragments were amplified using <i>UjWmv₁₀₀</i> (2 kb) (Pp14) as template
PPA119	U.A-B. <i>UjPACE</i> (<i>UjWmv₁₀₀</i>)	BspI	Fragment 1 amplified with primers BA114 and RA118	Fragment 2 amplified with primers RA119 and RA117	U(BB03)	Two PCR fragments were amplified using <i>UjWmv₁₀₀</i> (2 kb) (Pp14) as template
PPA1	U.C-D. <i>UjWmv₁₀₀</i>	BspI	Fragment 1 amplified with primers i165 and i166	Fragment 2 amplified with primers i167 and i168	U(BB03)	PCR fragment amplified using <i>UjWmv₁₀₀</i> gDNA as template. Multigenized for removing BspI/BsaI sites for Golden Gate cloning
PPA143	U.A-B. <i>UjPACE</i>	SfuI	<i>UjPACE</i> annealed with oligos XG71 & XG72		U(BB02)	Two PCR fragments were amplified using <i>UjWmv₁₀₀</i> gDNA as template
KGp145	U.A-B. <i>UjPACE</i>	SfuI	Fragment 1 amplified with primers XG20 and XG26		U(BB02)	Two PCR fragments were amplified using <i>UjWmv₁₀₀</i> gDNA as template
KGp146	U.A-B. <i>UjPACE</i>	SfuI	Fragment 1 amplified with primers XG20 and XG27		U(BB02)	Two PCR fragments were amplified using <i>UjWmv₁₀₀</i> gDNA as template
KGp147	U.A-B. <i>UjPACE</i>	SfuI	Fragment 1 amplified with primers XG20 and XG27		U(BB02)	Two PCR fragments were amplified using <i>UjWmv₁₀₀</i> gDNA as template
KGp148	U.A-B. <i>UjPACE</i>	SfuI	Fragment 1 amplified with primers XG20 and XG27		U(BB02)	Two PCR fragments were amplified using <i>UjWmv₁₀₀</i> gDNA as template
KGp149	U.A-B. <i>UjPACE</i>	SfuI	Fragment 1 amplified with primers XG20 and XG27		U(BB02)	Two PCR fragments were amplified using <i>UjWmv₁₀₀</i> gDNA as template
PPp10	U.A-B. <i>UjWmv₁₀₀</i> (8 kb)	SfuI	<i>UjWmv₁₀₀</i> (1 kb) amplified with primers XG108 and XG109		U(BB01)	PCR fragment amplified using <i>UjWmv₁₀₀</i> gDNA as template
PPp11	U.A-B. <i>UjWmv₁₀₀</i> (1 kb)	SfuI	<i>UjWmv₁₀₀</i> (1 kb) amplified with primers XG108 and XG109		U(BB01)	PCR fragment amplified using <i>UjWmv₁₀₀</i> gDNA as template
PPp12	U.A-B. <i>UjWmv₁₀₀</i> (1 kb)	SfuI	<i>UjWmv₁₀₀</i> (1 kb) amplified with primers XG108 and XG109		U(BB01)	PCR fragment amplified using <i>UjWmv₁₀₀</i> gDNA as template
CG10	<i>UjWmv₁₀₀</i> (<i>UjWmv₁₀₀</i>)	EcoRI	PCR fragment amplified with primers CG28 and CG31		Not applicable	Not applicable
CG11	<i>UjWmv₁₀₀</i> (<i>UjWmv₁₀₀</i>)	EcoRI	PCR fragment amplified with primers CG28 and CG28		U(BB02)	PCR fragment amplified using <i>UjWmv₁₀₀</i> gDNA as template
CG12	<i>UjWmv₁₀₀</i> (<i>UjWmv₁₀₀</i>)	EcoRI	PCR fragment amplified with primers CG28 and CG28		U(BB02)	PCR fragment amplified using <i>UjWmv₁₀₀</i> gDNA as template
CG13	<i>UjWmv₁₀₀</i> (<i>UjWmv₁₀₀</i>)	EcoRI	PCR fragment amplified with primers CG28 and CG28		U(BB02)	PCR fragment amplified using <i>UjWmv₁₀₀</i> gDNA as template
CG14	<i>UjWmv₁₀₀</i> (<i>UjWmv₁₀₀</i>)	EcoRI	PCR fragment amplified with primers CG28 and CG28		U(BB02)	PCR fragment amplified using <i>UjWmv₁₀₀</i> gDNA as template
CG15	<i>UjWmv₁₀₀</i> (<i>UjWmv₁₀₀</i>)	EcoRI	PCR fragment amplified with primers CG28 and CG28		U(BB02)	PCR fragment amplified using <i>UjWmv₁₀₀</i> gDNA as template
CG16	<i>UjWmv₁₀₀</i> (<i>UjWmv₁₀₀</i>)	EcoRI	PCR fragment amplified with primers CG28 and CG28		U(BB02)	PCR fragment amplified using <i>UjWmv₁₀₀</i> gDNA as template
CG17	<i>UjWmv₁₀₀</i> (<i>UjWmv₁₀₀</i>)	EcoRI	PCR fragment amplified with primers CG28 and CG28		U(BB02)	PCR fragment amplified using <i>UjWmv₁₀₀</i> gDNA as template
CG18	<i>UjWmv₁₀₀</i> (<i>UjWmv₁₀₀</i>)	EcoRI	PCR fragment amplified with primers CG28 and CG28		U(BB02)	PCR fragment amplified using <i>UjWmv₁₀₀</i> gDNA as template
CG19	<i>UjWmv₁₀₀</i> (<i>UjWmv₁₀₀</i>)	EcoRI	PCR fragment amplified with primers CG28 and XG24		U(BB02)	PCR fragment amplified using <i>UjWmv₁₀₀</i> gDNA as template
CG20	<i>UjWmv₁₀₀</i> (<i>UjWmv₁₀₀</i>)	EcoRI	PCR fragment amplified with primers CG28 and XG24		U(BB02)	PCR fragment amplified using <i>UjWmv₁₀₀</i> gDNA as template
CG21	<i>UjWmv₁₀₀</i> (<i>UjWmv₁₀₀</i>)	EcoRI	PCR fragment amplified with primers CG27 and XG24		U(BB02)	PCR fragment amplified using <i>UjWmv₁₀₀</i> gDNA as template
CG22	<i>UjWmv₁₀₀</i> (<i>UjWmv₁₀₀</i>)	EcoRI	PCR fragment amplified with primers CG27 and XG24		U(BB02)	PCR fragment amplified using <i>UjWmv₁₀₀</i> gDNA as template
CG23	<i>UjWmv₁₀₀</i> (<i>UjWmv₁₀₀</i>)	EcoRI	PCR fragment amplified with primers CG28 and CG28		U(BB02)	PCR fragment amplified using <i>UjWmv₁₀₀</i> gDNA as template
CG24	<i>UjWmv₁₀₀</i> (<i>UjWmv₁₀₀</i>)	BspI	Fragment 1 amplified with primers XG119 and CG43		U(BB03)	PCR fragment amplified using <i>UjWmv₁₀₀</i> gDNA as template
CG25	<i>UjWmv₁₀₀</i> (<i>UjWmv₁₀₀</i>)	BspI	Fragment 1 amplified with primers XG119 and CG43		U(BB03)	PCR fragment amplified using <i>UjWmv₁₀₀</i> gDNA as template
CG26	<i>UjWmv₁₀₀</i> (<i>UjWmv₁₀₀</i>)	BspI	Fragment 1 amplified with primers XG119 and CG43		U(BB03)	PCR fragment amplified using <i>UjWmv₁₀₀</i> gDNA as template
CG27	<i>UjWmv₁₀₀</i> (<i>UjWmv₁₀₀</i>)	BspI	Fragment 1 amplified with primers XG119 and CG43		U(BB03)	PCR fragment amplified using <i>UjWmv₁₀₀</i> gDNA as template
CG28	<i>UjWmv₁₀₀</i> (<i>UjWmv₁₀₀</i>)	BspI	Fragment 1 amplified with primers XG119 and CG43		U(BB03)	PCR fragment amplified using <i>UjWmv₁₀₀</i> gDNA as template
CG29	<i>UjWmv₁₀₀</i> (<i>UjWmv₁₀₀</i>)	BspI	Fragment 1 amplified with primers XG119 and CG43		U(BB03)	PCR fragment amplified using <i>UjWmv₁₀₀</i> gDNA as template

Supplementary Table 3. Continued.

Lil ref no.	Name	Plasmid construction				
		Restriction enzyme	Golden Gate modules used for assembly			
CGP4	U1E-F-1-2-NCS ₅ - <i>luc10p</i> -Npr1	Bsal	U1A-B-WD5 ₅ -[G090]	U1B-C- <i>oxY</i> [BB09]	U1D- <i>oxY</i> [BB09]	U1F-G- <i>oxY</i> [BB09]
CGP5	U1E-F-1-2-Ulq12 ₅ -MLS-ZAgFP	Bsal	U1A-B- <i>ulq12p</i>	U1B-C-NLS[BB09]	U1D-GFP[G011]	U1F-35S-T[G059]
CGP6	U1B-F-5-6- <i>PACE/MinW</i> ₅ -MLS-Z <i>mCherry</i>	Bsal	U1A-B- <i>PACE/MinW</i> ₅	U1B-C-NLS[BB09]	U1D-mCherry[G025]	U1F-NSP-T[G045]
CGP7	U1B-F-3-4- <i>luc2Z-NLS-ZAgFP</i>	Bsal	U1A-B-luc2[G082]	U1B-C-NLS[G060]- <i>oxY</i>	U1D-YFP[G012]	U1F-G- <i>oxY</i> [BB09]
pRAM5	U1B-F-3-4- <i>luc2Z-NLS-MinW</i>	Bsal	U1A-B-luc2[G082]	U1B-C- <i>luc2Z-NLS</i> [pRAM5]	U1D- <i>oxY</i> [BB09]	U1F-G- <i>oxY</i> [BB09]
CGP8	U1E-F-5-6-Uba ₅ -Myc-C _{50M}	Bsal	U1A-B- <i>luc2Z</i> [G082]	U1B-C- <i>oxY</i> [BB09]	U1D- <i>oxY</i> [BB09]	U1F-35S-T[G059]
CGP9	U1E-F-5-6-Uba ₅ -Myc-C _{50M}	Bsal	U1A-B- <i>luc2Z</i> [G082]	U1B-C- <i>oxY</i> [BB09]	U1D- <i>oxY</i> [BB09]	U1F-35S-T[G059]
CGP10	U1E-F-5-6-Uba ₅ -Myc-C _{50M}	Bsal	U1A-B- <i>luc2Z</i> [G082]	U1B-C- <i>oxY</i> [BB09]	U1D- <i>oxY</i> [BB09]	U1F-35S-T[G059]
CGP11	U1E-F-5-6-Uba ₅ -Myc-C _{50M}	Bsal	U1A-B- <i>luc2Z</i> [G082]	U1B-C- <i>oxY</i> [BB09]	U1D- <i>oxY</i> [BB09]	U1F-35S-T[G059]
CGP12	U1E-F-5-6-Uba ₅ -Myc-C _{50M}	Bsal	U1A-B- <i>luc2Z</i> [G082]	U1B-C- <i>oxY</i> [BB09]	U1D- <i>oxY</i> [BB09]	U1F-35S-T[G059]
CGP13	U1E-F-5-6-Uba ₅ -Myc-C _{50M}	Bsal	U1A-B- <i>luc2Z</i> [G082]	U1B-C- <i>oxY</i> [BB09]	U1D- <i>oxY</i> [BB09]	U1F-35S-T[G059]
CGP14	U1E-F-5-6-Uba ₅ -Myc-C _{50M}	Bsal	U1A-B- <i>luc2Z</i> [G082]	U1B-C- <i>oxY</i> [BB09]	U1D- <i>oxY</i> [BB09]	U1F-35S-T[G059]
CGP15	U1E-F-5-6-Uba ₅ -Myc-C _{50M}	Bsal	U1A-B- <i>luc2Z</i> [G082]	U1B-C- <i>oxY</i> [BB09]	U1D- <i>oxY</i> [BB09]	U1F-35S-T[G059]
pRA11	U1B-F-3-4-Ulq12 ₅ -Myc-Npr1	Bsal	U1A-B- <i>ulq12p</i> [G070]	U1E-C- <i>oxY</i> [G099]	U1D-mCherry[G025]	U1F-NSP-T[G045]

Supplementary Table 4: Name and sequences of primers used in this study. Primers with a reference number (ref no.) containing CC, MC, JL, KP, RA, XG, SZ or PP were generated by Chloé Cathebras, Marion Cerri, Jayne Lambert, Ksenia Vondenhoff, Rosa Elena Andrade, Xiaoyun Gong, Sarah Zeitlmayr and Priya Pimprikar respectively.

Primer ref no.	Sequence 5' - 3'
CC14	AAGAAGACAACAGAGGTCTCACAGATTCCAATTGAAGCTGTTGTTTTTTC
CC30	TTGAAGACCGTACGGGTCTCAGCGGACCTTTCATCTCACCCAACCCCT
CC31	GCGAAGACGTCAGAGGTCTCACAGAGGCAGAGTGTGAAAATATTGG
CC54	AAGAAGACAACAGAGGTCTCaCCTTAATCTCAGGGTCCATTTGCTCAT
CC55	CTGAAGACAGGATTGGAAGGGCATTACCCAATC
CC56	ATGAAGACCCAATCCTTTTCATAGAAACTGAAATTC
CC176	AACGTCTCACAGAGCTAGCTGATCCAATTAAGTACC
CC203	AACGTCTCAATTGATCCTTGACCTCTCCC
CC204	AACGTCTCAAAATCCCTGAGATGGTGTA
CC210	AACGTCTCACTACCTCCATCGTCTCTCTCTG
CC211	AACGTCTCAGATCTCTCATTCAGTCTAAATG
CC212	AACGTCTCAGATCCCTCTTATCACTAGCG
CC213	AACGTCTCATTGGTTCGGTCTGTTGAC
CC214	AACGTCTCACAACGAATATGGACGGAAG
CC263	AACGTCTCAGCGGTCCAAGGTAGACTTTACAGTTGC
CC264	AACGTCTCAAAGCGCCTTGCCCTTGTGTATTAC
CC267	AACGTCTCAGCTTTGTACGATTGCCATGTGGCAC
CC268	AACGTCTCAGCTTCACCTGCTTACACTTGTGGG
CC253	AACGTCTCAGCTTCGATTGCACGTTTTAG
CC287	AACGTCTCAATGCGCAGAGAGGCCACAAAGAGGCGAGA
CC288	AACGTCTCACATTCACAAATGATCGTACAAAAATTTGTGTACCTAAAAATGC
CC289	AACGTCTCAATGTGGCAACGGTTTGGCAGCCACAAAGAGGCGAGA
CC290	AACGTCTCAACATGGCAGAACCTGCAAAATTTGTGTACCTAAAAATGC
CC311	AACGTCTCAGTAGCCTTGCCCTTGTGTATTAC
CC440	AACGTCTCAGCGGCCACCCAAACATATGTGGTGG
CC443	AACGTCTCATTGGGACTTAATCCCGAAGTAGG
CC471	CCCGTCTCACAACACCTGCTTACACTTGTGGGTCCT
CC472	CCCGTCTCACAATGTACGATTGCCATGTGGCA
MC119	ATGAAGACTTTACGGGTCTCaGCGGGACCAAGTCTCATAACATAGATCA
JL65	ATGAAGACTTTACGGGTCTCTCACCATGGAATATGGTTCATTACTAGTGC
JL66	TTGAAGACTTGAACACAGGAAGGGCTAAAGA
JL67	ATGAAGACTTGTTCGAAAGAGGCACCGG
JL68	TTGAAGACTTAGATTCTTGATCCCCACCCTC
JL69	ATGAAGACTTATCTTCTTATACCTTTGGAAGCCGCGCTCTTCTTCTGGTGGAAAGAAAGTCAGGCGAGAAAAGACGAACCAA GGCAGAAAAGACTATCAG
JL70	TTGAAGACTTCAGAGGTCTCTCCTTAGATGGGCTGCTATTGC
KP50	ATCGTCTCAGCGGCTGCTTTGGACTATATTTCTTTGAG
KP52	TACGTCTCTCAGAGCTGCTTCTTCTTACCTC
KP58	ATCGTCTCATACAACATGACACACGGATG
KP59	TACGTCTCTTGTAAAAATGGTATGTCCTAGACAAAC
KP60	TACGTCTCTGGAGACCAGCTACACTCAAATG
KP61	ATCGTCTCACTCCAATCGAAGGTATATTAGTATGGATC
KP62	TACGTCTCTGCAGGTTGTGGGTTCATTTATTG
KP63	ATCGTCTCACTGCCGCTAATCAGGAAGCA
KP84	TACGTCTCACAGAGCTAGCTGATCCAATTAAGTACCTG
KP91	ATCGTCTCAGCGGGCTCCGTTTGGTCAACAGAC
KP92	ATCGTCTCTAAGCTAATTTGCAGCGACTTTTCTC
KP93	TACGTCTCAGCTTATATCGCAGCGACCAG
RA114	ACGAAGACAATACGTACGTCTCAGCTTATATCGCA
RA115	AAGAAGACAAGCTCAAATTTGTGTACCTAAAAATGC
RA116	TCAGAAGACAAGAGCCCAAGAGGC
RA117	AAGAAGACAACAGATACGTCTCACAGAGCTAGCTG
RA118	AAGAAGACAAGACGATACGGATCCACAAATTTGTGTACCTAAAAATGCAA
RA119	TCAGAAGACAAGTCTTAGATAGTCTGTGAGCCCAAGAGGC
RA124	AAGAAGACAACATGTGCGATGGAGCAAAATTTGTGTACCTAAAAATGC
RA125	TCAGAAGACAATGTGGCGTGTCTCACAGGAGCCCAAGAGGC

Supplementary Table 4. Continued.

Primer ref no.	Sequence 5' - 3'
RA126	AAGAAGACAAACATGTCAGATGGACAAAATTTGTGTACCTAAAAATGC
RA127	TCAGAAGACAAAATGTGTCGTACGGACATGAGCCACAAGAGGC
RA130	AAGAAGACAAACATGTCGGATGCAGAAAATTTGTGTACCTAAAAATGC
RA131	TCAGAAGACAAAATGTGGCACAACCAAGAGCCCAAGAGGC
RA87	ATGAAGACTTTACGGGTCTCATCTGTGCTTACACTTGTGGGTCT
RA88	ATGAAGACTTCAGAGGTCTCAGGTGCTAGCTGATCCAATTAAGTACCT
SZ02	ATCGTCTCCAGAATTATTACTGATAAAAAATCAAATGTTGC
SZ07	ATCGTCTCGCATGTGGCAGCAGAGAGCAGATTTTAAGGTTCACTACTCTATTTCT
SZ08	TACGTCTCACATGGCAATCGTACAAAATCCAGAGTGGTGAGGAT
SZ09	ATCGTCTCGATCGTCTTAGATAGTCTGTGATTTTAAGGTTCACTACTCTATTTCT
SZ10	TACGTCTCACGATACGGATCCACAATCCAGAGTGGTGAGGAT
XG105	TAGAAGACTAATGTAAGAAGTAGGAAATTTGTGTACCTAAAAATGCAA
XG106	TAGAAGACTAACATGTGGCAATCAGGCAGGAGCCACAAGAGGCGAGA
XG107	TAGAAGACTAGACACATGTGTCAGAAGGAGAAAATTTGTGTACCTAAAAATGCAA
XG108	TAGAAGACTATGTCTAAGGACAGGAGCCACAGAGGCGAGA
XG109	TAGAAGACTACTGATGTTGGTTGGATCAAATTTGTGTACCTAAAAATGCAA
XG110	TAGAAGACTATCAGCGTAGCGTCCAGGAGCCACAAGAGGCGAGA
XG23	TAGAAGACTACACCTGCTTACACTTGTGGGTCCCTA
XG24	TAGAAGACTACAGATATCGTCTCACAGAGCTAGCTGATCCAATTAAGTAC
XG32	TACGTAACGTCTCAGCGGTGTACGATTGCCATGTGGCAGCAGAGAG
XG33	GGTGCTCTCTGCGTGCCACATGGCAATCGTACACCGCTGAGACGTTA
XG71	ATCGTCTCAGCGGTGTACGATTGCCATGTGGCAGCAGAGAGTCTGTGAGACGAT
XG72	ATCGTCTCACAGACTCTCTGCGTGCCACATGGCAATCGTACACCGCTGAGACGAT
XG79	CTGAAGACTATAACGTAACGTCTCAGCGGGCTCCATGCGACATGTGGCGTGTCTCACAGCACCAGTCTTCTT
XG80	AAGAAGACTTGGTGTCTGTGAGCACGCCACATGTGCGATGGAGCCCGCTGAGACGTTACGTATAGTCTTTCAG
XG81	CTGAAGACTATAACGTAACGTCTCAGCGGTGTCCATCTGACATGTGTGCTGAGACATCACCAAGTCTTCTT
XG82	AAGAAGACTTGGTGTCTGTGAGCACGCCACATGTGCGATGGAGCCCGCTGAGACGTTACGTATAGTCTTTCAG
XG85	CTGAAGACTATAACGTAACGTCTCAGCGGTCTGATCCGACATGTGGCACAACCAACCAAGTCTTCTT
XG86	AAGAAGACTTGGTGTCTGTGAGCACGCCACATGTGCGATGGAGCCCGCTGAGACGTTACGTATAGTCTTTCAG
PP168	AAGAAGACAATACGGGTCTCACACCATGGAAGGGAGGGGTTTCTG
PP179	AAGAAGACAACAGAGGTCTCACCTTCATTTTTTCAGTTTCTGATAG
PP204	ATGAAGACTTTACGGGTCTCACACCATGGGATATGATCAAACCAG
PP208	TAGAAGACAAAGTCTTTTCATAGAAACTGAAATTC
PP211	ATGAAGACTTGACTTGGAAAGGCATTACCCAATC
PP212	ATGAAGACTTCAGAGGTCTCACCTTTGATGGACGAAGAGAAGAGAGGAGCATG

12. Acknowledgements

First of all, I would like to express my deepest gratitude and thanks to my supervisor Prof. Dr. Martin Parniske, who has supported me throughout my doctoral thesis. I am very thankful for his guidance, encouragements, feedback and stimulating suggestions. Martin was always open for discussions, his enthusiasm for science and outstanding knowledge have been a constant source of inspiration and motivation for me. I am especially grateful to him for giving me the freedom to pursue “my own” scientific ideas and side projects as well as for giving me the opportunity to attend many international conferences.

I am very grateful to all the reviewers for taking their precious time and effort to evaluate this thesis.

Big thanks go to all past and present members of the Genetics Department and especially to the members of the Parniske group for the continuous help and support. Special thanks go to Dr. Martina Katharina Ried who introduced me into the research topic and taught me many experimental procedures. Thanks to Dr. Marion Cerri and Dr. Katja Katzer for their help and guidance in the lab and for their valuable advices, scientific input and discussions. I would like to also thank to Prof. Dr. David Chiasson for all the advices and help with cloning and yeast work and for the continuous scientific discussions we had at the bench. Thanks also to greenhouse members, especially Anna, for taking care of my plants.

I want to thanks the *PACE* making team, Xiaoyun, Rosa, Ksenia and Max for the great time we had while working together and for all the fruitful discussions that enabled us to bring this challenging and exciting project forward. I would also like to thank Philipp for his insights on my projects, his help and advices on various experimental procedures and for the fun times we had in the lab.

A big thank you goes to the best lab technician Jessica. Thanks a lot for your help in the lab, for answering my questions, for the fun times and for your personal support.

Thanks also go to my previous office mates Corinna, Andy and Michi for their help, kindness, and fun in everyday lab life.

During those years, I had the pleasure to supervise and teach Jonas Hammerl, who was a fabulous Master student. I would like to thank him for his dedication and outstanding work.

I also had the chance and pleasure of meeting some awesome colleagues that became my friends during this time, Rosa, Constance, Benjamin, Xiaoyun, Aline, Nimisha, Juan, Fang-

Acknowledgements

Yu, Rafa and Katy. Thank you all for your personal support, help and for the great times we had together. Thank you for always being on my side.

In the end, I would like to thank my love ones outside of the lab bubble. Big thanks go to my friends Laura and Benoit as well as to the past and current members of my “climbing crew”, Simon, Florian, David, Michael, Michał, Tobias, Milan and Clemens for all the support and encouragements you gave me during the period of this doctoral thesis. Very special thanks and gratitude go to my parents who always believed in me and unconditionally supported me throughout all these years. Lastly, I would like to thank Veit for always being there for me.

13. Curriculum Vitae

Chloé Cathebras

EDUCATION

2015 - 2022 **Doctoral study** in Plant Molecular Biology and Genetics, Institute of Genetics, University of Munich (LMU), Germany

2013 - 2015 **Master** in Functional Biology of Plants, University of Montpellier, France

2012 - 2013 **Bachelor** in Functional Biology of Plants, University of Montpellier, France

2010 - 2012 **DUT** (two-year university degree in technology) in Bioengineering and Environmental Engineering), University of Perpignan, France

PROFESSIONAL EXPERIENCE

SEP 2015 - present **Doctoral Thesis**
 Institute of Genetics, University of Munich (LMU), Germany
 Supervisor: Prof. Dr. Martin Parniske
 Project 1: Study of the roles and dynamics of *cis*-regulatory elements during the establishment of the nitrogen-fixing root nodule symbiosis.
 Project 2: *In vivo* study of the CCaMK/CYCLOPS complex structure and interactome in the model legume *Lotus japonicus*.

JAN 2015 - JUN 2015 **Master Thesis**
 Institute of Genetics, University of Munich (LMU), Germany
 Supervisor: Prof. Dr. Martin Parniske
 Project: Analysis of the connections between lateral root development and nodule organogenesis in *Lotus japonicus*.

MAR 2014 - JUN 2014 **Internship**
 Department of Biotechnology, Mahidol University, Bangkok, Thailand
 Supervisor: Dr. Unchera Viboonjun
 Project: Optimization of a protein extraction method for rubber particles from rubber tree (*Hevea brasiliensis*), investigation of the proteome alterations of rubber particles and isolation of potential protein markers for rubber yield.

APR 2013 - JUL 2013 **Bachelor Thesis**
 CIRAD research institute, Montpellier, France
 Supervisor: Dr. Hâna Chair
 Project: Isolation and characterization of microsatellite markers in *Xanthosoma sagittifolium* for genetic studies, and cross amplification in related species.

APR 2012 - AUG 2012 **Internship**
 Phytocontrol laboratory, Nîmes, France
 Supervisor: Delphine Milletti
 Project: Development and application of an Aflatoxin M1 extraction method and dosing method on HPLC-FL, analysis of various mycotoxins in food on HPLC-FL.

MANUSCRIPTS IN PREPARATION & PUBLICATION

Cathebras C, Sandré A, Ried MK* & Parniske M*, Common symbiosis genes stimulate lateral root emergence via the activation of *NIN* in *Lotus japonicus* and *Dryas drummondii*. *Manuscript in preparation*

Cathebras C*, Gong X*, Andrade RE, Vondenhoff K, Keller J, Delaux P-M, Griesmann M & Parniske M, Acquisition of a *cis*-regulatory element in the *NIN* promoter enabled the emergence of the nitrogen-fixing root nodule symbiosis. *Manuscript under review*.

Cathebras C, Traore R, Malapa R, Risterucci A-M & Chair H (2014) Characterization of microsatellites in *Xanthosoma sagittifolium* (Araceae) and cross-amplification in related species. *Applications in Plant Sciences* 2: 1400027

TALKS

2020 "Evolution of the nitrogen-fixing root nodule symbiosis". Virtual seminar in symbiosis, September 2020, ZOOM conference organised by Dugald Reid, Katharina Markmann, Myriam Charpentier and Pierre-Marc Delaux

2016 "Do you want to join the complex? Toward the identification fo new CCaMK/CYCLOPS interactors". Lightning talk, ENFC 2016, Budapest, Hungary.

POSTER COMMUNICATIONS (presenter(s) underlined)

2019 Cathebras C & Parniske M, *In vivo* FRET-FLIM to investigate the CCaMK/CYCLOPS complex interactome in root hair cells. iMMM 2019, Torino, Italy.

2018 Cathebras C & Parniske M, *In vivo* FRET-FLIM to investigate the CCaMK/CYCLOPS complex interactome in root hair cells. ENFC 2018, Stockholm, Sweden.

2018 Vondenhoff K, Gong X, Cathebras C, Andrade RE, Griesmann G & Parniske M, A *cis*-regulatory element enables the emergence of the root nodule symbiosis. ENFC 2018, Stockholm, Sweden.

2017 Cathebras C, Ried MK & Parniske M, The CCaMK/CYCLOPS complex regulates lateral root formation in *Lotus japonicus*. Plant biology of the next generation, SFB924 conference, Freising, Germany.

2017 Cathebras C, Ried MK & Parniske M, The CCaMK/CYCLOPS complex regulates lateral root formation in *Lotus japonicus*. ICNF 2017, Granada, Spain.

2016 Sandré A, Cathebras C, Bellon P, Andrade RE, Gong X & Parniske M, Do you want to join the complex? Towards the identification of new CCaMK/CYCLOPS interactors. ENFC 2016, Budapest, Hungary.

2015 Cathebras C, Ried MK & Parniske M, The CCaMK/CYCLOPS complex regulates lateral root formation in *Lotus japonicus*. Cell biology at the plant-microbe interface, 36th New Phytologist symposium, 2015, Munich, Germany.

WORKSHOPS

2015 "BioVoxel, processing and analysis of scientific images", two days workshop, University of Munich (LMU), Germany

2016 "Eoda, data mining with R", two days workshop, Technical University of Munich (TUM), Freising, Germany

2017 "Evolution of regulatory networks", two days workshop organised by Prof. Dr. Martin Parniske (LMU), Center for Advanced Studies der LMU (CAS), Munich, Germany

2019 "R course", one day workshop organised by Alexandre Magalhães (TUM), Technical University of Munich (TUM), Freising, Germany

2019 "Plant microbiome", two days workshop co-organized by Prof. Dr. Martin Parniske (LMU) and Prof. Dr. Caroline Gutjahr (TUM), Center for Advanced Studies der LMU (CAS), Munich, Germany

2020 "FLIM, online symposium", 5 days online workshop co-organized by CMCB Light Microscopy Facility of Technische Universität Dresden, Imaging Network of WWU Münster, Center of Advanced Imaging of HHU Düsseldorf University and the Core Facility Bioimaging at the Biomedical Center of the LMU München, Germany

SKILLS

MICROSCOPY: confocal microscopy (CLSM), multiphoton imaging, fluorescence lifetime imaging (FLIM), *in vivo* FRET-FLIM, fluorescence microscopy

MOLECULAR BIOLOGY: DNA/RNA extraction, yeast one-hybrid, yeast one-hybrid screen, yeast two-hybrid, Golden Gate cloning, genotyping

PLANT BIOLOGY: root transformation, root phenotyping, plant inoculation, vibratome and microtome sectioning

MICROBIOLOGY: bacteria culture, bacteria transformation, *Rhizobia* Nod Factors extraction and purification on HPLC

SOFTWARES:

- Adobe illustrator: scientific poster design, figure preparation and illustration for publication
- Affinity designer: scientific poster design, figure preparation and illustration for publication
- Affinity publisher: data formatting for publication
- ImageJ and Fiji: image processing and image analysis
- Becker & Hickl SPC and SPCImage: FLIM data recording and analysis
- Leica SP8 Falcon FLIM and PicoQuant SymPhoTime 64: notions - hands-on sessions at the Center of Advanced Light Microscopy of the TUM and the Core Facility Bioimaging at the Biomedical Center of the LMU, with Leica and PicoQuant FLIM specialists
- CLC main workbench: cloning
- Microsoft office: data processing with Excel, data presentation with PowerPoint
- R: data illustration and statistical analysis

TEACHING:

- Responsible of the Leica SP5 CLSM and Becker & Hickl TCSPC system at the institute of genetic, LMU (training of all the new doctoral students and postdocs at the microscope for the last 3 years)
- Lecturer for computational biology course: "image processing and analysis with ImageJ (Fiji)" (lecture and exam preparation, grading Master students for the last 2 semesters)
- Supervision of 3 Master students during the course of my doctoral thesis

SCIENTIFIC WRITING:

- Co-writing of a DFG (German research fundation) grant proposal
- Reviewing of several (>10) manuscripts for high ranking journals
- Writing manuscripts

LANGUAGE PROFICIENCY: English (fluent), French (native speaker)

